SAND2016-1349PE

Sandia National Laboratories

SECANT QKD Grand Challenge LDRD

Sandia Enabled Communications and Authentication Network using Quantum Key Distribution

Sandia National Laboratories

LDRD

Chip-scale Quantum Photonics

Paul Davids, and Team

U.S. DEPARTMENT OF ENERGY

NNSA National Nuclear Security Administration

Sandia National Laboratories is a multi-program laboratory managed and operated by Sandia Corporation, a wholly owned subsidiary of Lockheed Martin Corporation, for the U.S. Department of Energy's National Nuclear Security Administration under contract DE-AC04-94AL85000. SAND NO. 2011-XXXXP

Team

- *SPD Development:* Chris DeRose, Nick Martinez, Andrew Starbuck, Andy Pomerene, Reinhard Brock, Doug Trotter.
- *Heterogeneous Integration:* Bruce Burckel, Andy Pomerene, Chris DeRose, Erik Skogen, Jeff Cederberg, Anna Pedretti-Tauke.
- *CV-QKD & QCFC:* Chris DeRose, Daniel Soh, Mohan Sarovar, Andrew Hollowell, Mark Ballance, Chris Nordquist, Ryan Camacho.

Chip-scale Quantum Photonics

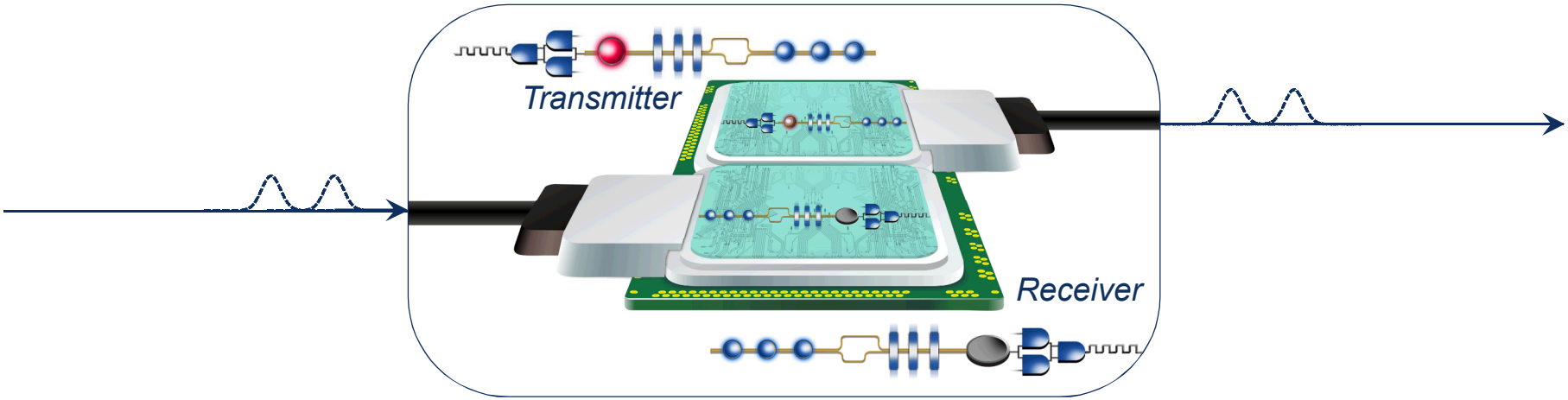

- Develop a chip-scale quantum photonics platform.
- Leverage Si Photonics development for large scale integration.
- Why?
  - Multi-node complex quantum circuits for quantum networks.
- 1st Application: Quantum Key Distribution

State of the Art

- Many groups pursuing chip-scale quantum photonics
  - Bristol, NIST, UCSD, MIT, Oxford, ORNL, LANL, Duke, Toshiba, CUDOS ….. and many more.
- Sandia is uniquely positioned
  - Co-located CMOS fabrication facility with III-V fabrication facility.
  - CMOS compatible Si photonics platform.
  - III-V Photonics platform and high performance electronics.

Core Silicon Photonics

Sandia National Laboratories

Free-carrier Effect (high-speed)

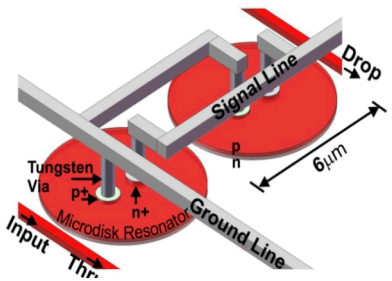

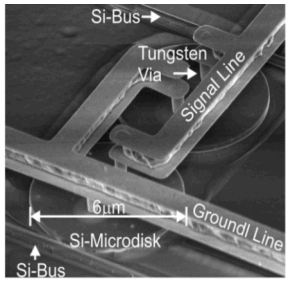

Fast Reconfigurable Interconnects

3.2fJ/bit at 12Gb/s

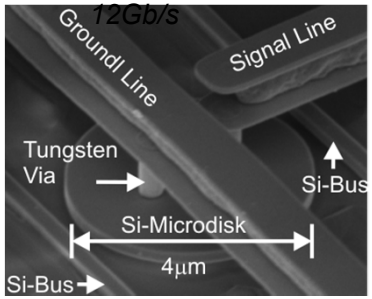

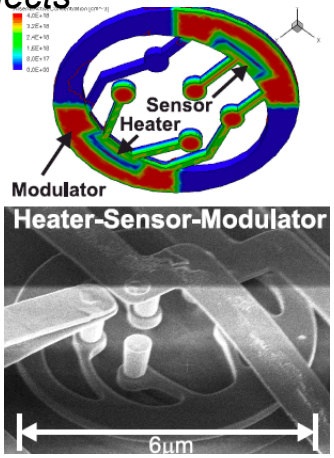

Resonant Optical Modulator/Filter

Thermally stabilized modulator

Broadband Mach-Zehnder Filter/Switch < 1V-cm at 10 Gb/s

Thermal Optic Effect (wide-band)

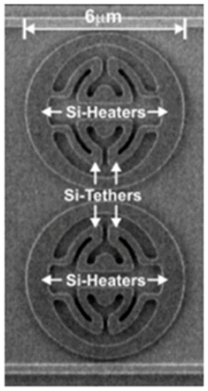

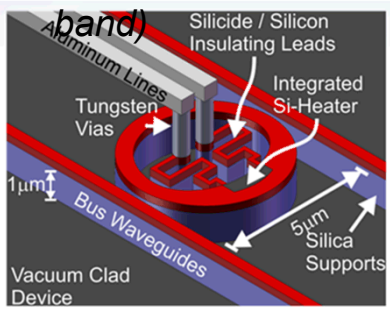

Tunable Resonant Filt

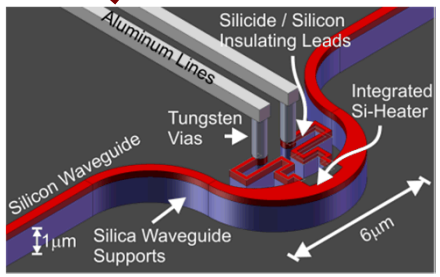

Thermo-optic Phase Shifter

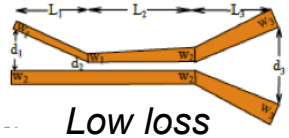

Low loss optical coupler

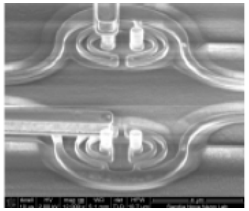

Switch Arrays

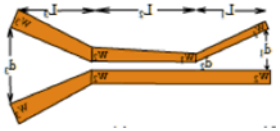

High-speed Ge Detector in

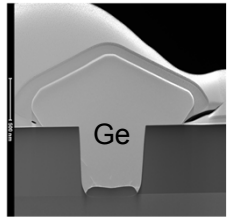

Si Photonics-CMOS Integration

Integration Advantages

- High data rate – multiple wavelengths per channel
  - Requires dense integration.
  - High index contrast system – compact devices
- CMOS compatible photonics
  - Leverage existing infrastructure
  - Large number of active devices (SPAD's)
  - Low cost
- High efficiency
  - Compact devices – give lower dark current
  - Ge on Si offers best chance for integrated compact devices.

Optical Transceiver for Exascale

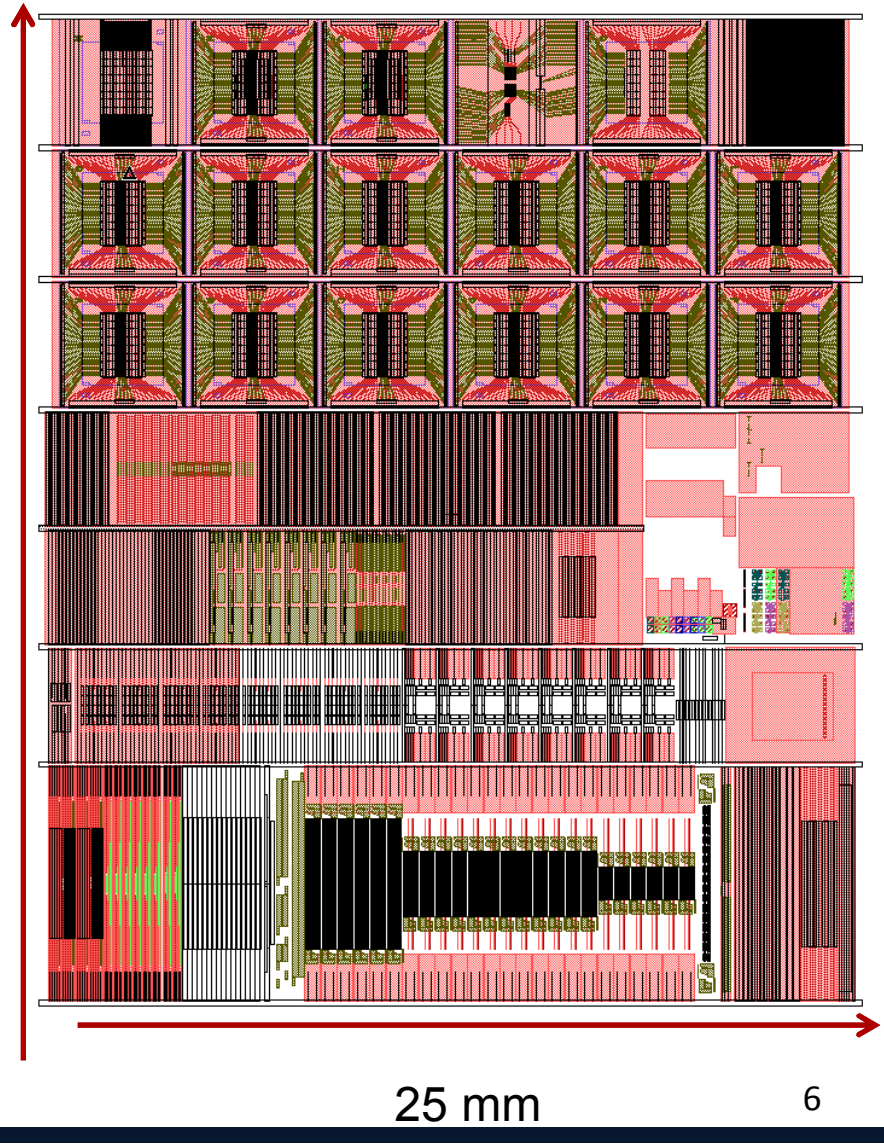

Chip-scale Quantum Photonics Platform

Sandia National Laboratories

- Key Platform Components
  - Single Photon Detection (SPD) Capability
  - Single Photon Source (SPS)
- Heterogeneous integration methods
  - Enable integration of SPS
  - Non-linear media and incompatible new devices
- Differences between bench-top and chip-scale quantum optics.
  - Loss, polarization, dispersion and mode conversion.
  - Waveguide non-linearities

Outline

- Highlight early progress in 3 areas:
  - Integrated Single Photon Avalanche Detector (SPAD)
  - Heterogeneous integration of III-V laser source on Si Photonics substrate.
  - Complex integrated quantum optoelectronic circuits

Ge in Modern CMOS

Germanium old semiconductor technology.

- Indirect Bandgap at 0.66 eV.
- Direct Bandgap at 0.8 eV (1550 nm) in telecom band.
- Not efficient optical emitter.

Selective epitaxial growth of Ge on Si has enabled advanced strain engineering in modern CMOS.
Fully CMOS Compatible.
High electron and hole mobilities.

Ge optoelectronics: direct bandgap at 1550nm implies good absorption.

Strain engineering in CMOS

Intel 45nm

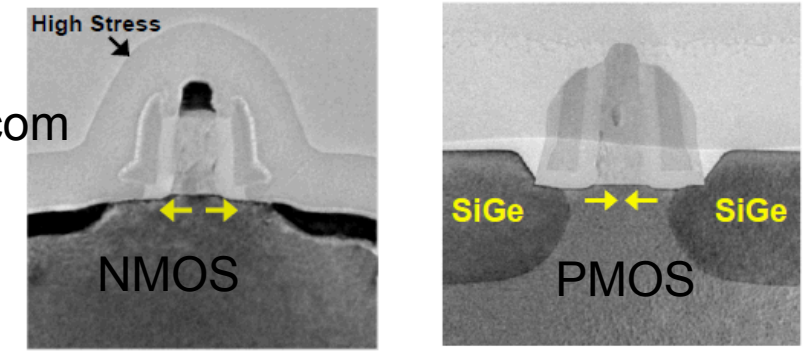

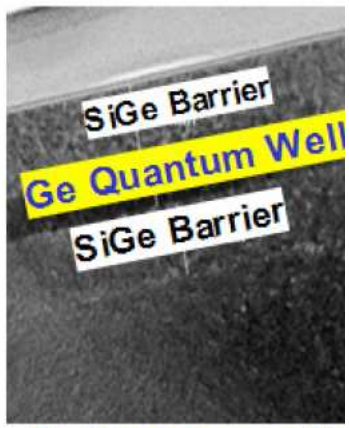

Ge Quantum-well

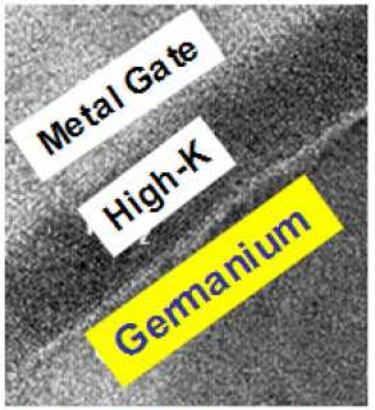

Ge MISFET Transistor

Sources: (1) ESSDERC 2008, (2) www.intel.com/silicon research/R&D pipeline

Ge on Si Detector Development

Compact high speed photodiode

Sandia

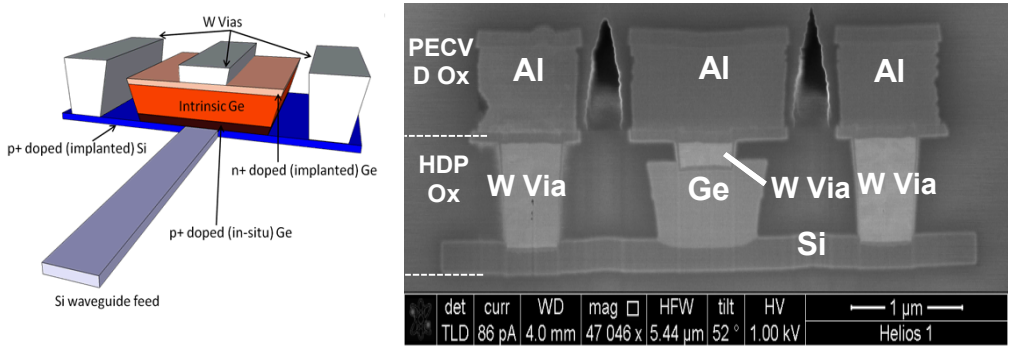

Ge on Si Avalanche Photodiode

Intel, UCSB, UVa

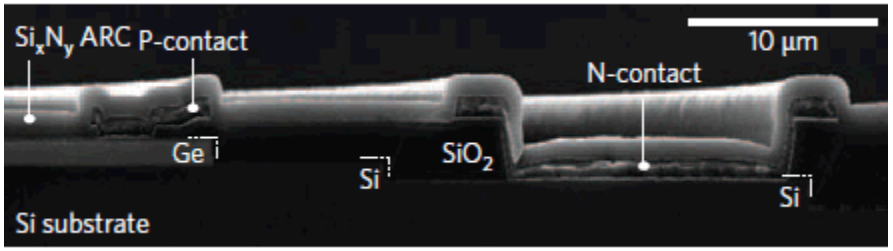

NATURE PHOTONICS | VOL 3 | JANUARY 2009 | www.nature.com/naturephotonics

5 December 2011 / Vol. 19, No. 25 / OPTICS EXPRESS 24897

- Integrated waveguide Ge on Si photodetector demonstrated best in class performance.
- Ge on Si linear mode separate absorption multiplication avalanche photodiode demonstrated 340 GHz gain bandwidth product.
- **Combining new device concepts would enable integrated single photon detection and launch Quantum Si Photonics.**

Separate absorption and charge multiplication APD.

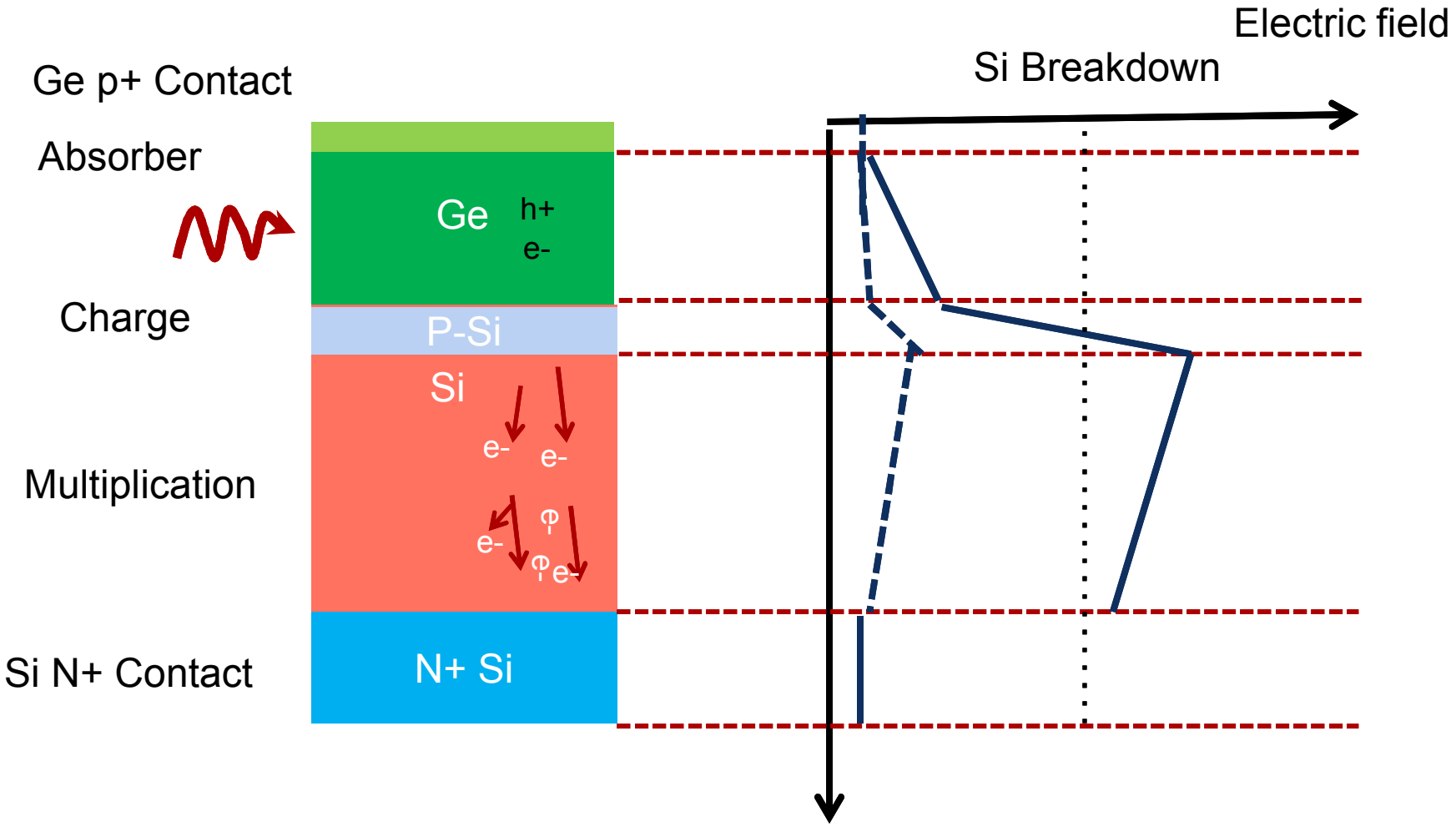

Separate absorption and charge multiplication APD.

Two types of Ge on Si SACM

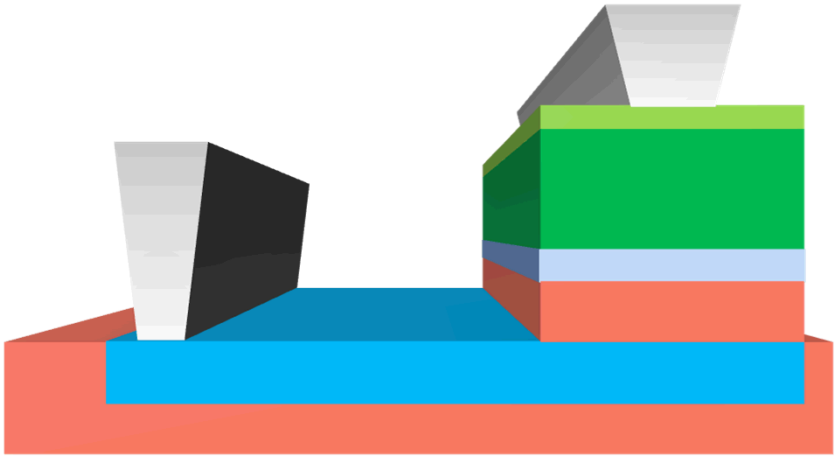

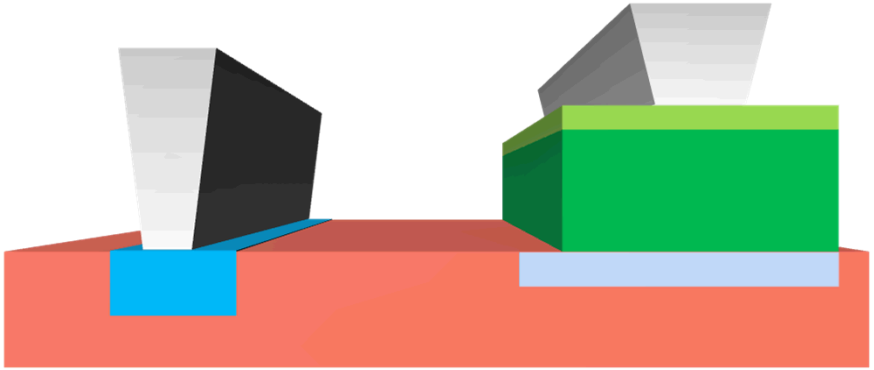

- Selective Si & Ge epi growth.
- In-situ doped charge layer.
- Vertical multiplication.

- Selective Ge epi growth.
- Implanted charge layer
- Lateral multiplication.

Integrated Waveguide Coupled SPD

Sandia National Laboratories

Two coupling types

For vertical and lateral APD

Si end-fired

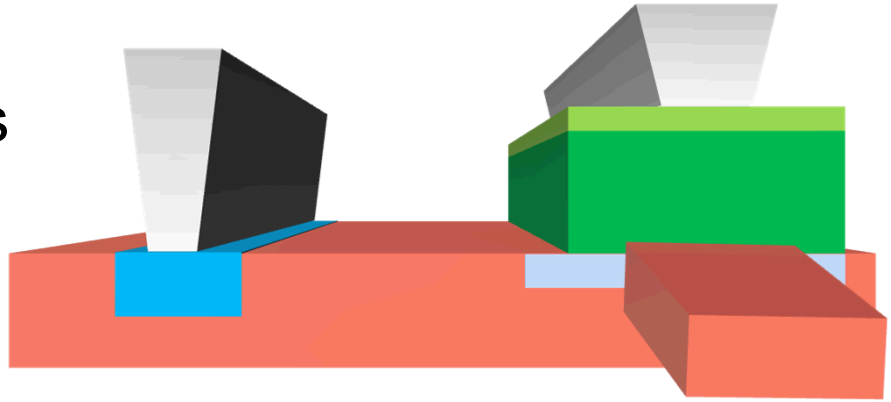

Evanescent coupled

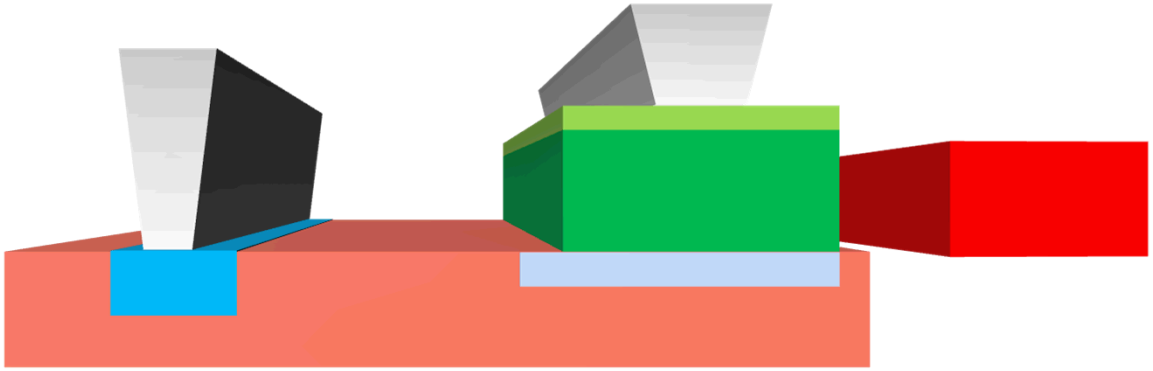

P+ Ge

Ge

Si

P-Si

N+ Si

Nitride

SPAD Test-Chip

- SPD test –chip
- 24 wafers
- Lateral and vertical designs
- Si and nitride waveguide coupled
- 10,000 SPD device variations.
- Automated testing required

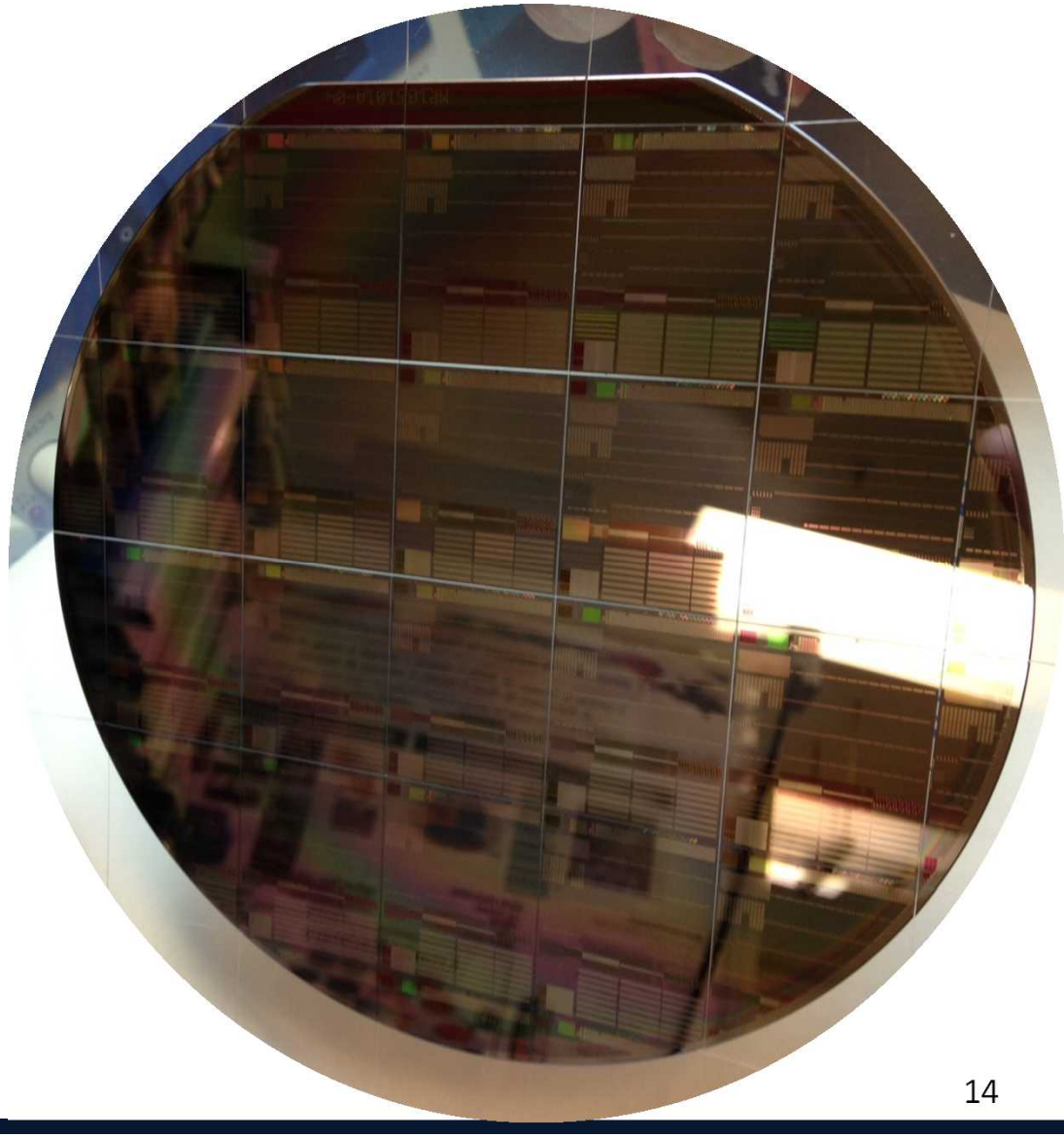

Integrated lateral APD results

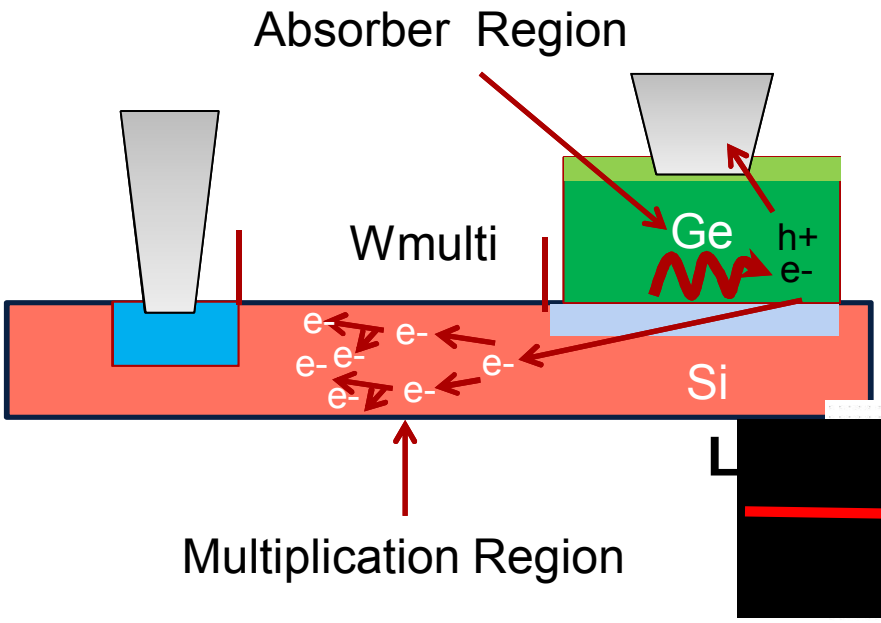

Lateral APD in X-section

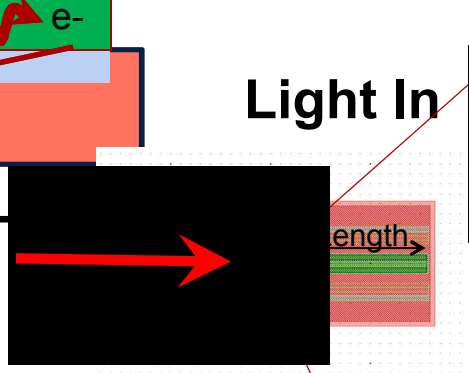

Top down view

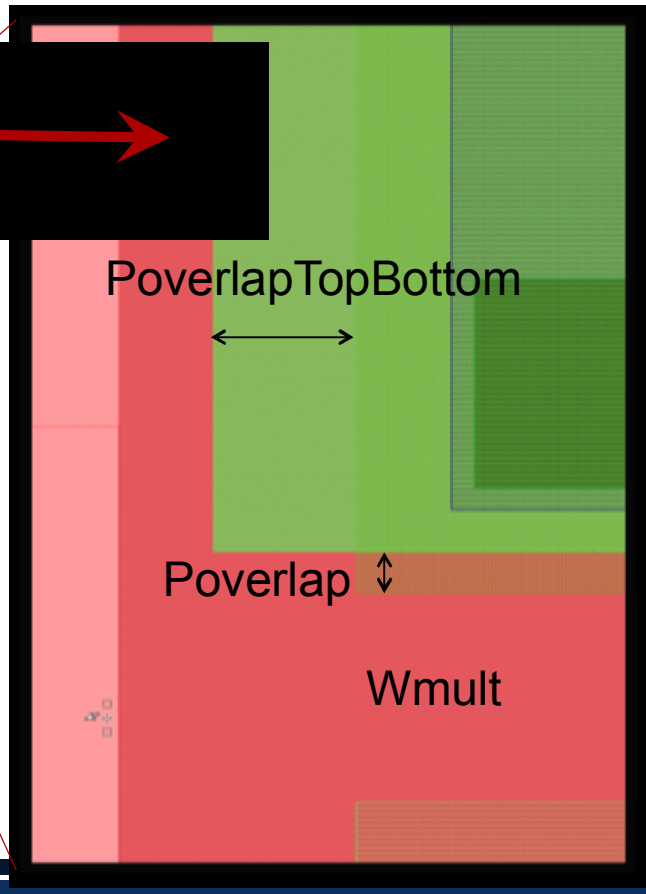

Top down view shows variation of multiplication Width and p-Charge layer overlap.

Together with implant doses we vary these parameters.

Die Map: Yield & Calibration

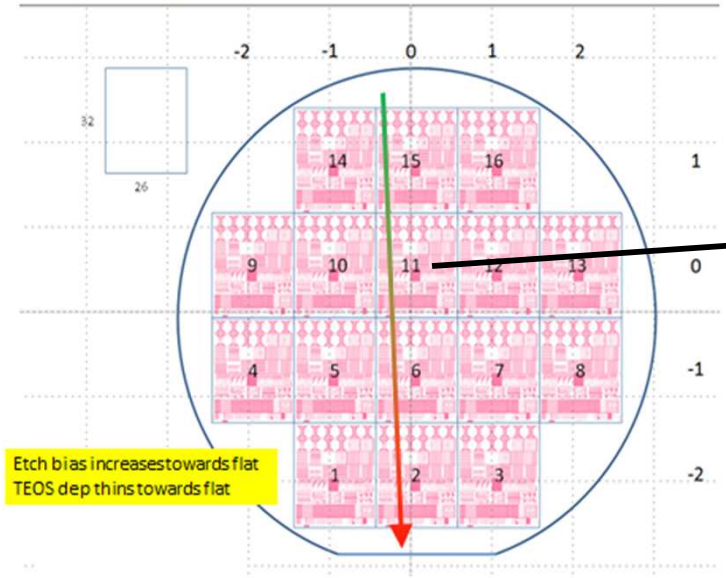

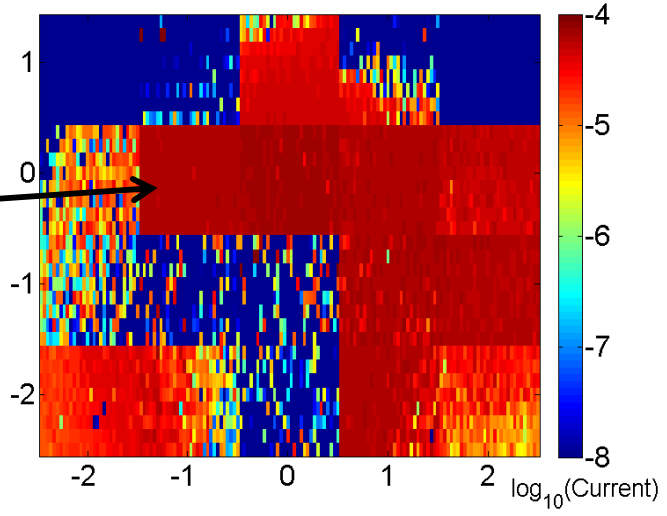

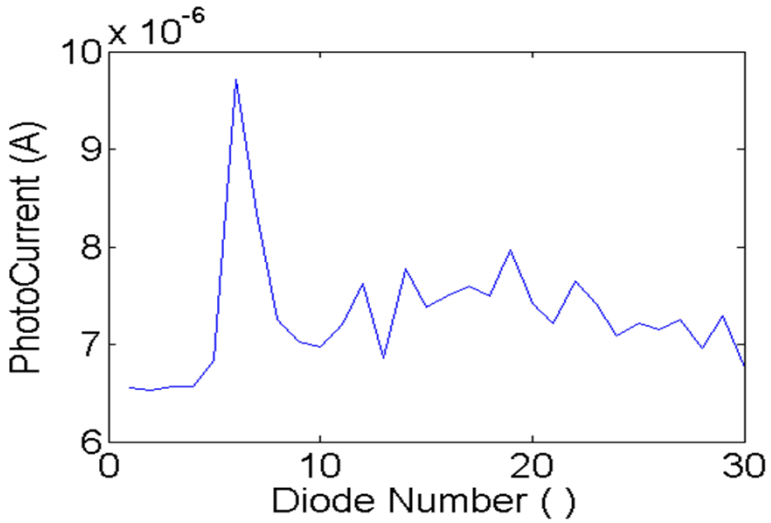

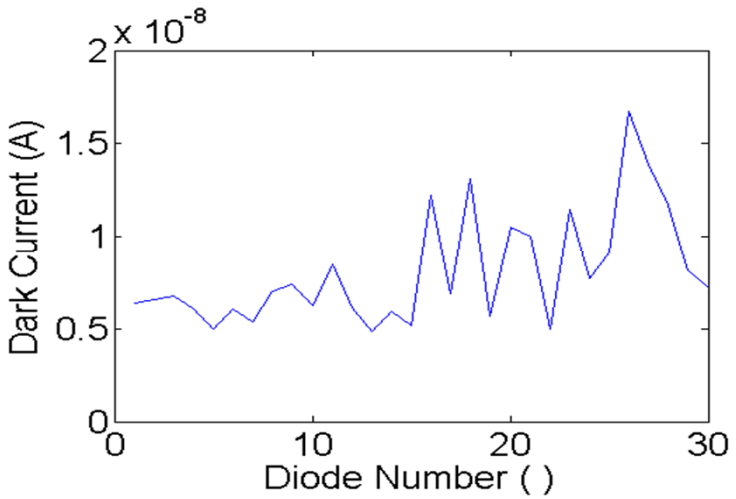

Experimental illumination condition

- Done with 100 uW incident on grating coupler
- Wavelength set to 1540 nm.
- Estimate ~ 8 uA photocurrent in equivalent PIN structure.
- Fiber array position optimized fo each measurement.

- 1000 APD measurements
- APD Gain approximated by

$$M = (i_{light} - i_{dark})/8uA$$

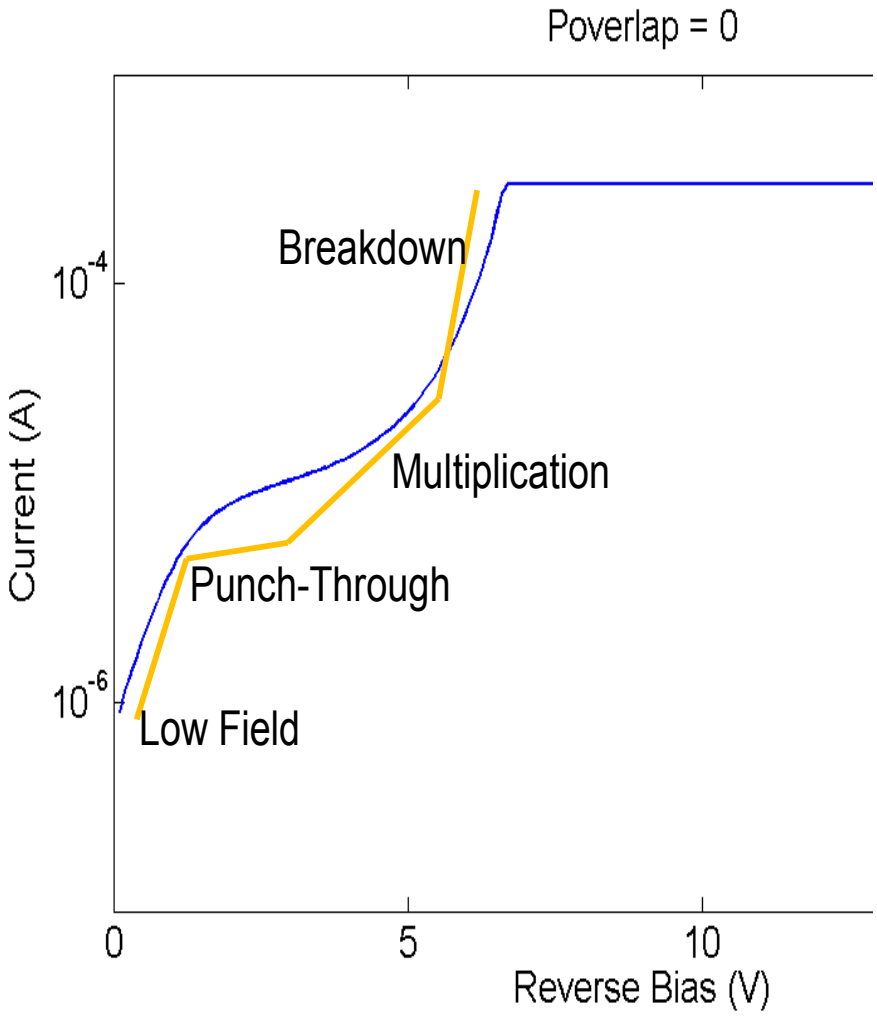

Linear mode APD measurements

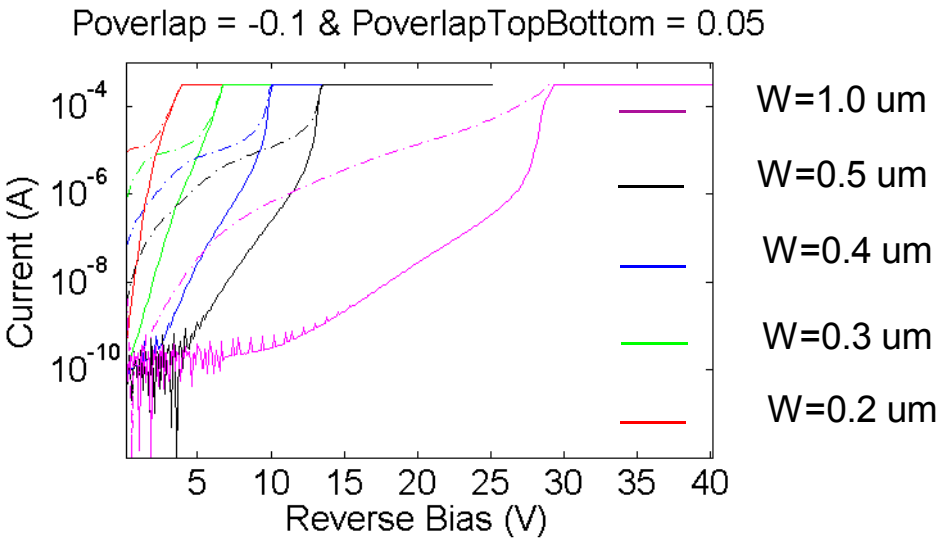

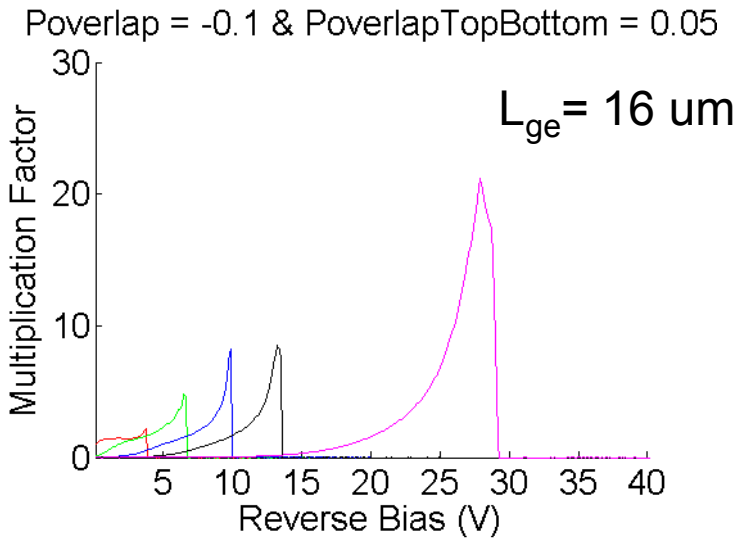

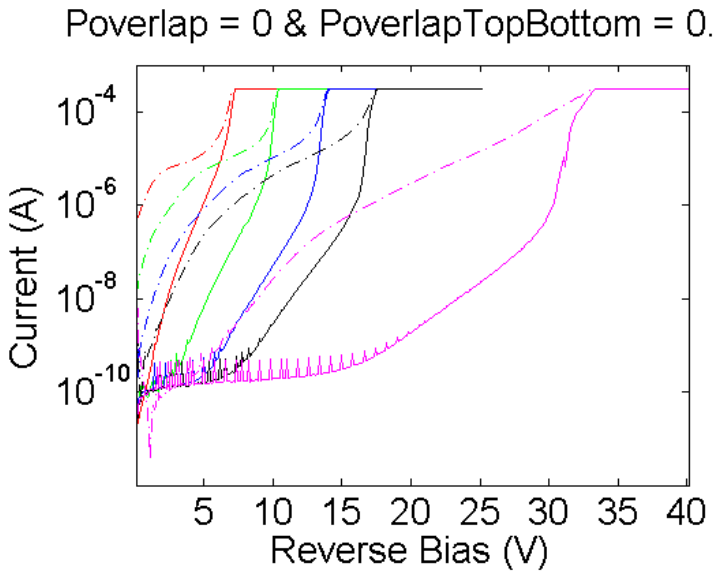

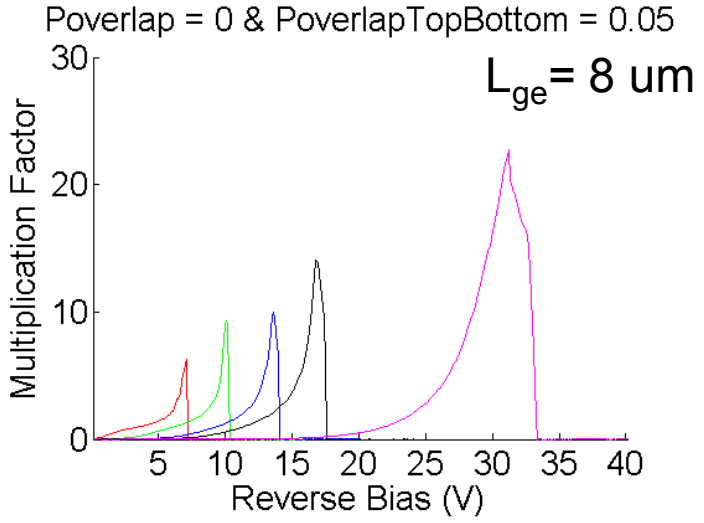

Summary of Linear mode APD's

- Waveguide coupled linear mode APD's show multiplication gain exceeding M> 20.
- Compact nature of device ~16 μm^2 gives
  - Higher strain and responsivity for wavelengths > 1550 nm.
  - Low dark current.
  - Low capacitance.
- High speed testing underway for determination of gain-bandwidth product.
- Useful in low noise receiver application.

Geiger mode operation enables single photon detection.

Geiger mode APD (SPD)

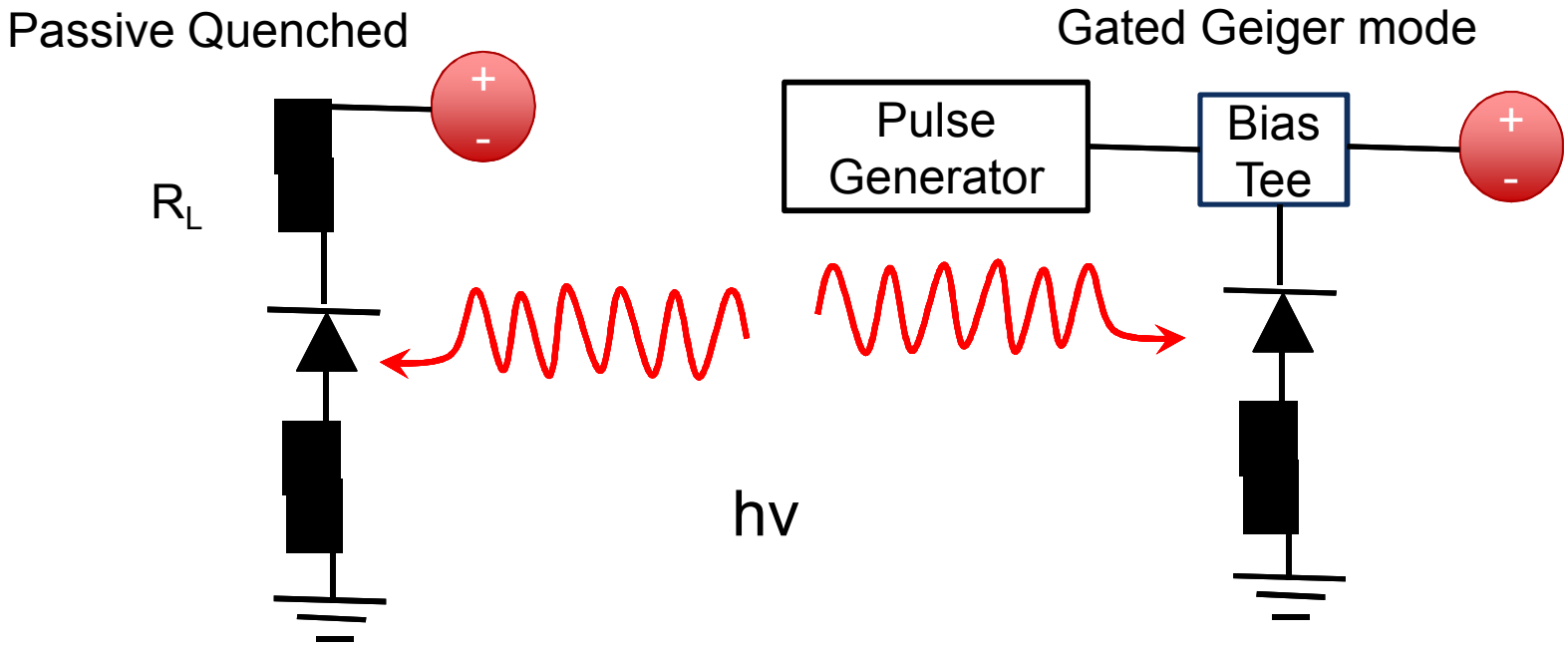

- Two types of Geiger mode operation
  - Passively quenched
    - External quench resistor R_l
  - Gated Geiger mode
    - Electronic gate and photon pulse are timed with variable delay.

Initial Passive Quenched GM

Sandia National Laboratories

Low Dark Count Detection

- Our Selective Ge on Si gives low defect count at Si/Ge interface.
- Leverages our Ge on Si process:
- Apply analytic tools to reduce defects at interface.
  - Very low threading dislocations.
- Field engineering and Vertical designs reduce dark current levels.

Our Ge device

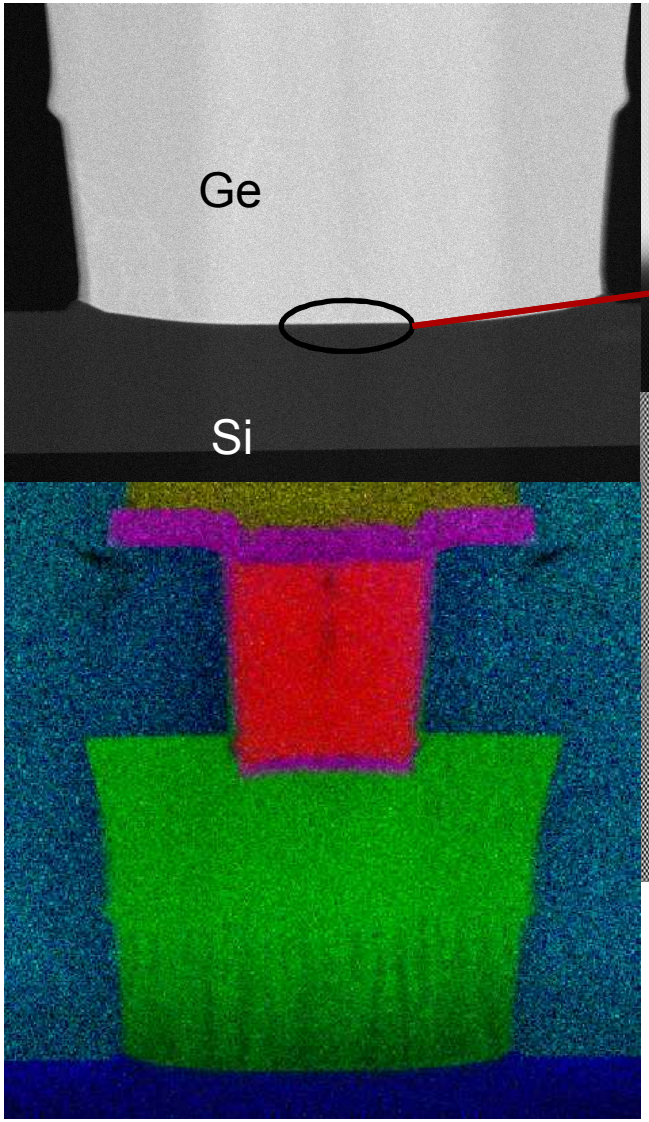

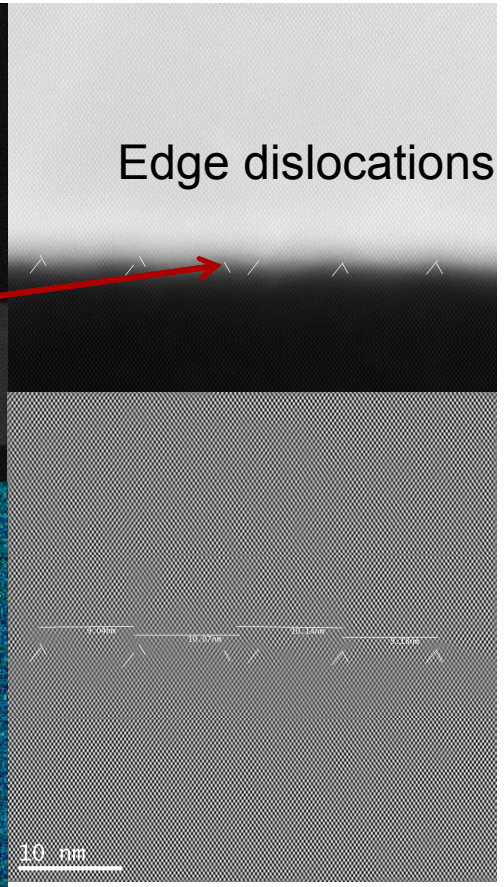

Outline

- Highlight early progress in 3 areas:
  - Integrated Single Photon Avalanche Detector (SPAD)
  - Heterogeneous integration of III-V laser source on Si Photonics substrate.
  - Complex integrated quantum optoelectronic circuits

InP Lasers & PIC Platform

1550 nm wavelength

- State-of-the-art discrete photonic component performance from a single chip
- DBR lasers, EAMs, WGs, High-gain SOAs, High-Psat SOAs, Evanescent PD.

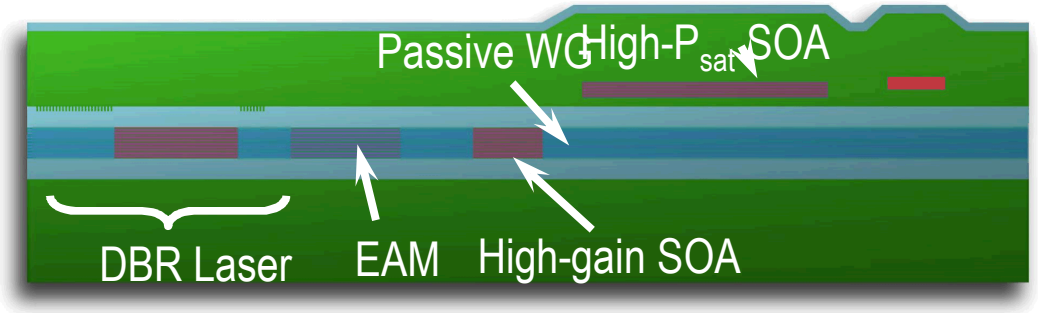

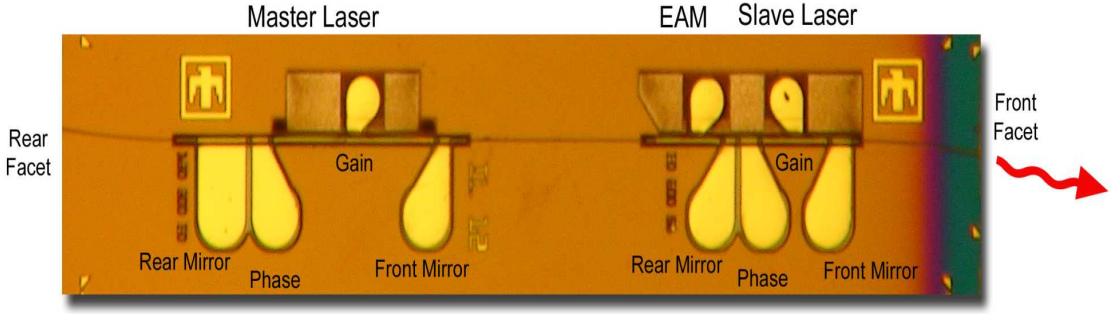

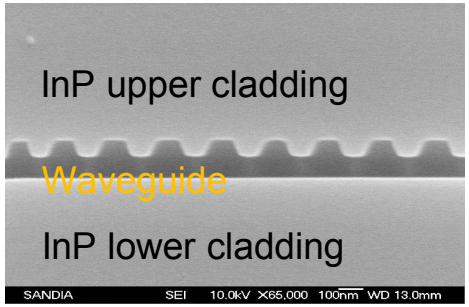

InP to Si Waveguide Grating Coupling

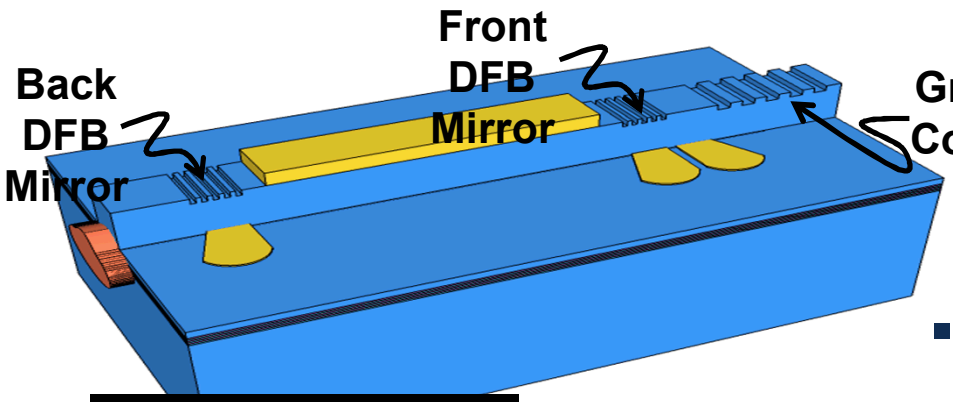

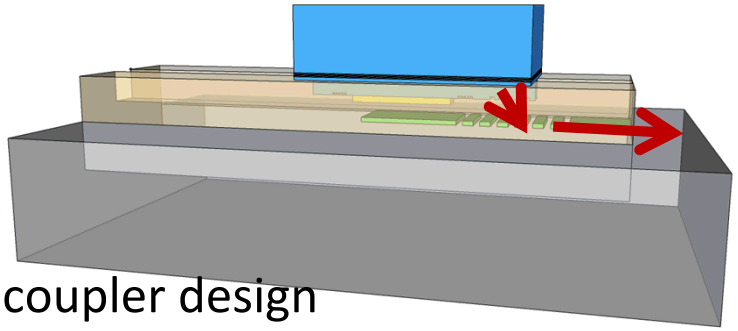

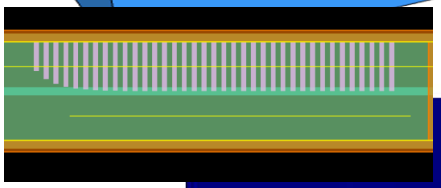

InP coupler

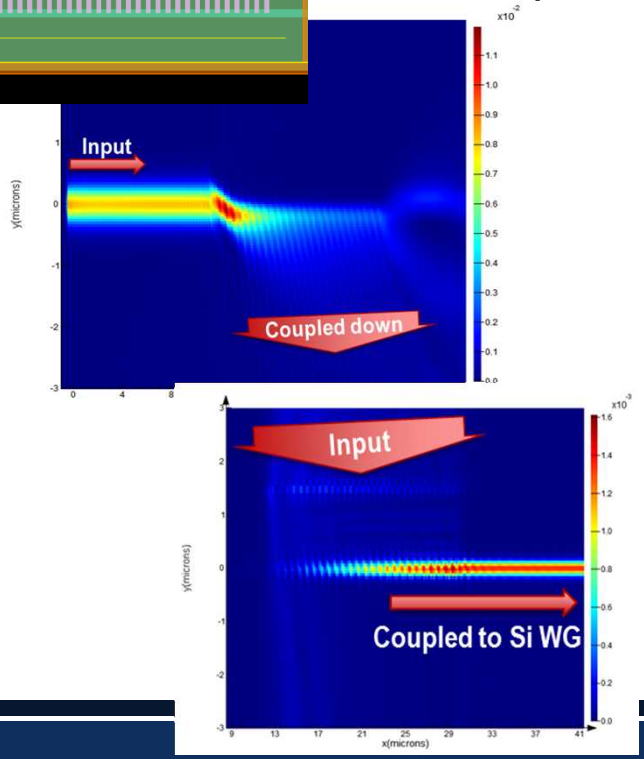

- InP coupler design
  - > 52% power coupled down
  - < 5° farfield angle
- Si coupler design
  - Input the InP coupler mode field
  - ~30% is coupled into the Si WG
- Next step
  - Combine InP and Si simulations
    - Will allow more design optimization

Grating Couplers

- InP-to-Si grating couplers
  - 2nd order grated designed to have light exit chip vertically
  - Allows for optimized mode shape for larger alignment tolerances
    - > 1 µm
  - Avoids flip chip integration
    - Light exits InP chip through the substrate
    - Couples into the top of the Si chip
    - Top contacts on both chips

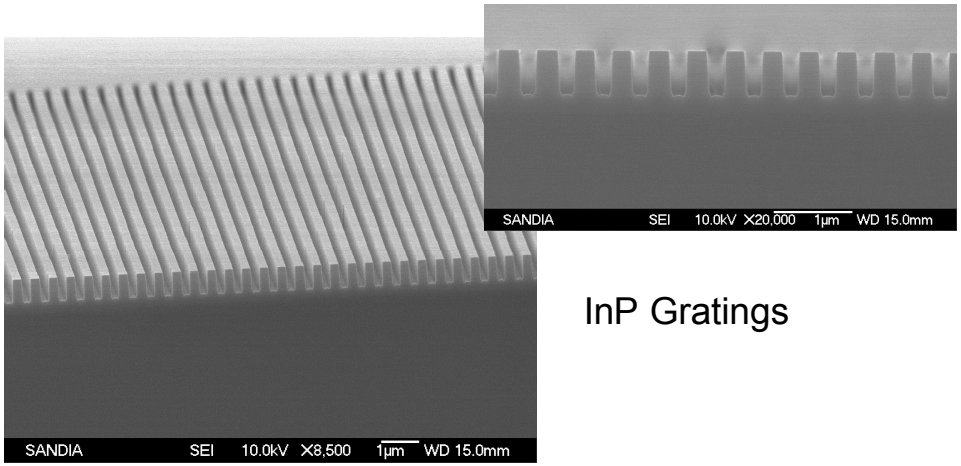

InP Gratings

- Process development
  - Developing InP ICP etch process for high aspect ratio gratings
    - ~500 nm pitch
    - Targeting 1 µm depth
  - InP gratings defined by ebeam lithography
    - Allows for many different designs on a single wafer
  - Complementary Si and InP masks are currently being laid out
    - Access alignment tolerances
    - Demonstrate laser to Si waveguide coupling
  - Si gratings will leverage previous work for fiber coupler

Heterogeneous Kinematic Mounting

- Precision kinematic mounting for general integration of devices with Si Photonics substrate.
- Nitride posts mate with Si pyramids
- FC 150 bonder used to mate parts

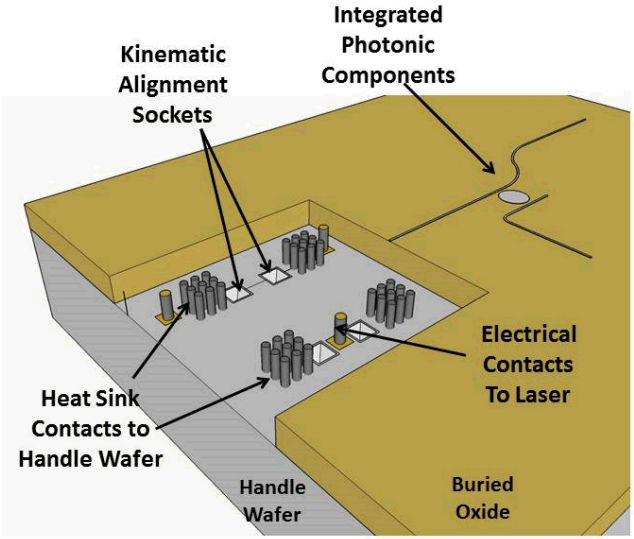

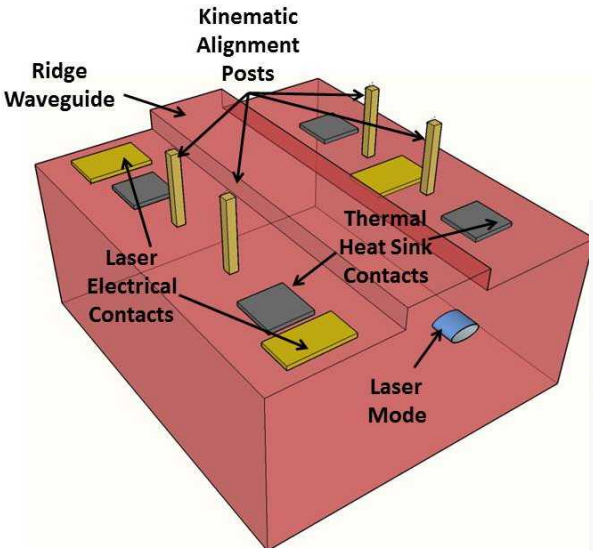

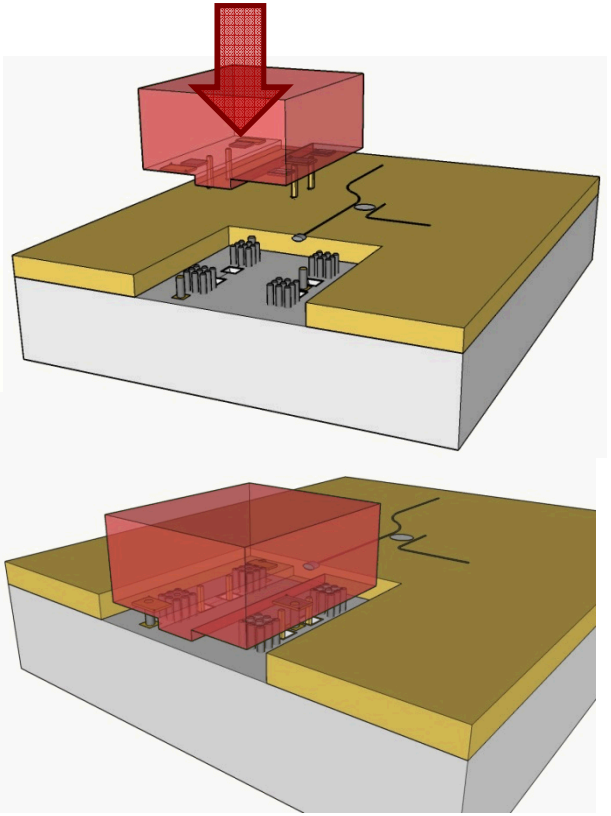

Precision alignment

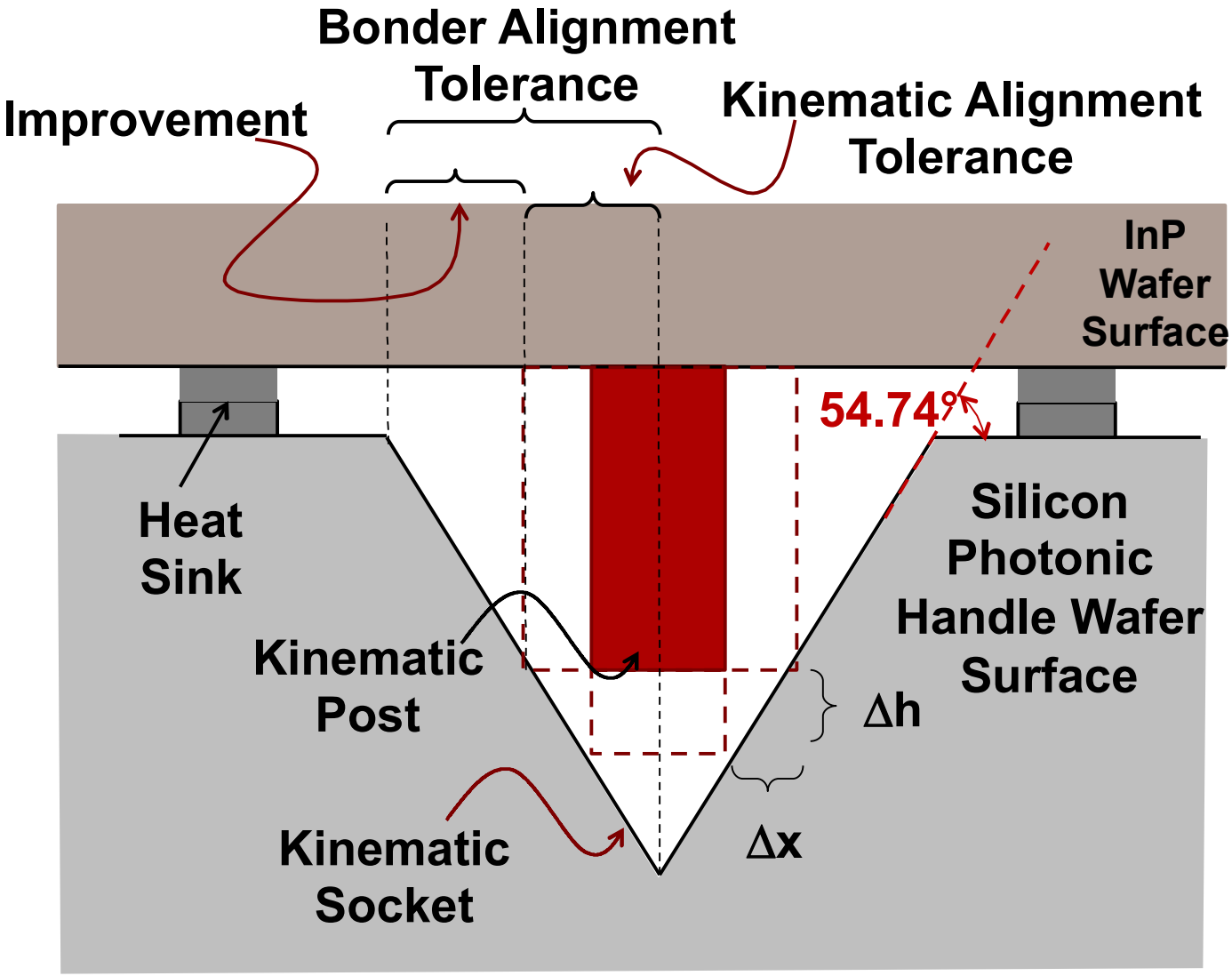

Socket & Post Process flow

Sandia National Laboratories

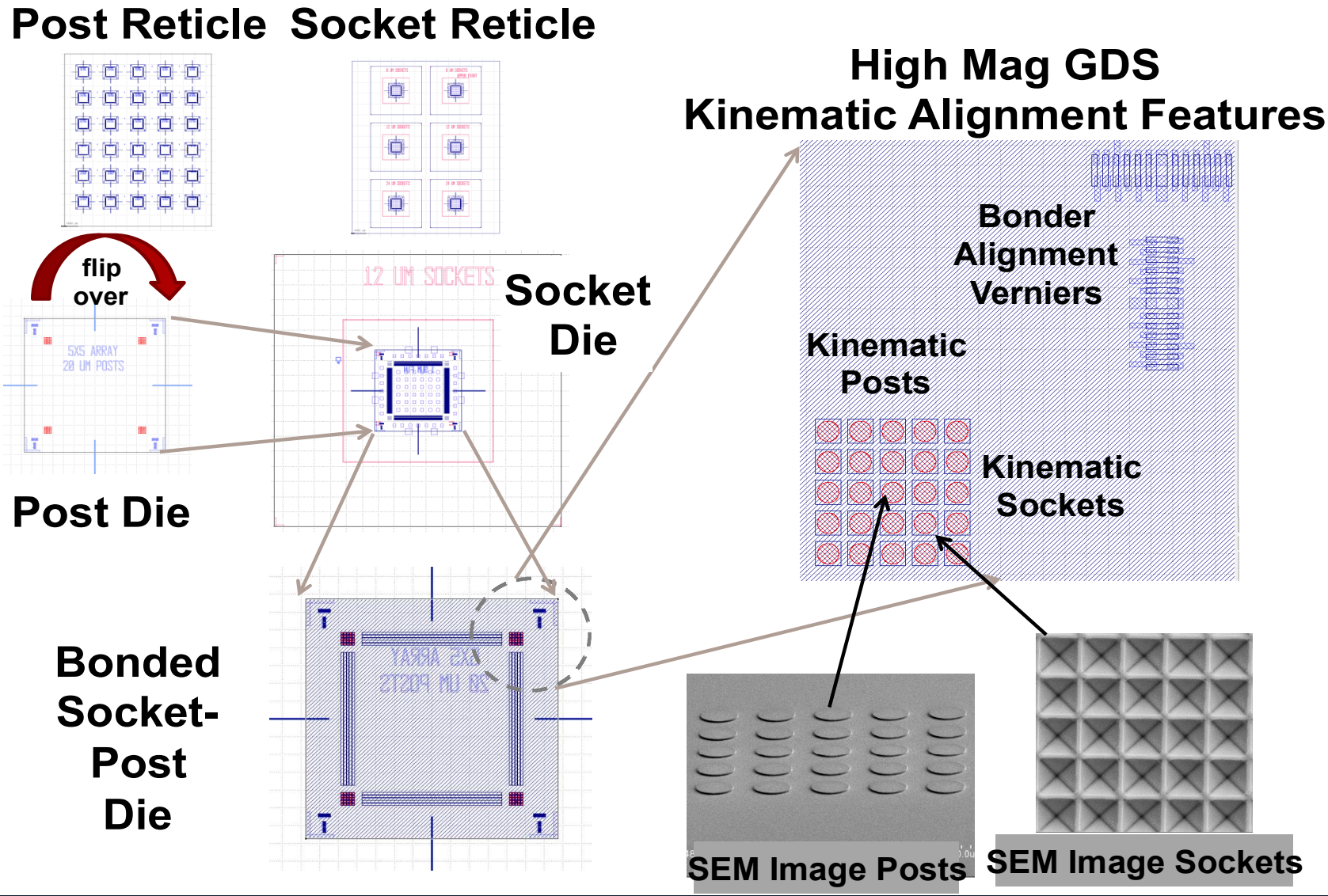

Heterogeneous Integration

Sandia National Laboratories

- InP chip with grating coupling to Si Photonics carrier designed and currently in process.
- Developed general sub-micron alignment and bonding of full processed devices onto Si substrate.
- Socket and post test chip fabricated and currently under test.
- Use cases:
  - III-V actives with Si
  - Fiber alignment.
  - Non-linear crystals not compatible with CMOS processing.
  - Etc….

Outline

- Highlight early progress in 3 areas:
  - Integrated Single Photon Avalanche Detector (SPAD)
  - Heterogeneous integration of III-V laser source on Si Photonics substrate.
  - Complex integrated quantum optoelectronic circuits

Quantum Photonics: CVQKD Tx/Rx

- What do you do with these building blocks?
- Implement a CV-QKD transceiver on-chip.
  - Chip-scale version of bench top design.
  - P. Jouguet, S. Kunz-Jacques, A. Leverrier, P. Grangier, and E. Diamanti. Experimental demonstration of long-distance continuous-variable quantum key distribution. Nature Photonics, 7(5):378–381, 2013.
- Explore simple quantum coherent feedback and control circuit.
  - H. Mabuchi. Coherent-feedback quantum control with a dynamic compensator. Physical Review A, 78(3):032323, 2008.

CV-QKD Tx/Rx

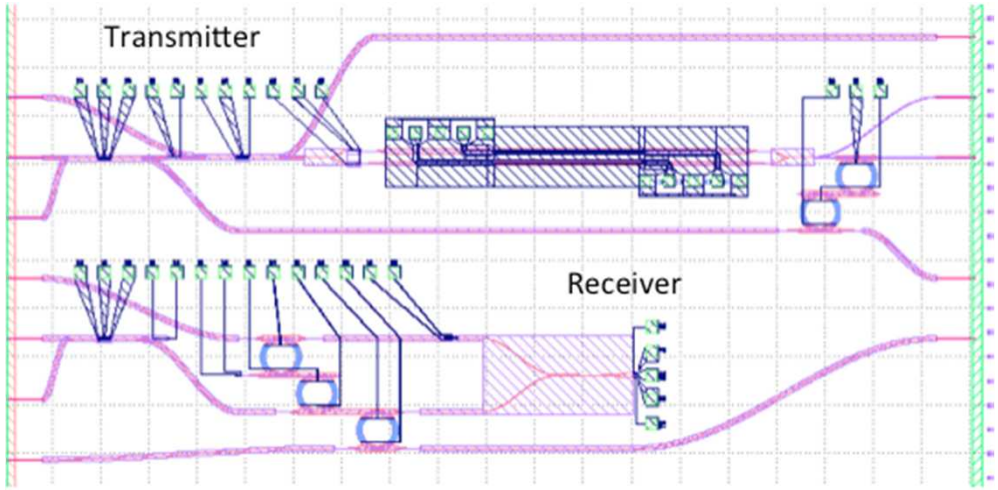

Coherent Quantum Feedback & Control

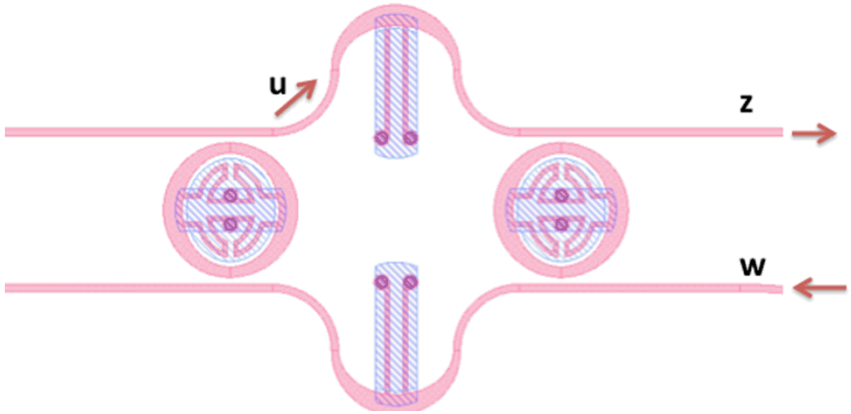

Bench-top CV-QKD link

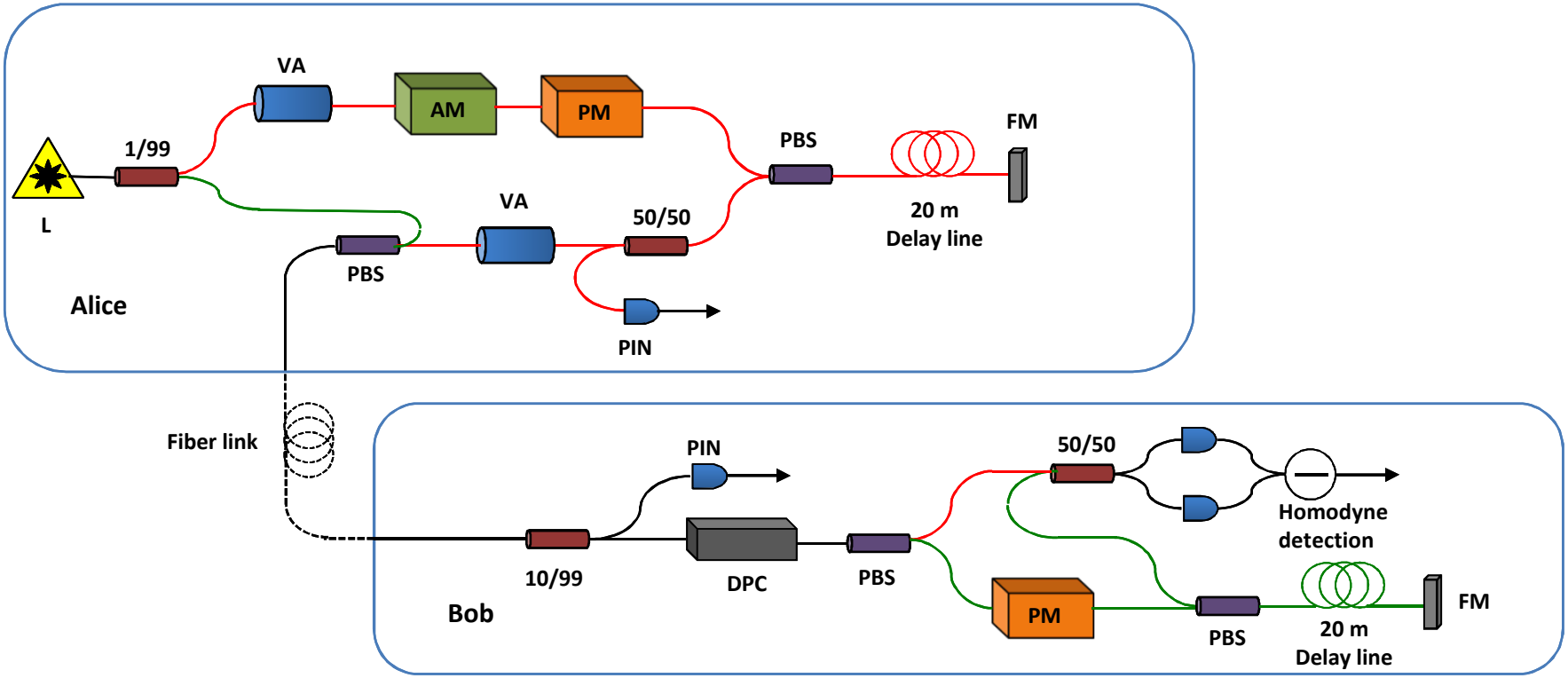

Current State of the Art CV-QKD link using coherent state source

P. Jouguet, S. Kunz-Jacques, A. Leverrier, P. Grangier, and E. Diamanti. Experimental demonstration of long-distance continuous-variable quantum key distribution. Nature Photonics, 7(5):378–381, 2013.

Heterodyned Chip-scale CV-QKD

Designed by C. DeRose, D. Soh, M. Sarovar

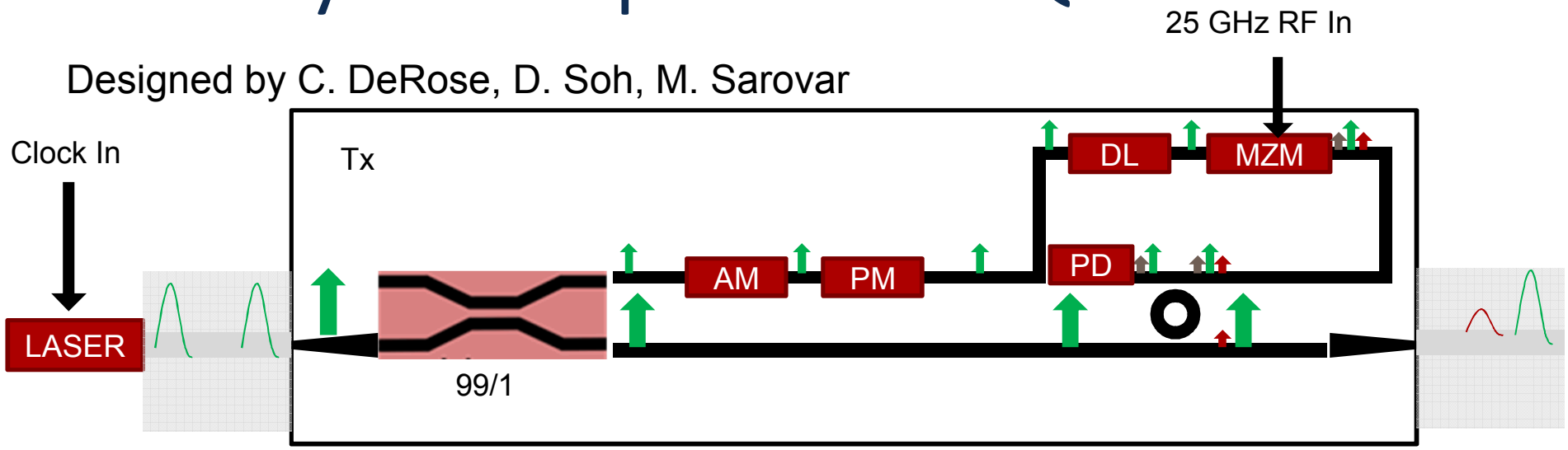

- 1 ns pulse
- 1 MHz rate
- SMF-28 coupled
- Requirement for filter suppression?

AM – amplitude modulator, PM – phase modulator, DL – 2 ns delay line, MZM – Mach-Zehnder modulator, PD - photodiode

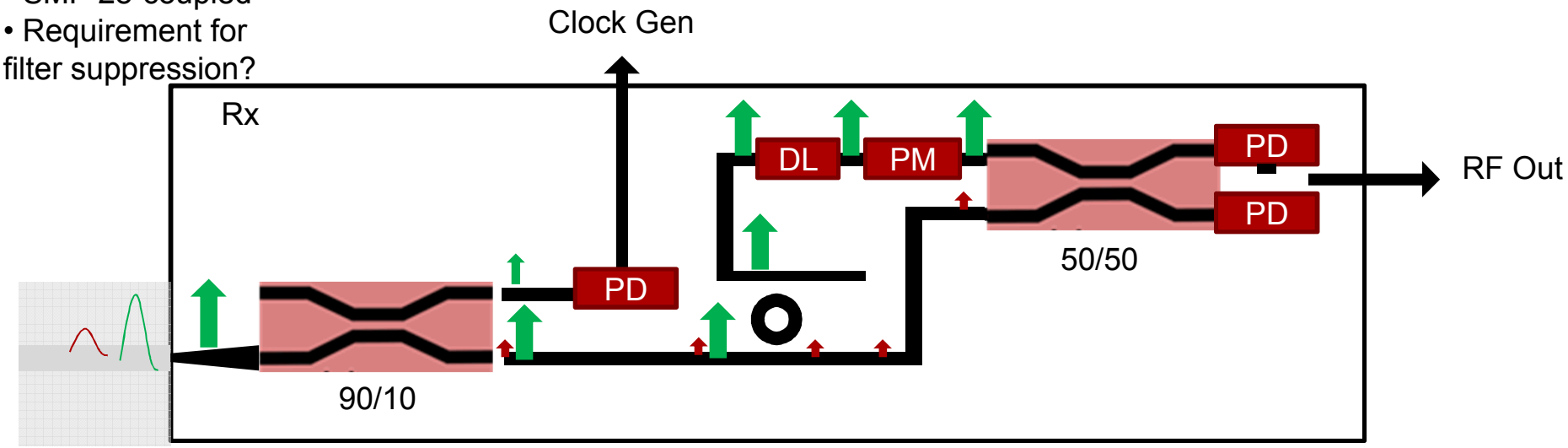

Summary

- We are at the early stages of development of a chip-scale quantum photonics platform.
- We are developing
  - Single Photon Detectors based on Ge on Si Gm-APD's.
  - An integrated InP laser source onto Si Photonics substrate.
  - A heterogeneous integration approach that will enable general integration of complex devices and new materials onto active Si substrate.
  - Complex quantum photonic circuits for exploration of new ideas.
  - An electronic and optical packaging scheme (not discussed).
- We are leveraging multiple efforts
  - III-V optoelectronics development
  - Si Photonics development
  - RF/optoelectronics/CMOS/pakaging

Sandia National Laboratories

Thank You !

Sandia National Laboratories

BACKUP

Bench-top CV-QKD link

Recent Publication using
COTS fiber optics.

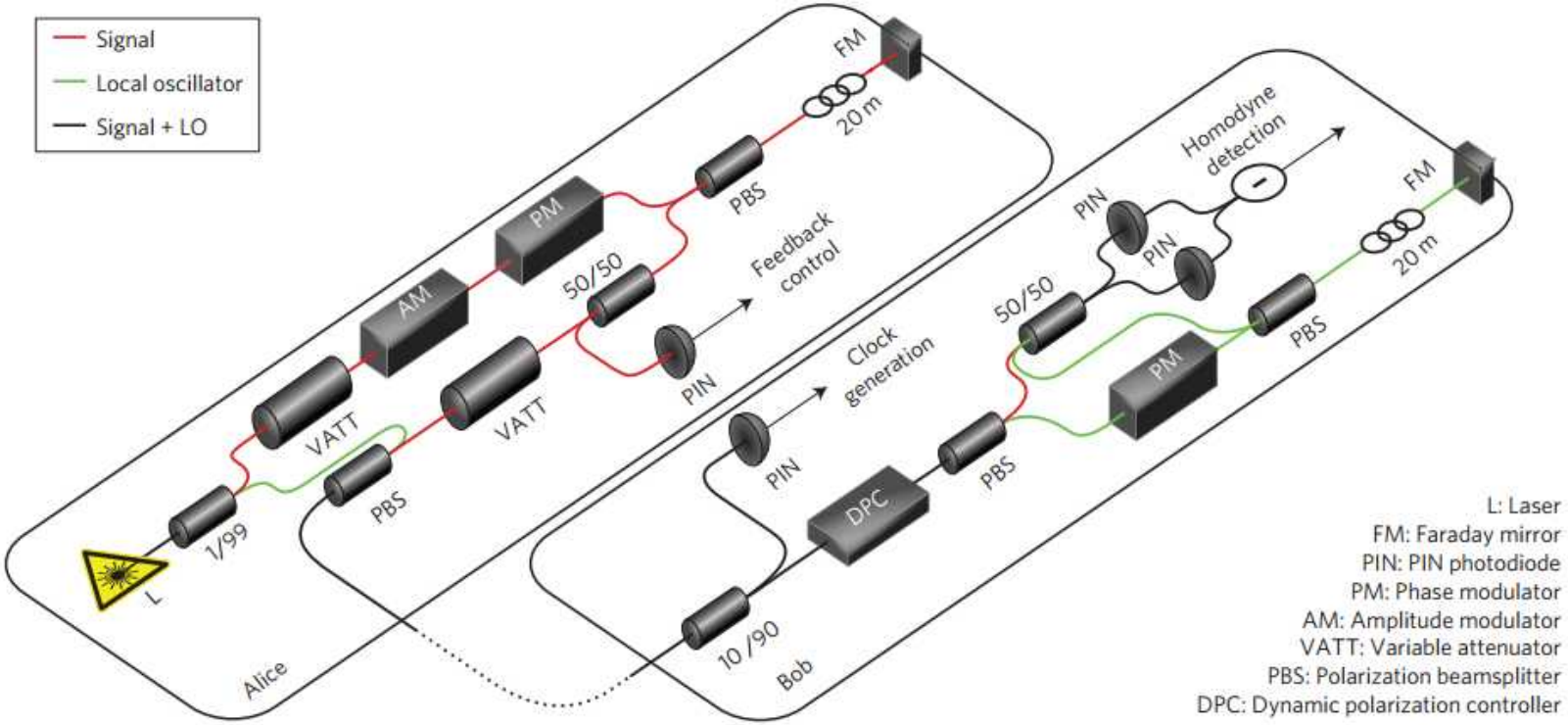

P. Jouguet, S. Kunz-Jacques, A. Leverrier, P. Grangier, and E. Diamanti. Experimental demonstration of long-distance continuous-variable quantum key distribution. Nature Photonics, 7(5):378–381, 2013.

CV-QKD fiber test bed

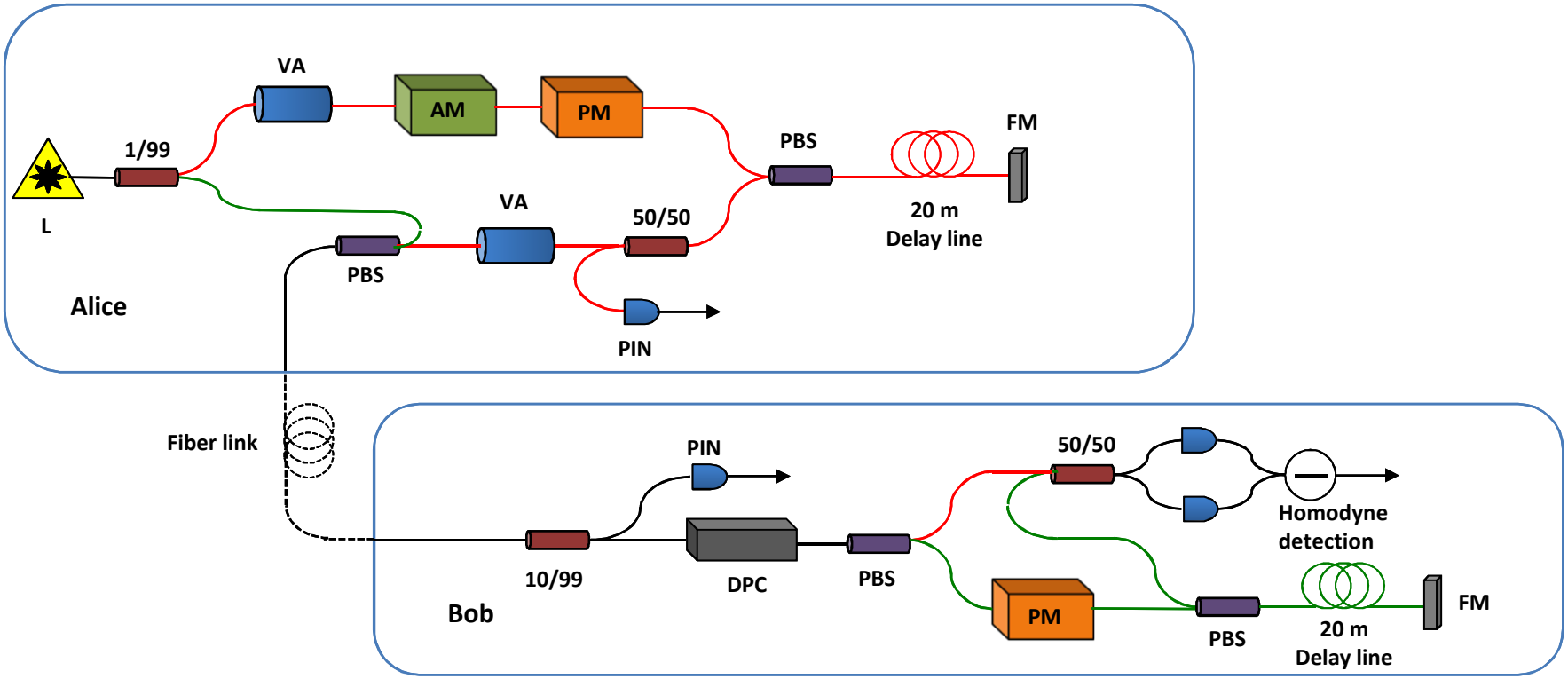

- Coherent source is a CW laser.
- Bob randomly chooses measuring quadrature by phase-shifting the local oscillator.
- Eve randomly chooses measuring quadrature by phase-shifting the local oscillator.
- Eve's quadrature measurement squeezes the light (reduces the noise) in measured quadrature, but greatly increases the noise in the other quadrature (uncertainty principle).
- Local oscillator is temporally multiplexed and transmitted in the same fiber.

InP to Si Waveguide Grating Coupling

Sandia National Laboratories

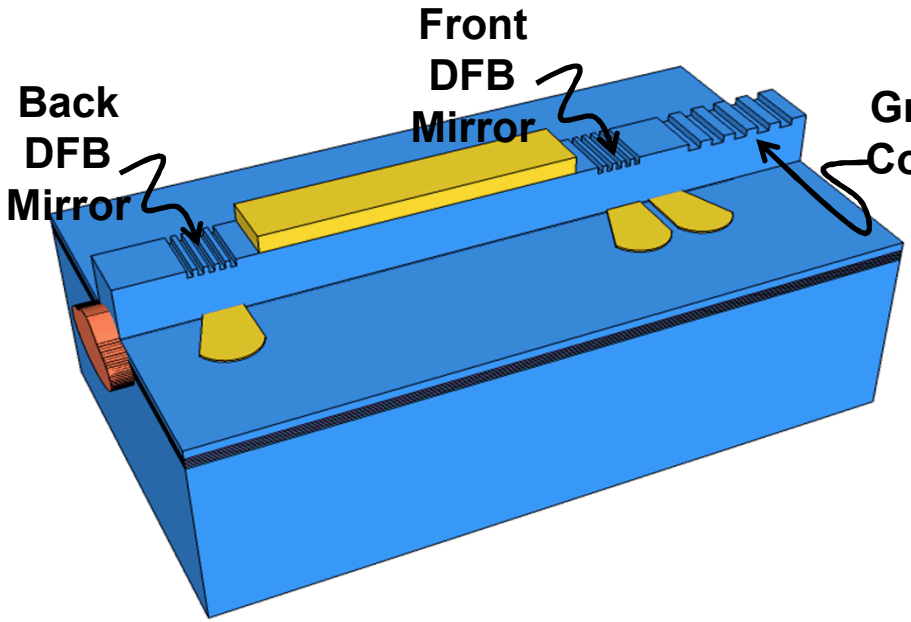

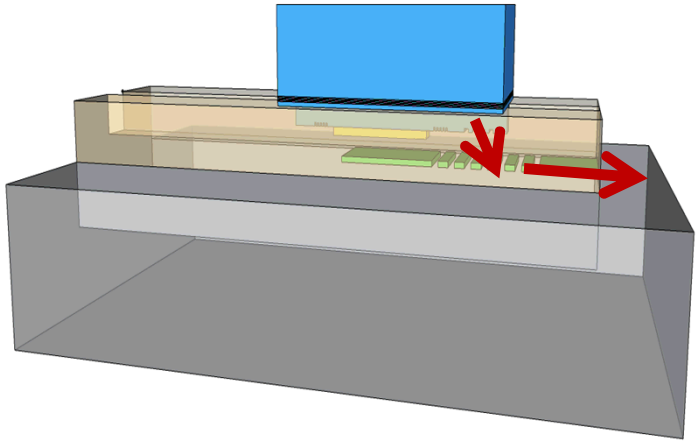

InP-to Si Grating Simulations

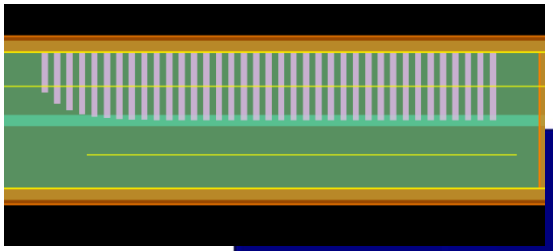

InP coupler

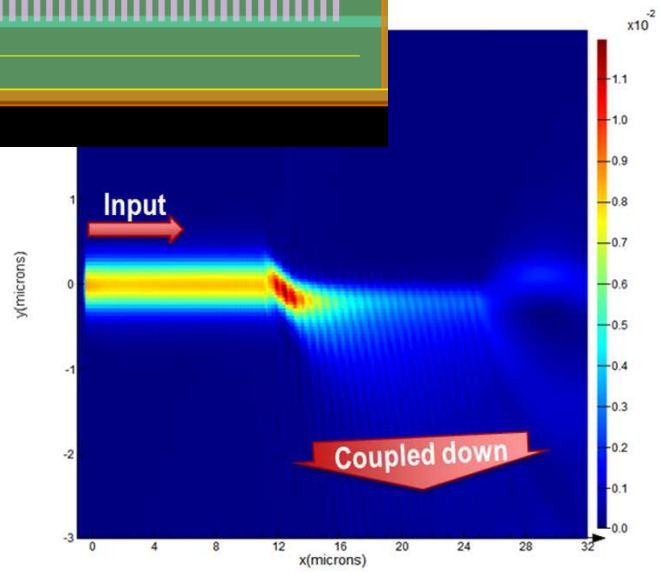

- InP coupler design
  - > 52% power coupled down
  - < 5° farfield angle
- Si coupler design
  - Input the InP coupler mode field
  - ~30% is coupled into the Si WG
- Next step
  - Combine InP and Si simulations
    - Will allow more design optimization

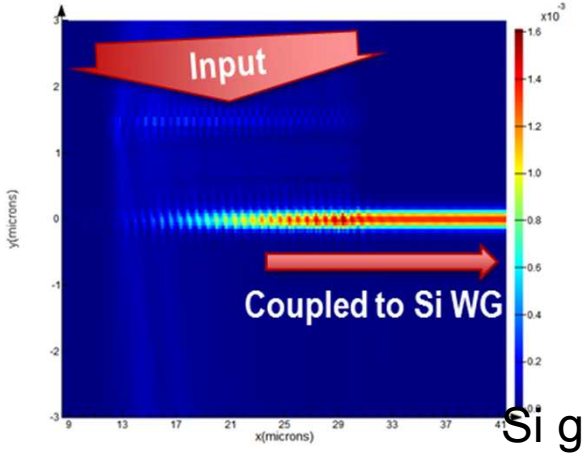

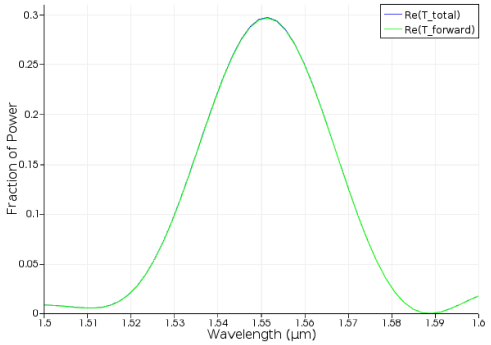

Si grating coupler

Device Simulations

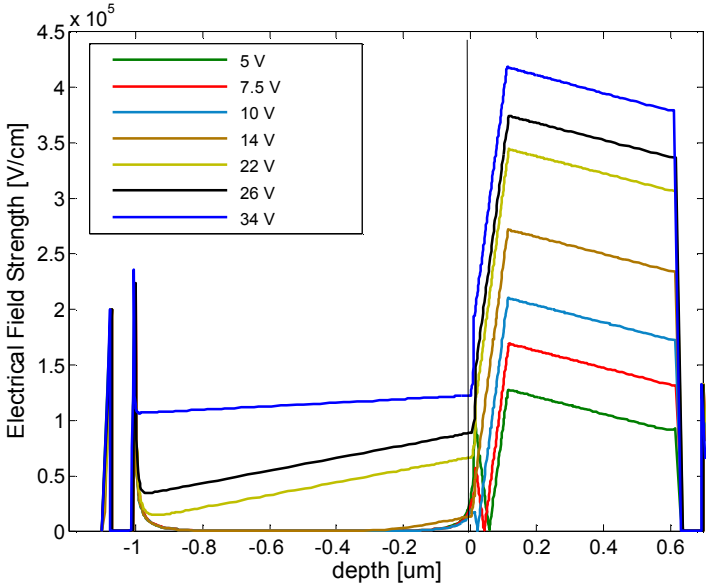

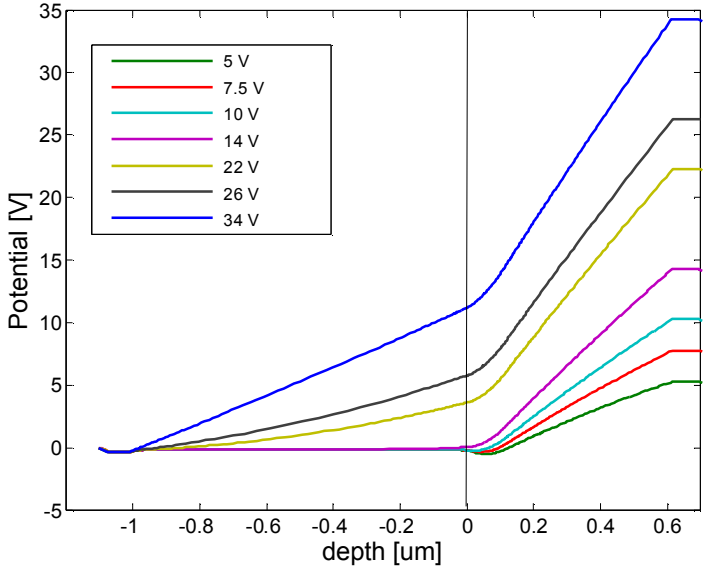

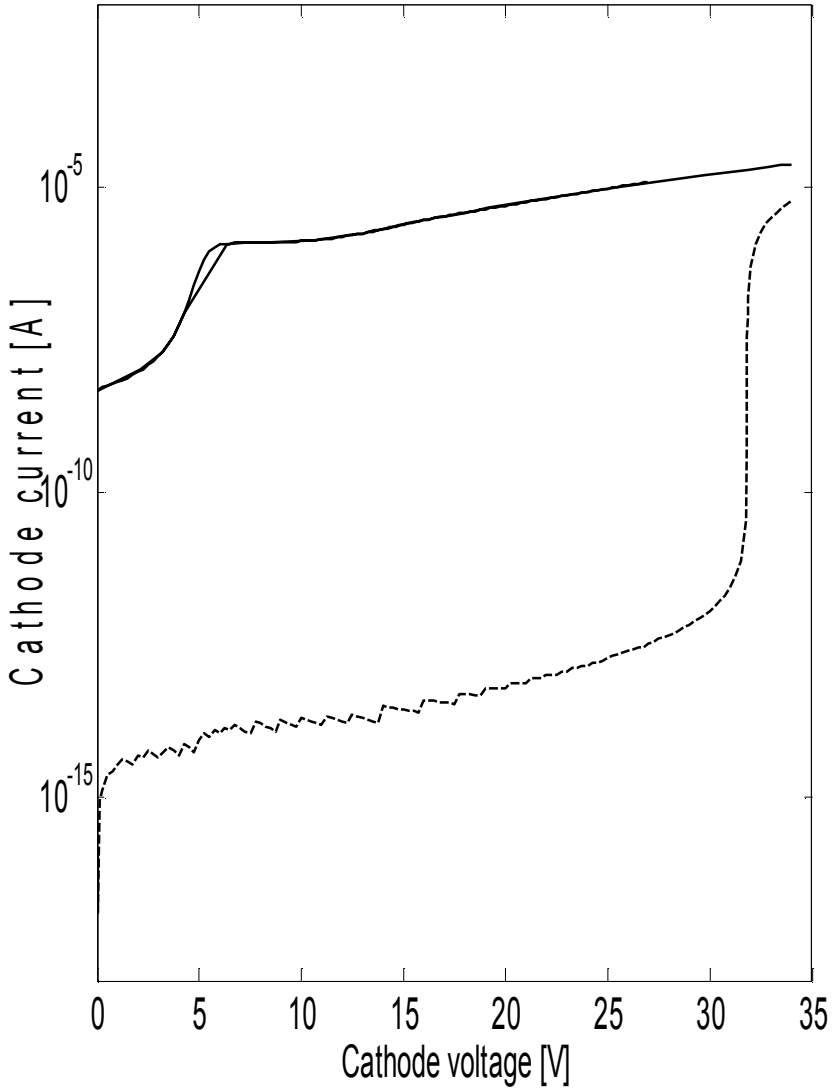

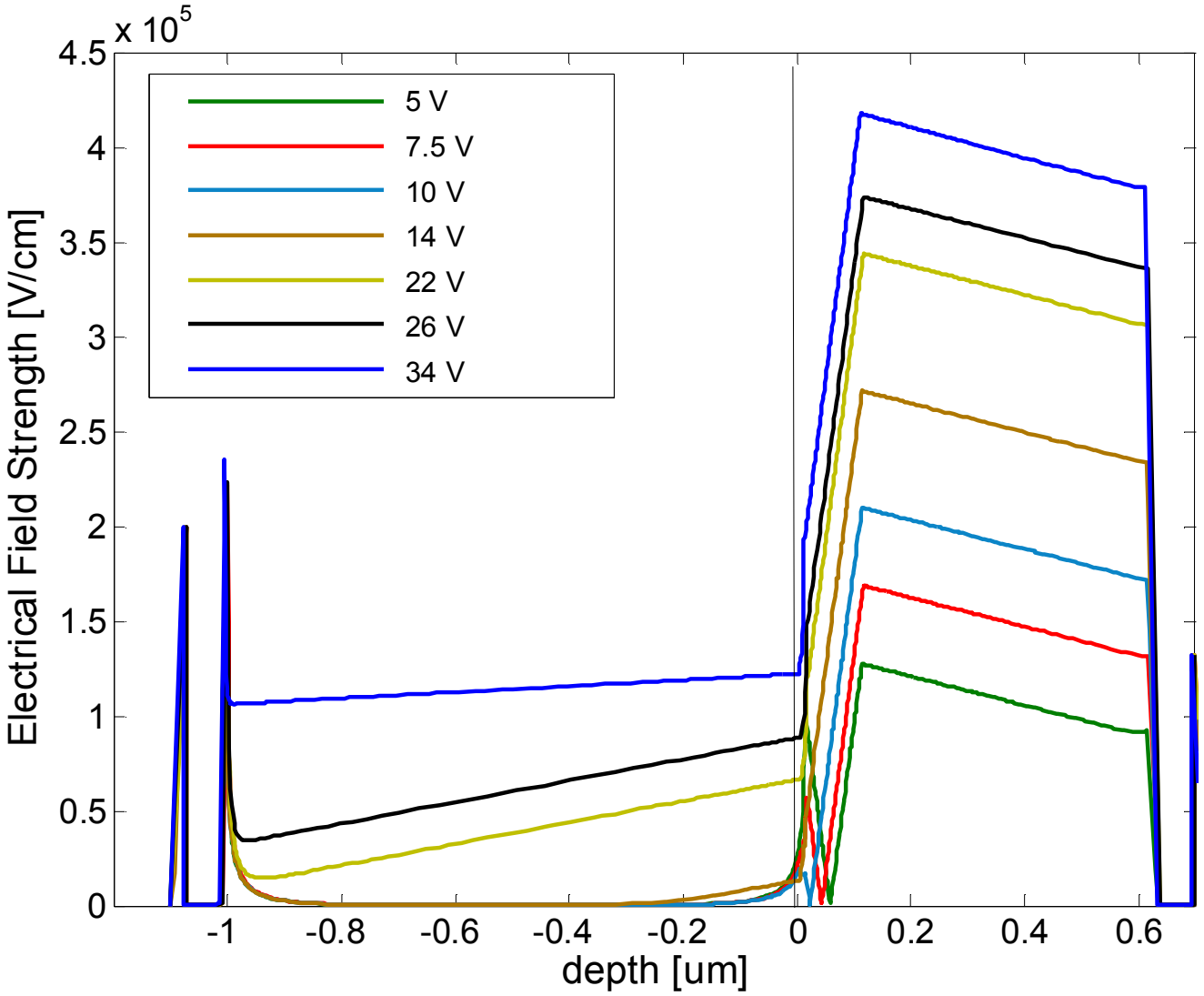
x 10^5
4.5
4
3.5
3
2.5
2
1.5
1
0.5
0
Electrical Field Strength [V/cm]
5 V
7.5 V
10 V
14 V
22 V
26 V
34 V
-1
-0.8
-0.6
-0.4
-0.2
0
0.2
0.4
0.6
depth [um]

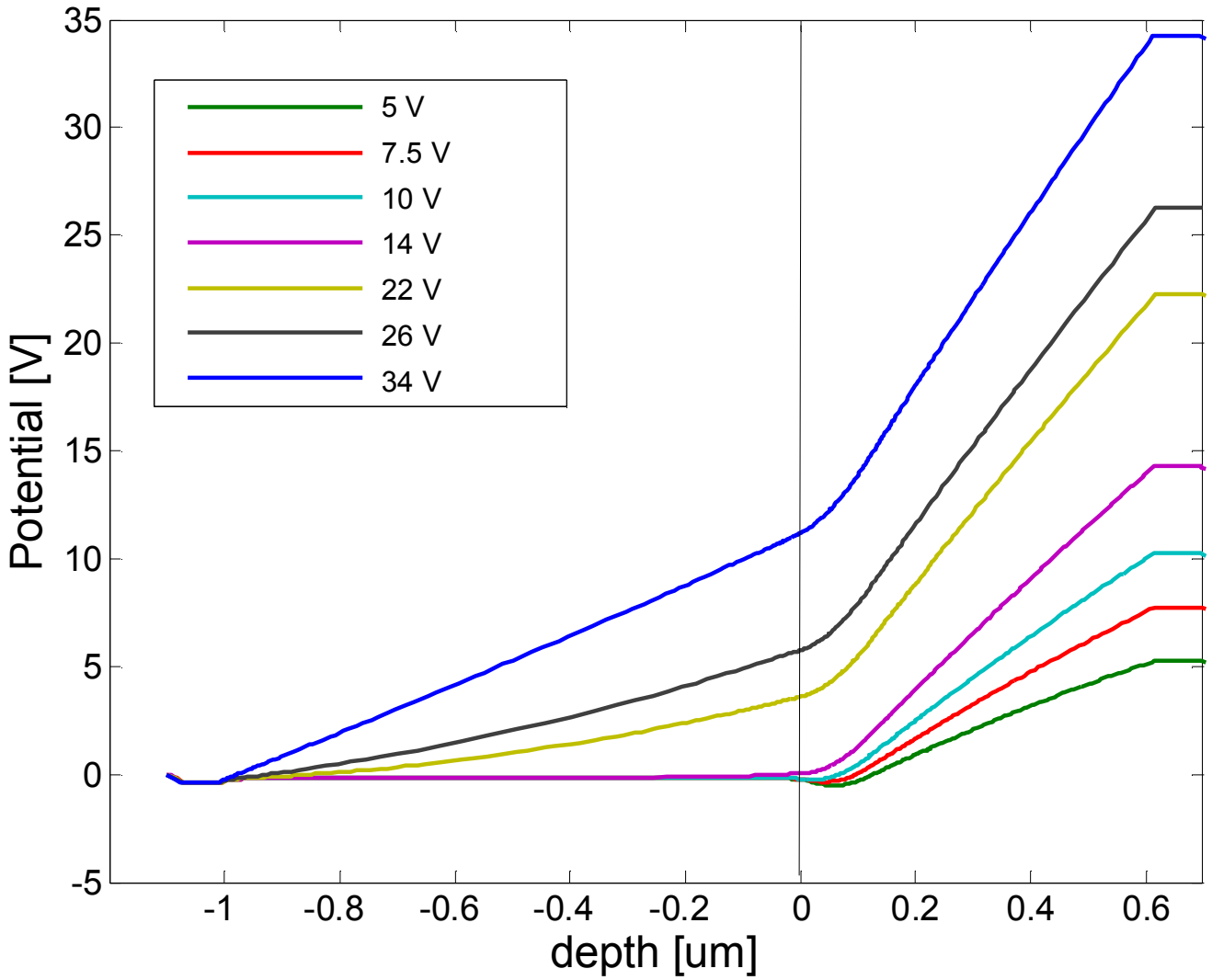
5 V
7.5 V
10 V
14 V
22 V
26 V
34 V
Potential [V]
depth [um]
35
30
25
20
15
10
5
0
-5
-1
-0.8
-0.6
-0.4
-0.2
0
0.2
0.4
0.6

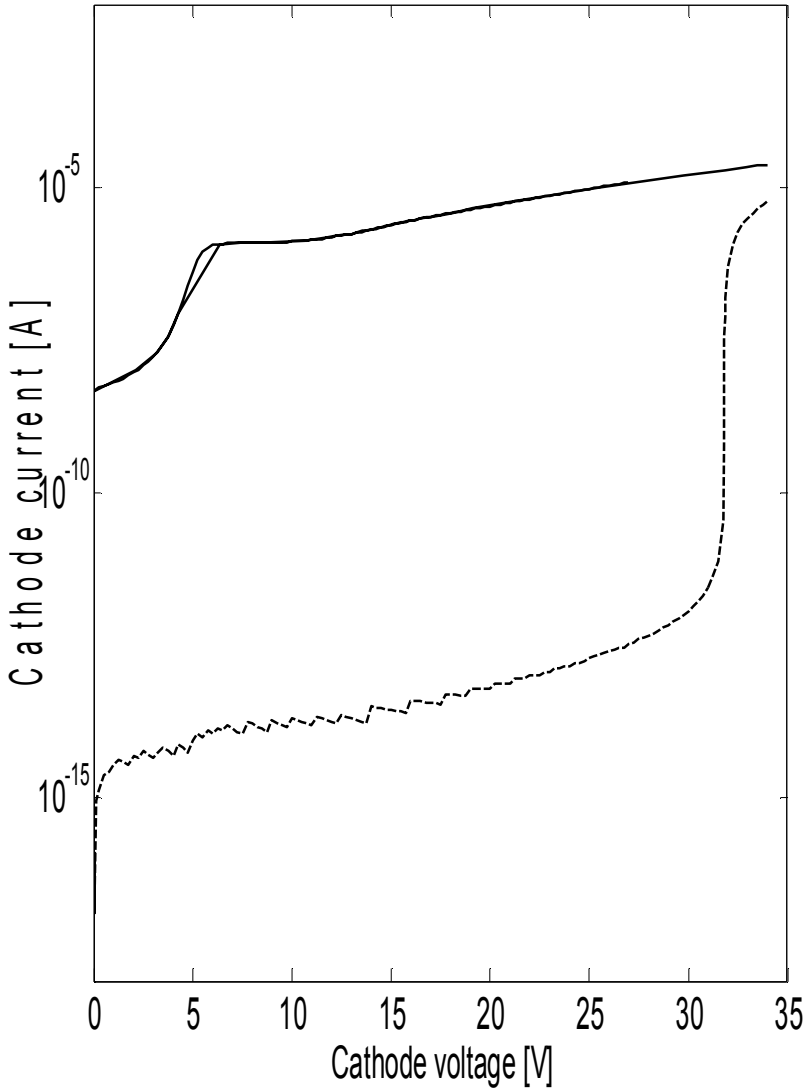
Cathode current [A]
10^-5
10^-10
10^-15
0
5
10
15
20
25
30
35
Cathode voltage [V]

Integrated Waveguide Coupled SPAD

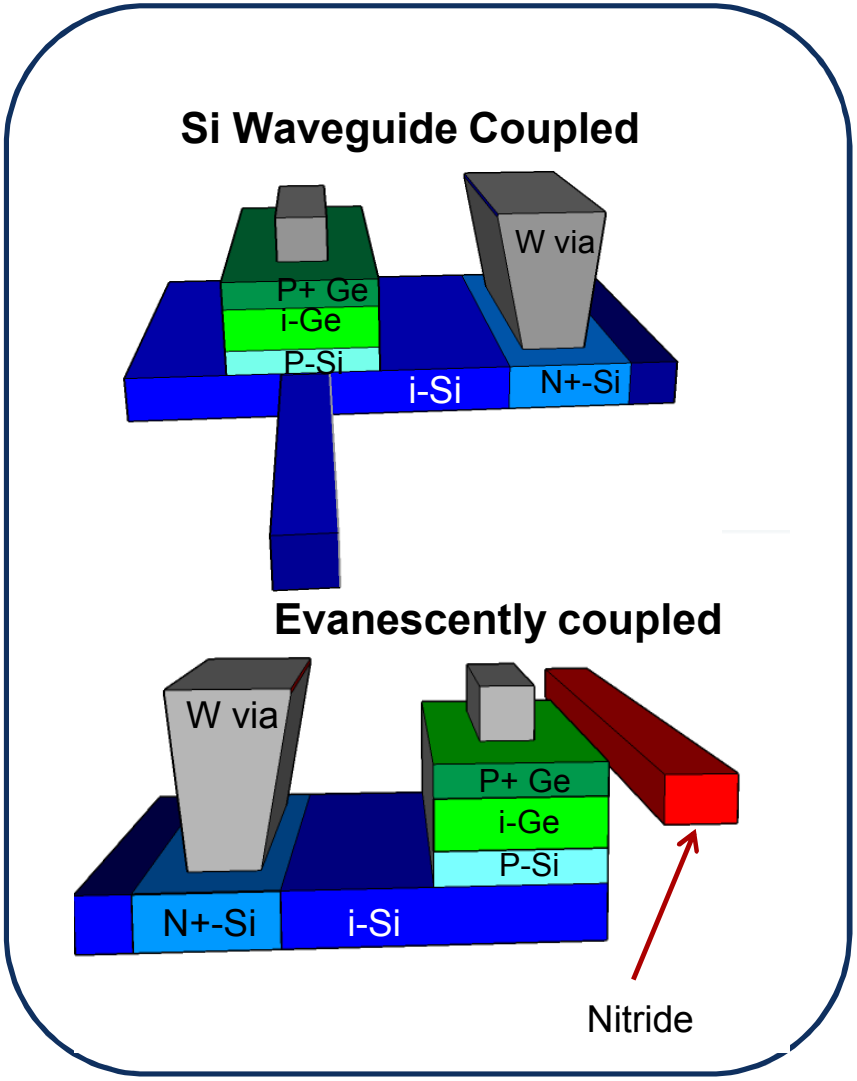

- ***Separate absorption and charge multiplication APD***
- Lateral and Vertical (not shown) APD designs.
- Selective Ge on Si Epitaxial growth.
  - Vertical design uses Si selectrive epitaxial growth.
- Waveguide-Coupling
  - Si end-fired
  - Nitride waveguide evanescent coupled

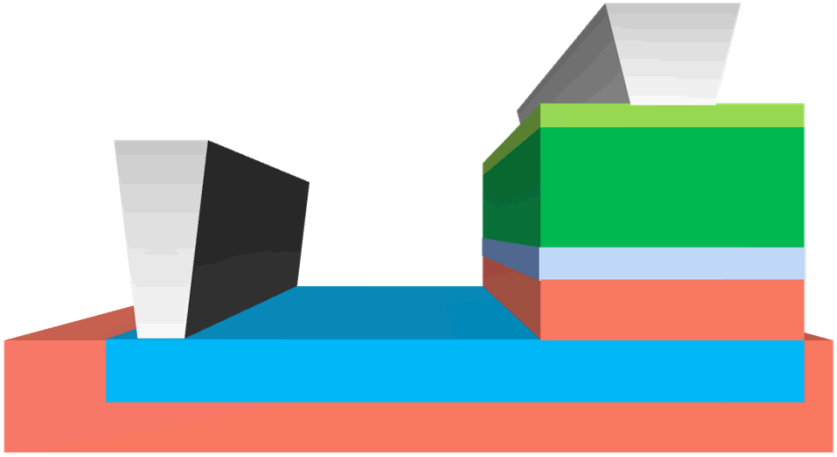

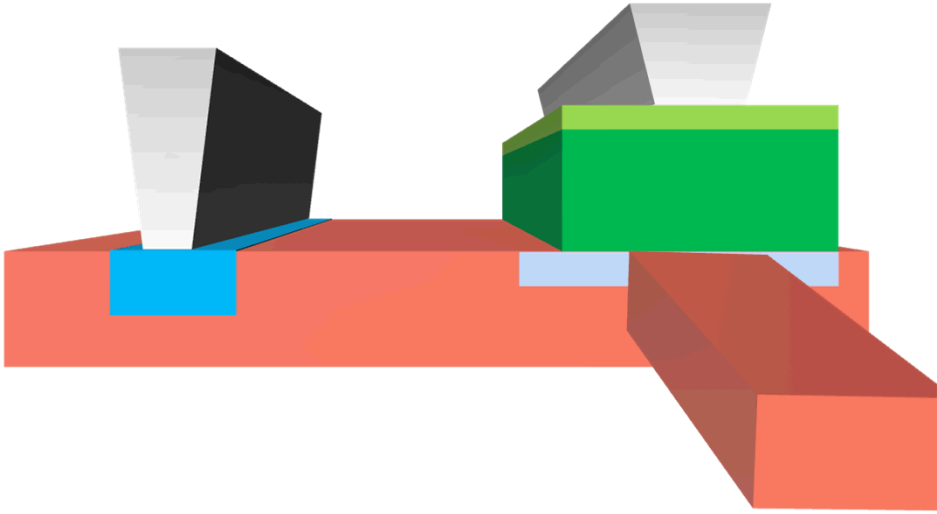

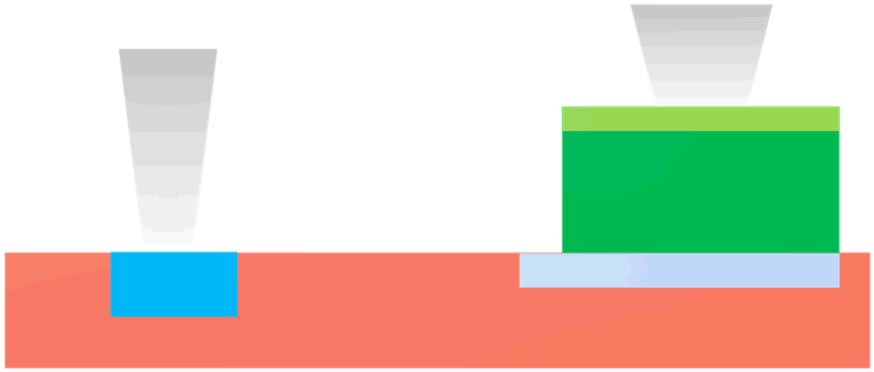

P+ Ge

Ge

Si

P-Si

N+ Si

Integrated lateral APD results

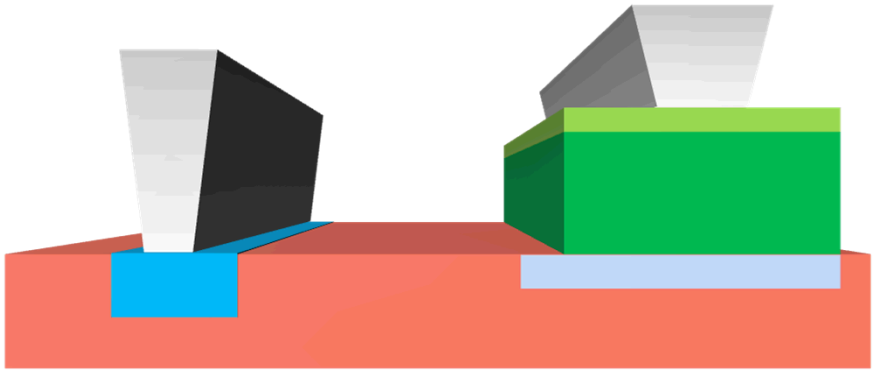

Top down view shows variation of multiplication
Width and p-Charge layer overlap.

Together with implant doses we vary these parameters.

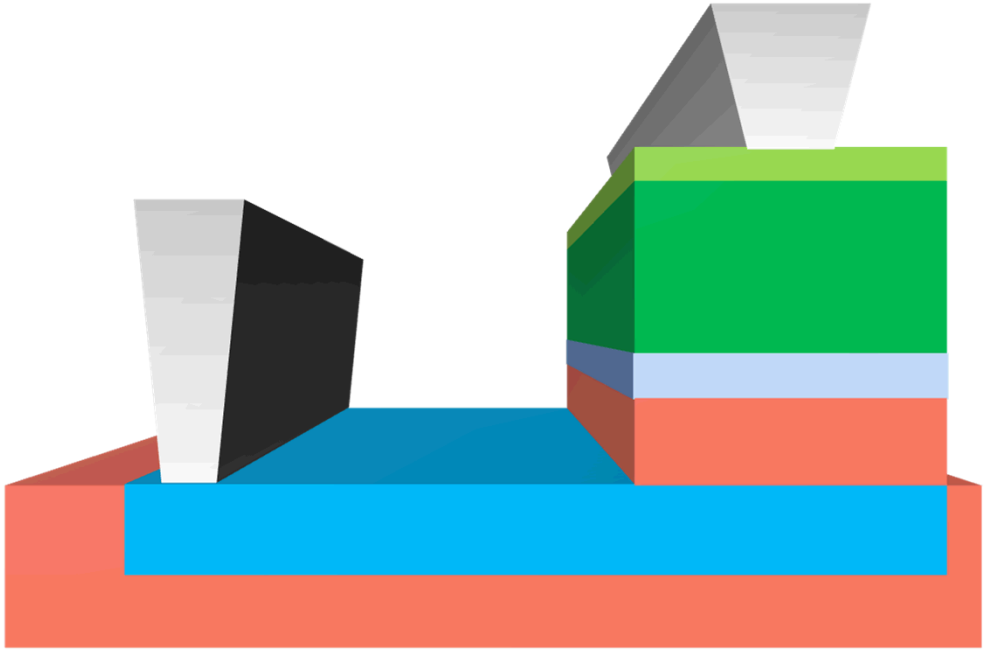

Top down view shows variation of multiplication Width and p-Charge layer overlap.

Together with implant doses we vary these parameters.

Light On (Dashed Curve) L = 16

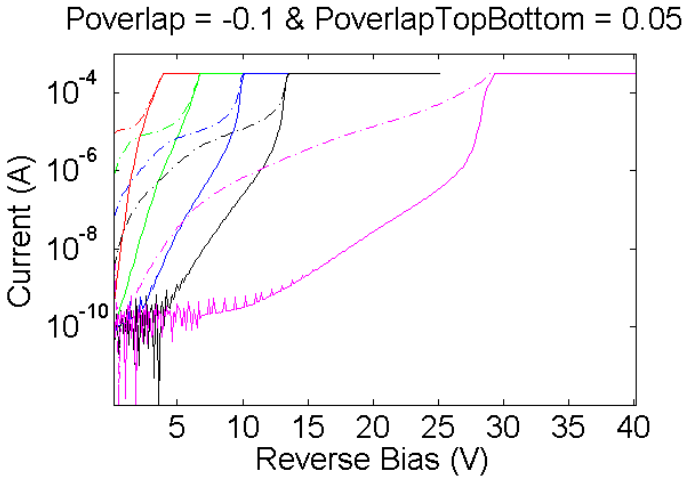

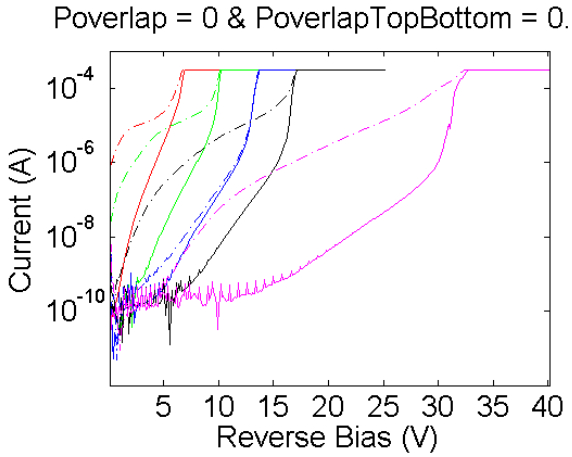

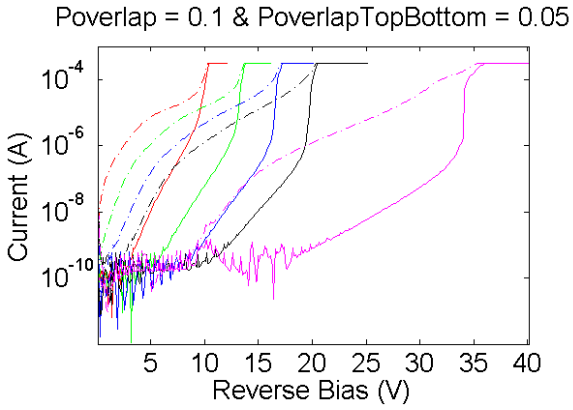

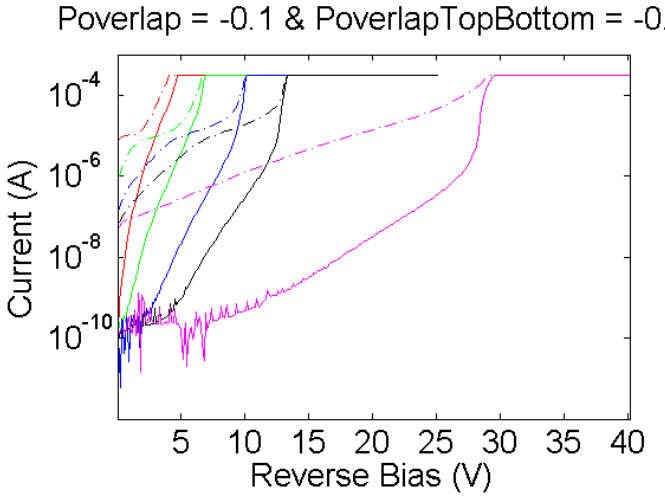

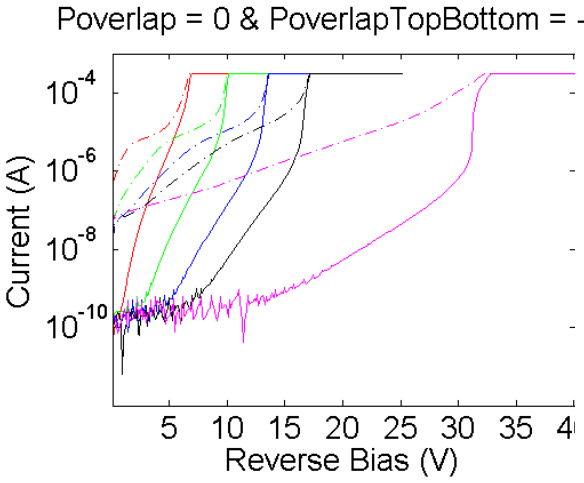

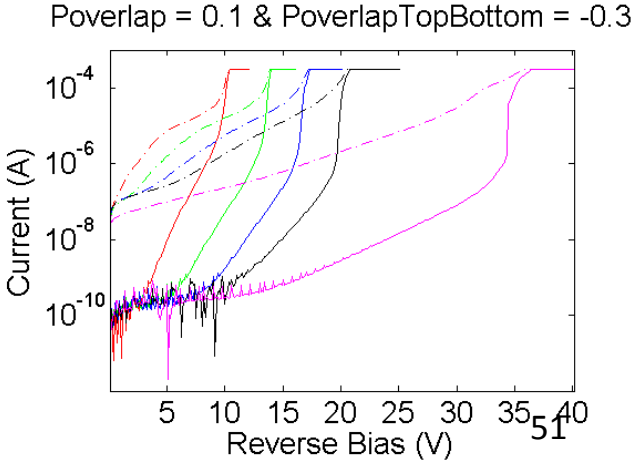

Light On (Dashed Curve) L = 8

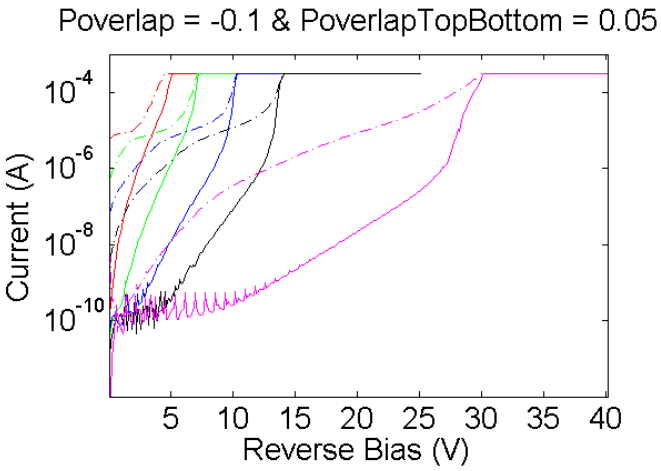

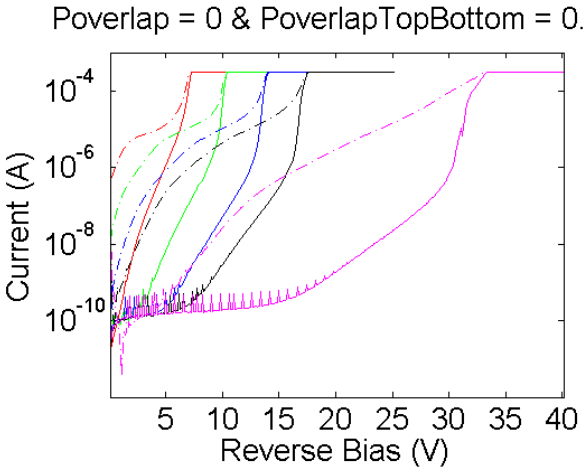

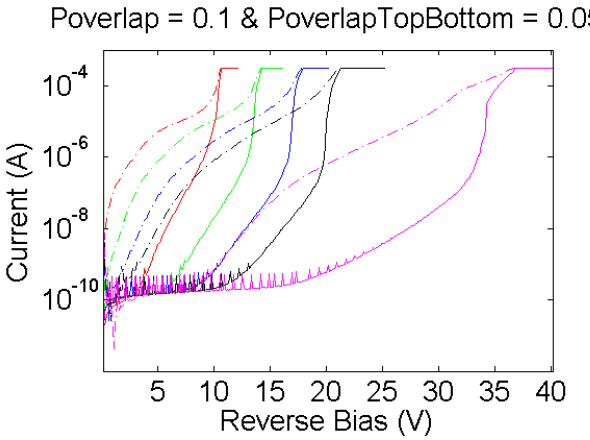

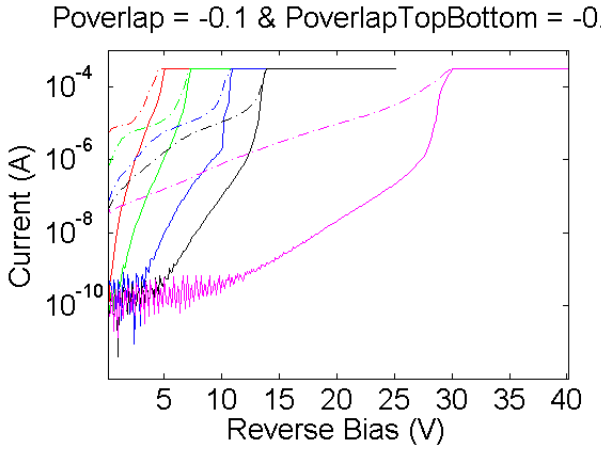

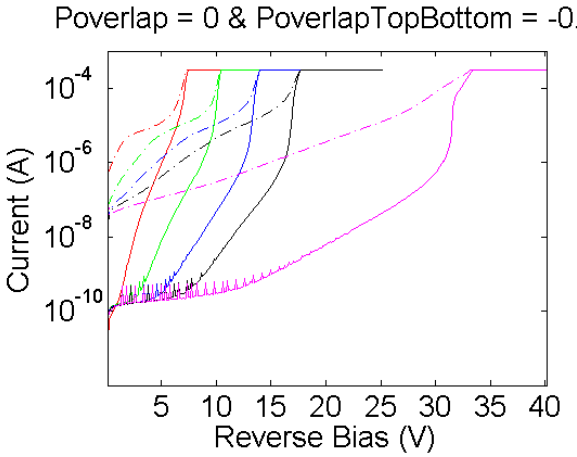

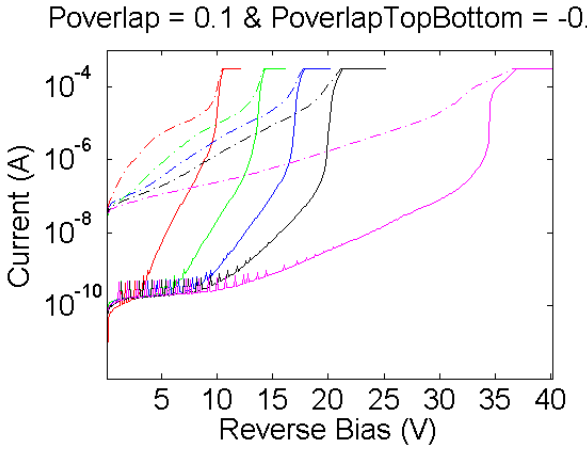

Multiplication L = 16

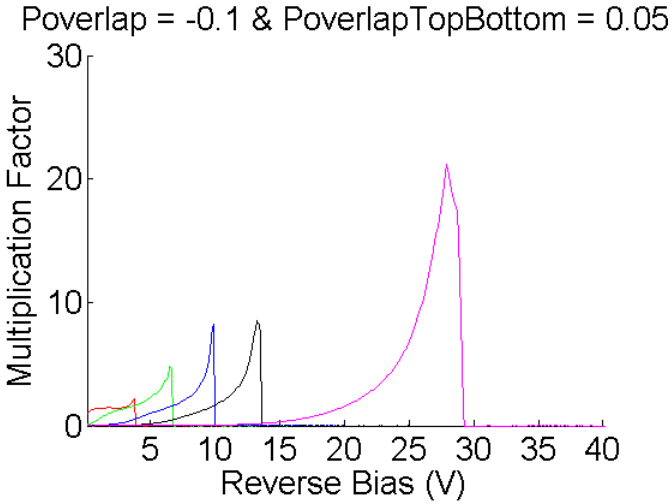

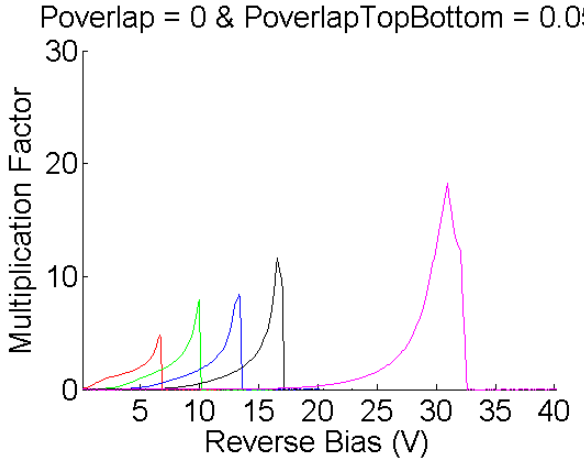

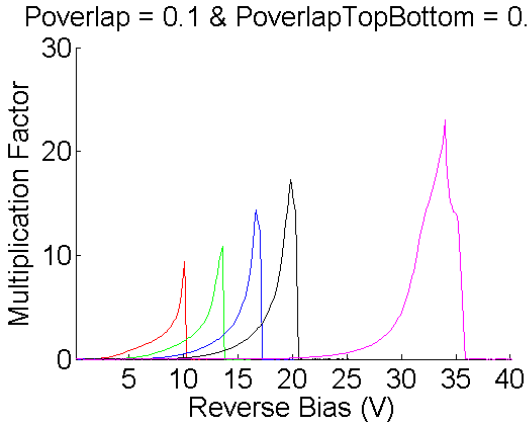

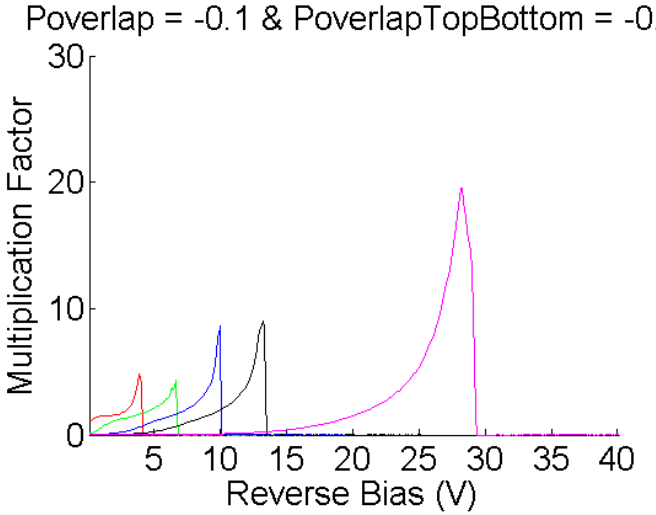

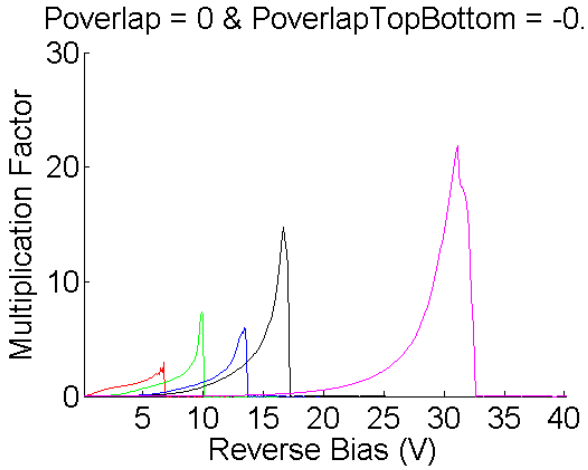

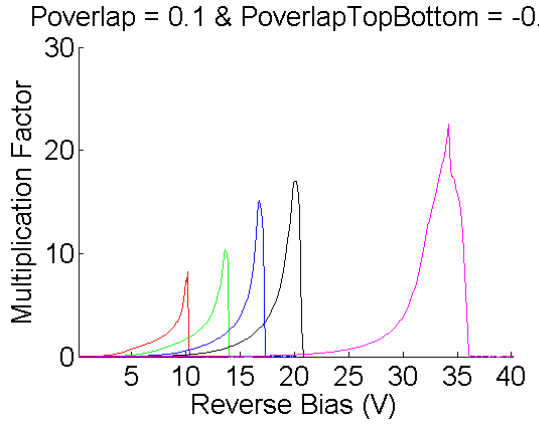

Multiplication L = 8

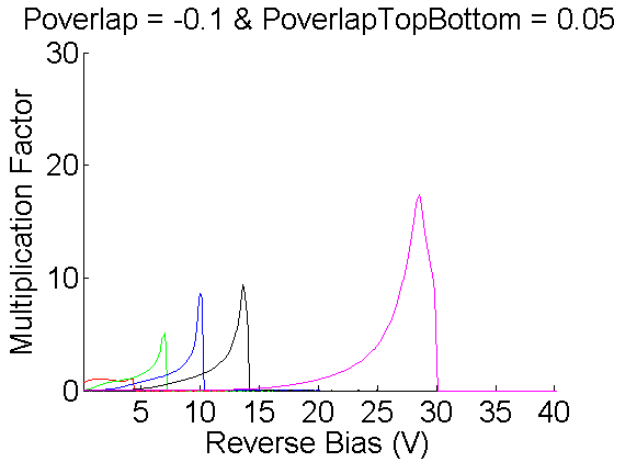

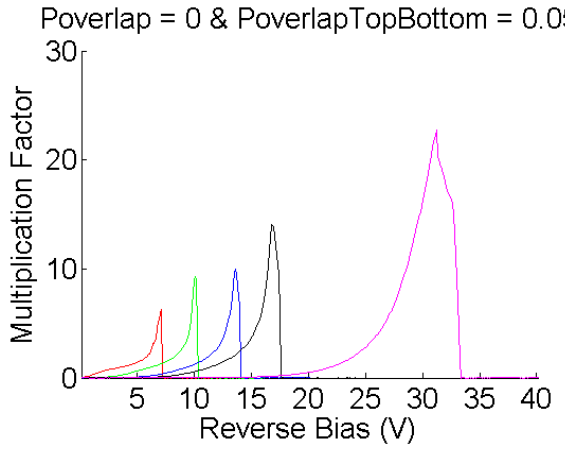

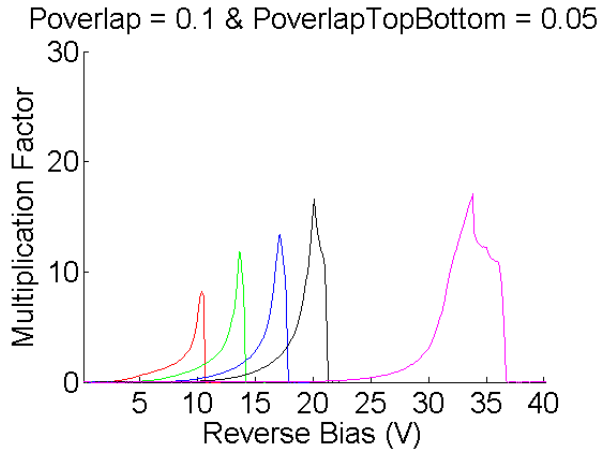

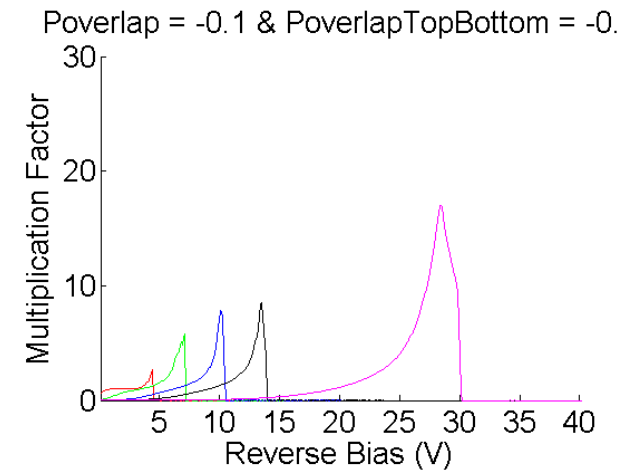

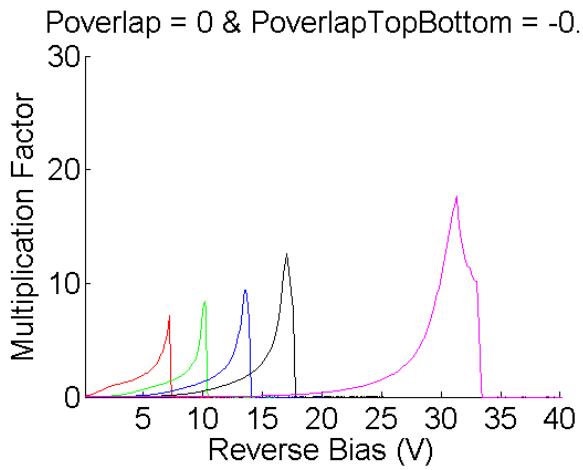

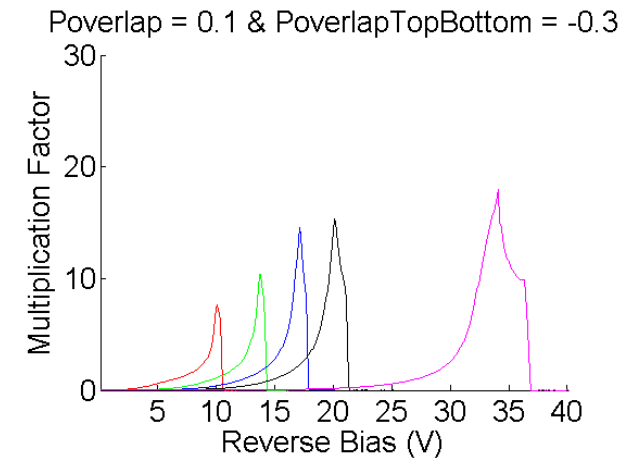

Initial Passive Quenched GM

Optical Properties of Doped Ge

Sandia National Laboratories

Tight binding band-structure

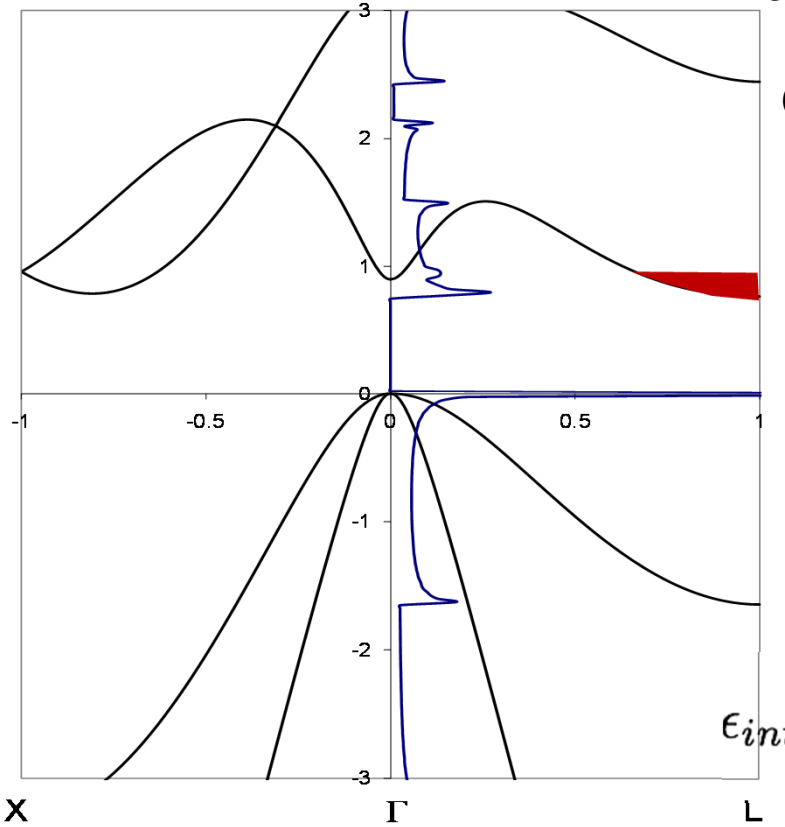

Can we determine validity of band-filling and strain models for PL & EL signatures?

Optical Properties of Heavily Doped Semiconduc

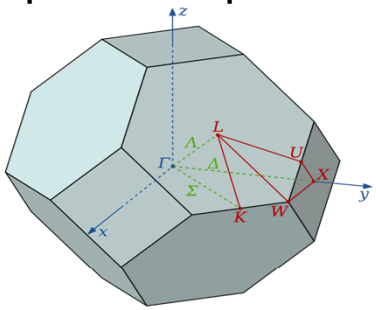

J. Jung, T. G . Pederson, JAP,113,114904,(2013)

$$\epsilon(\omega) = \epsilon_{inter}(\omega) + \epsilon_{intra}(\omega)$$

$$\epsilon_{intra}(\omega) = \frac{e^2}{8\pi^3\epsilon_0\hbar^2\omega^2}\sum_n \int \frac{\partial E_{n\mathbf{k}}}{\partial \mathbf{k}} f'(E_{n\mathbf{k}})d\mathbf{k}$$

$$\epsilon_{inter}(\omega) = 1 + \frac{e^2\hbar^2}{8\pi^3\epsilon_0 m^2}\sum_{n\neq m} \int \frac{f(E_{n\mathbf{k}}) - f(E_{m\mathbf{k}})}{E_{m\mathbf{k},n\mathbf{k}}[E^2_{m\mathbf{k},n\mathbf{k}} - (\hbar\omega)^2]} M_{m,n}(\mathbf{k})d\mathbf{k}$$

Indirect Bandgap in Strained Ge

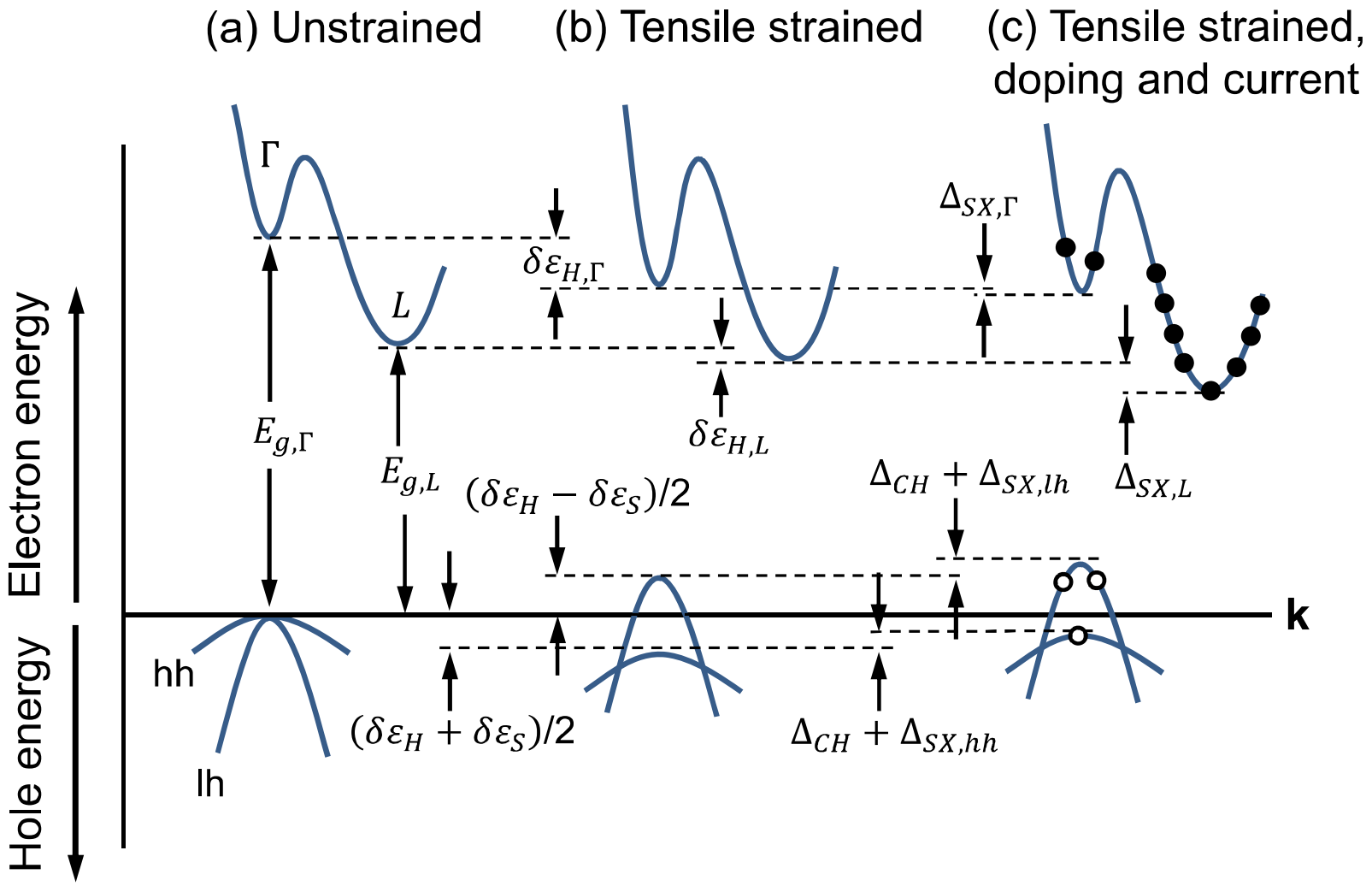

Waveguide Coupled SPAD

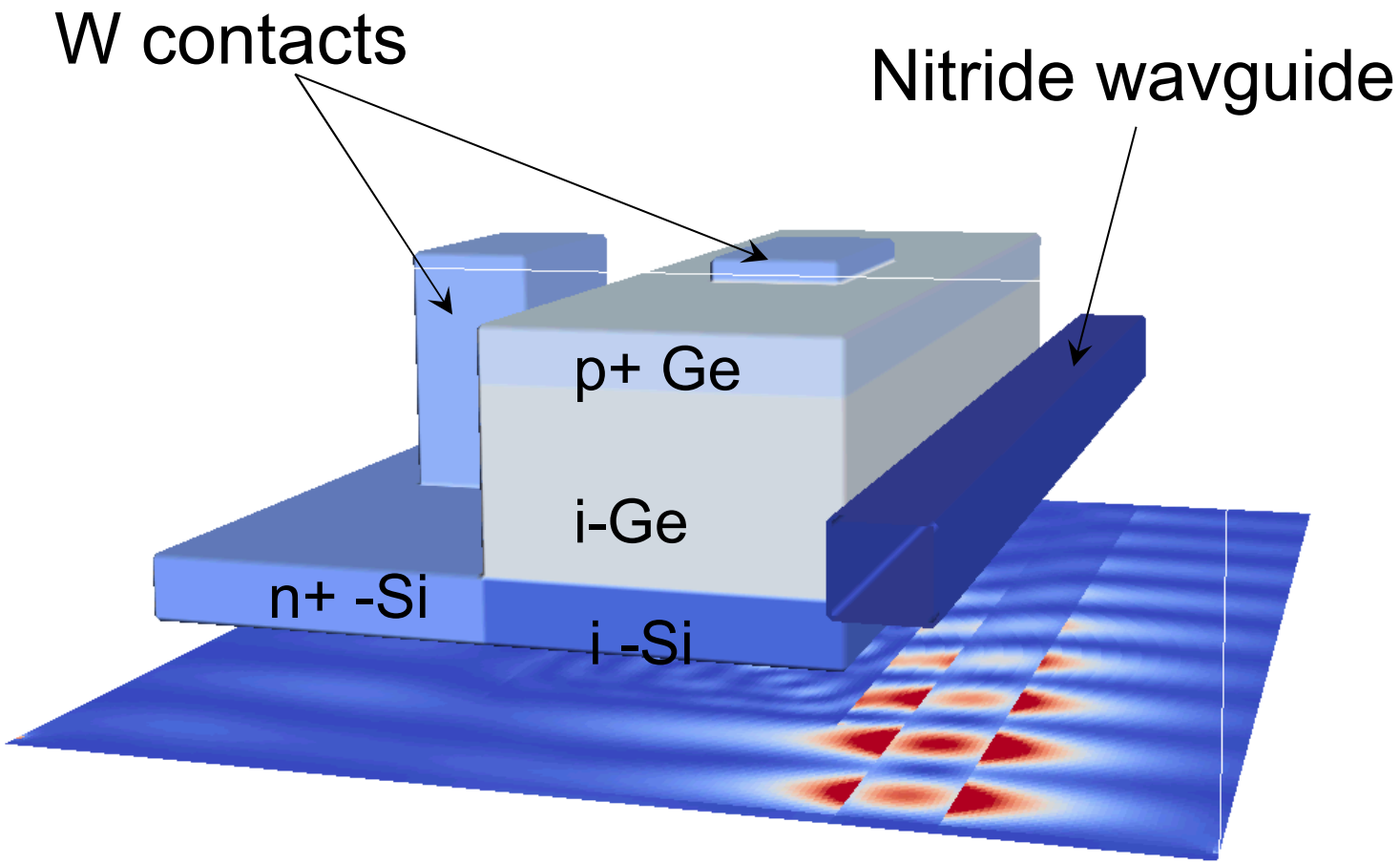

Ge Photodetector Development

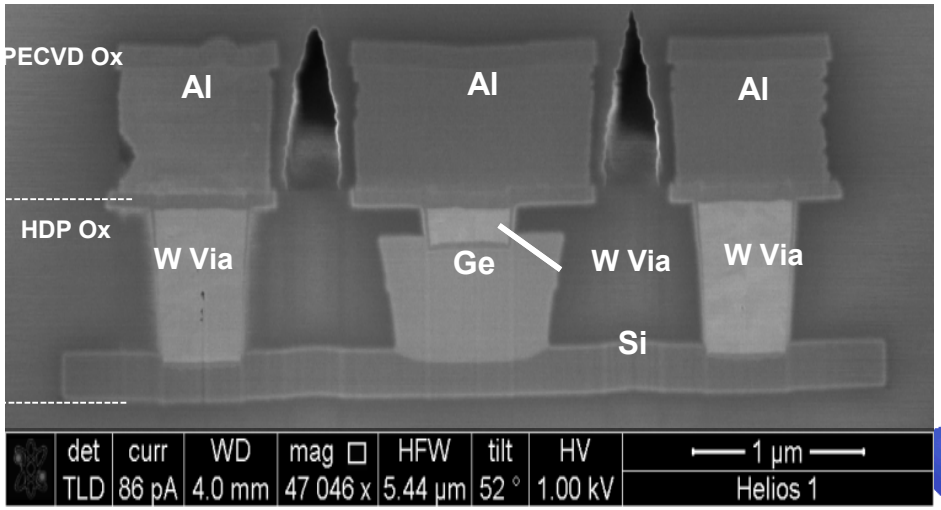

Generation rate

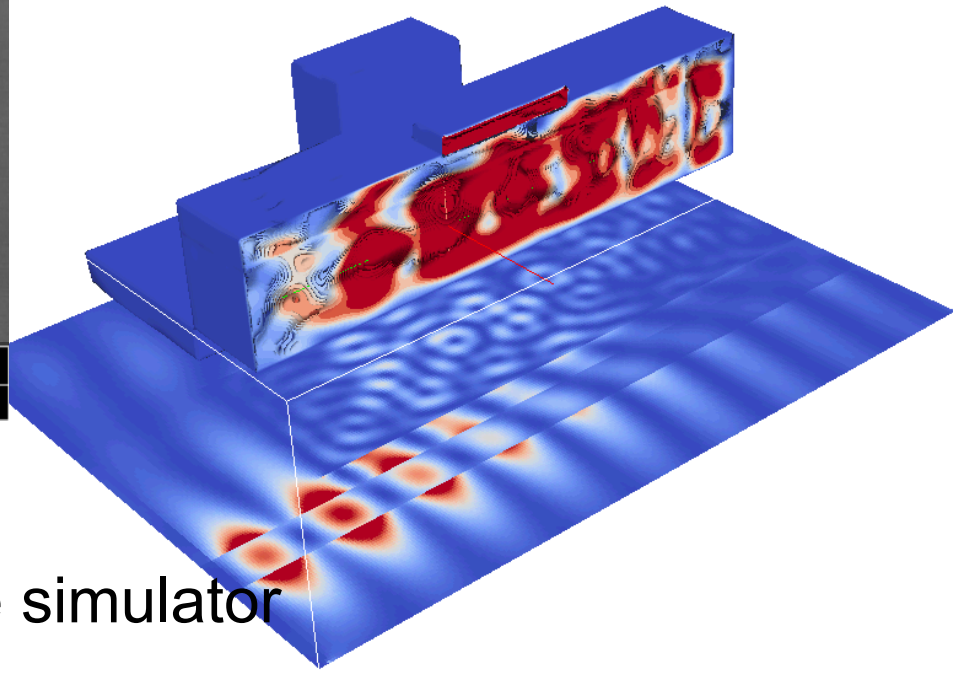

Input Generation rate into Device simulator
Synopsis drift-diffusion.
APD simulations currently underway.

C. T. DeRose, D. C. Trotter, W. A. Zortman, A. Starbuck, M. Fisher, M. R. Watts, and P. S. Davids, "Ultra compact 45GHz CMOS compatible Ge waveguide photodiode with low dark current," *Optics Express*, vol. 19, no. 25, p. 24897, 2011.

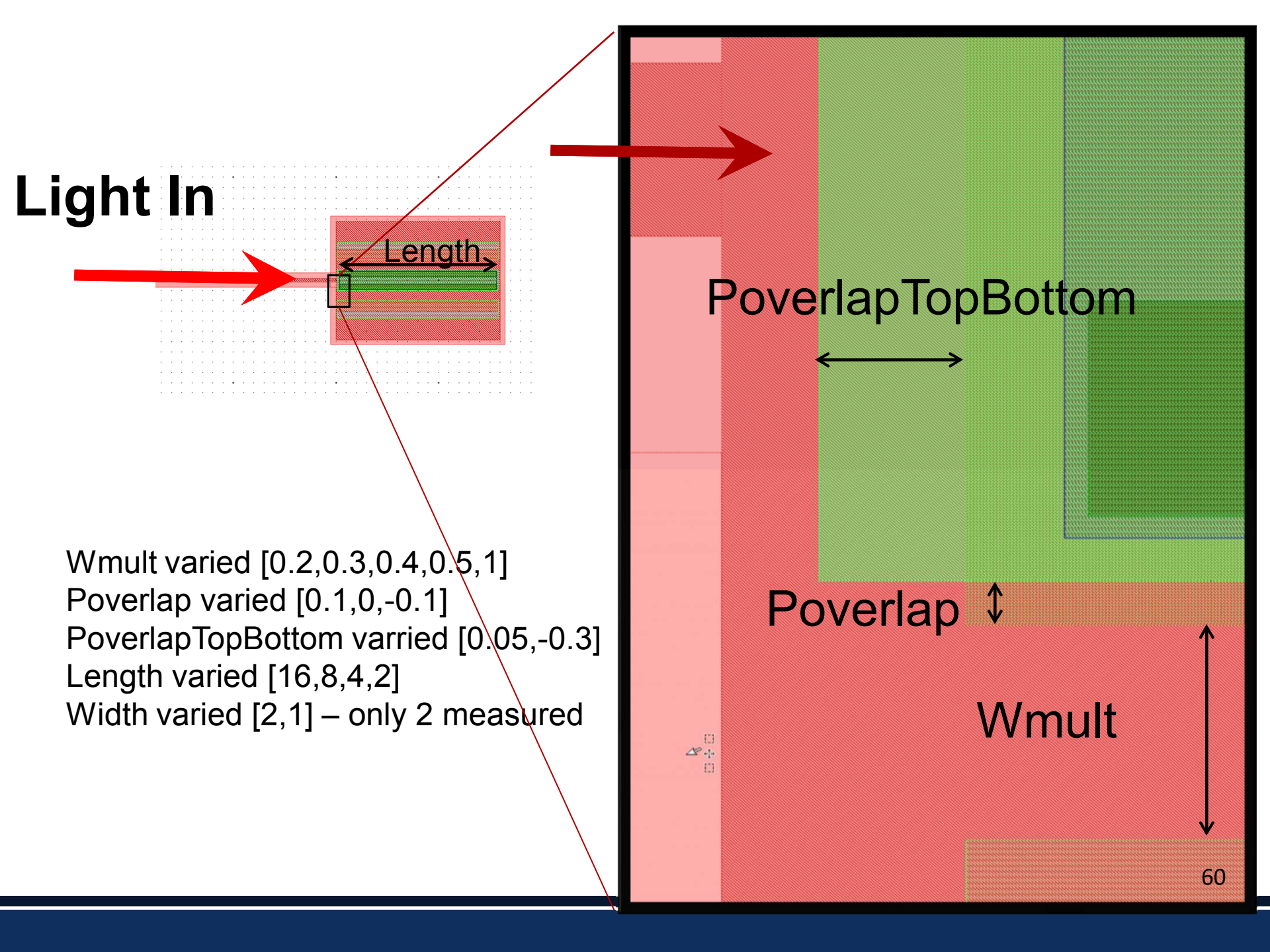

Wmult varied [0.2,0.3,0.4,0.5,1]
Poverlap varied [0.1,0,-0.1]
PoverlapTopBottom varried [0.05,-0.3]
Length varied [16,8,4,2]
Width varied [2,1] – only 2 measured

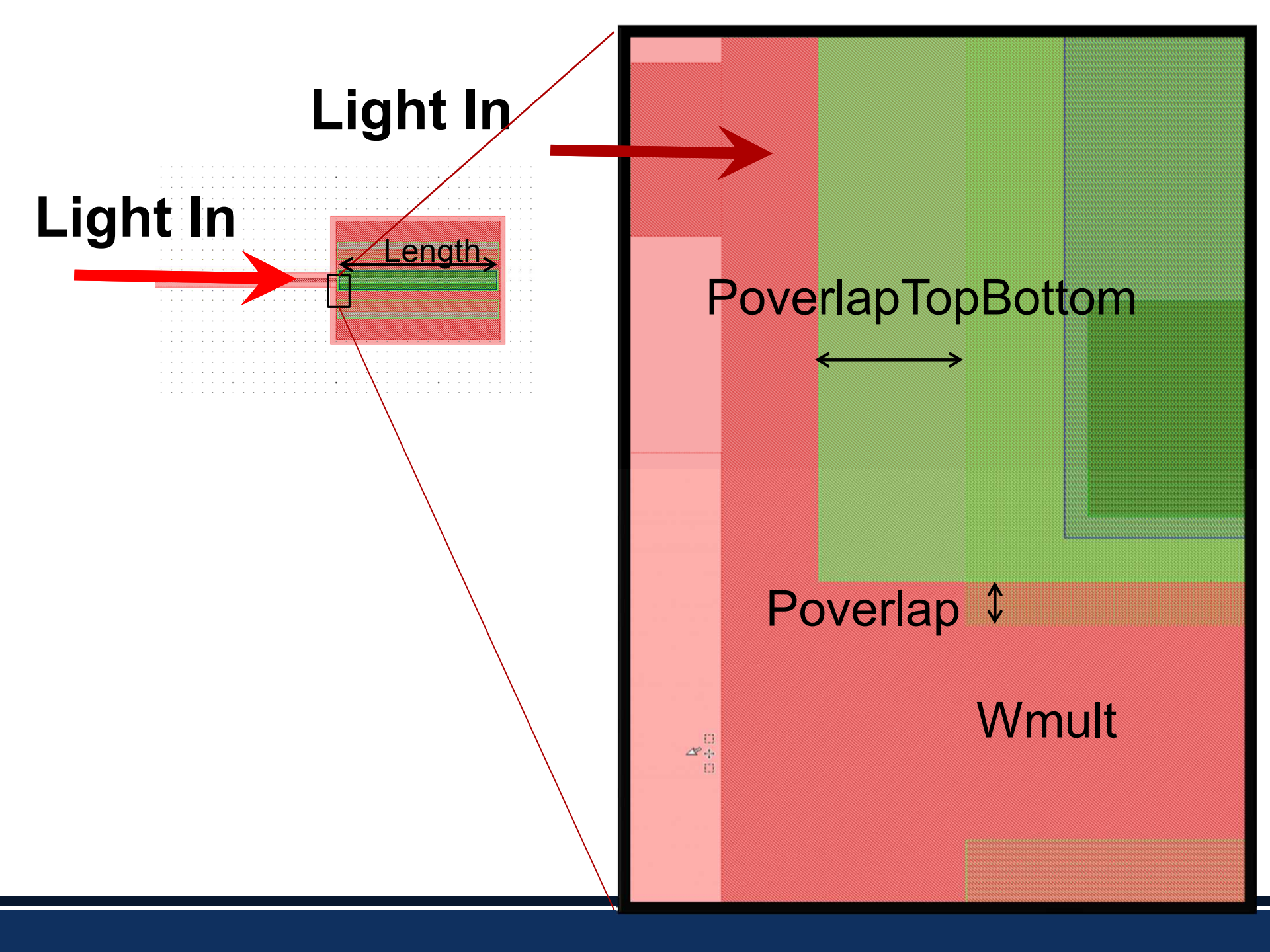
Light In
Light In
Length
PoverlapTopBottom
Poverlap
Wmult

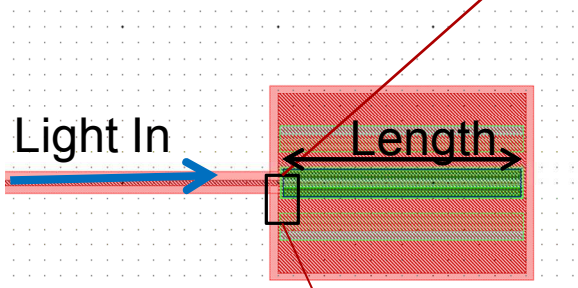

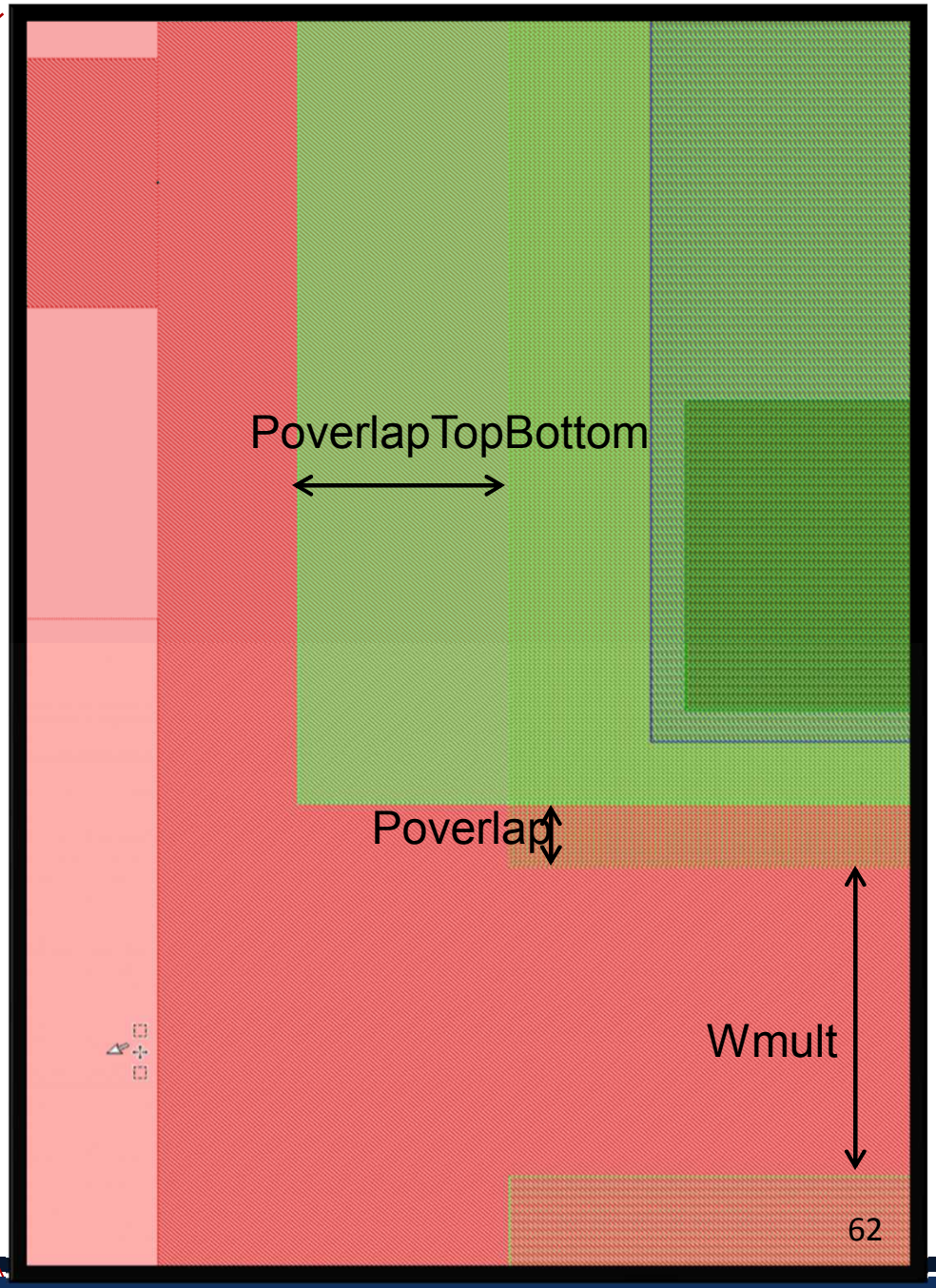

Wmult varied [0.2,0.3,0.4,0.5,1]
Poverlap varied [0.1,0,-0.1]
PoverlapTopBottom varried [0.05,-0.3]
Length varied [16,8,4,2]
Width varied [2,1] – only 2 measured

Die Map

- All measurements presented here were on 1051A W2 Die (0,0)

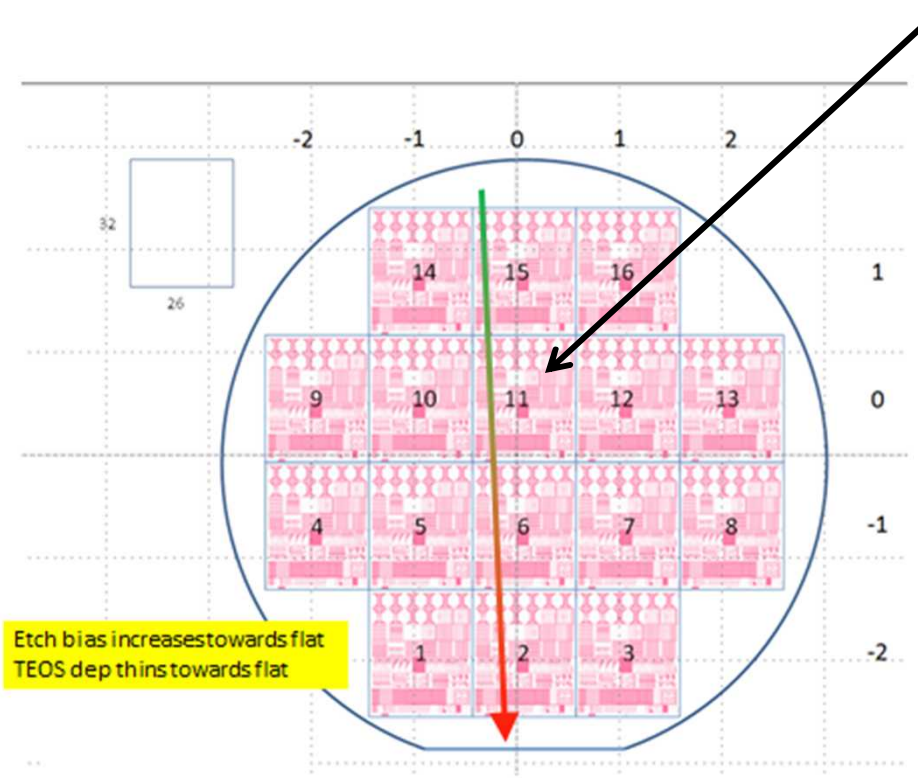

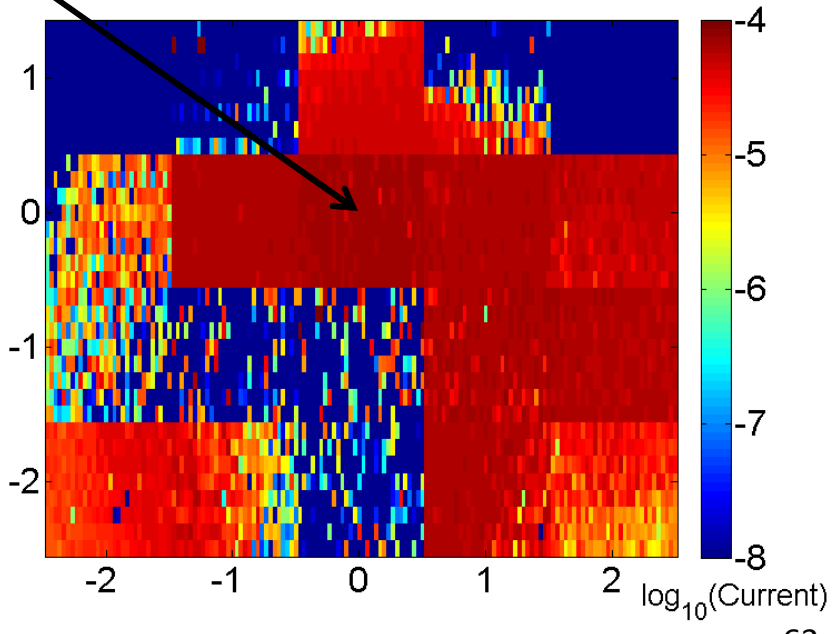

Dark Characteristics L = 16

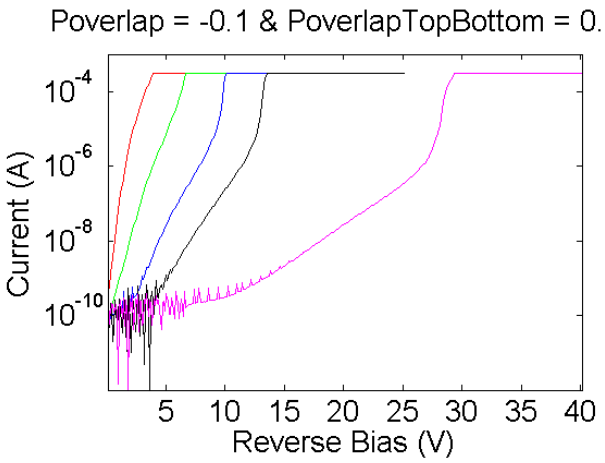

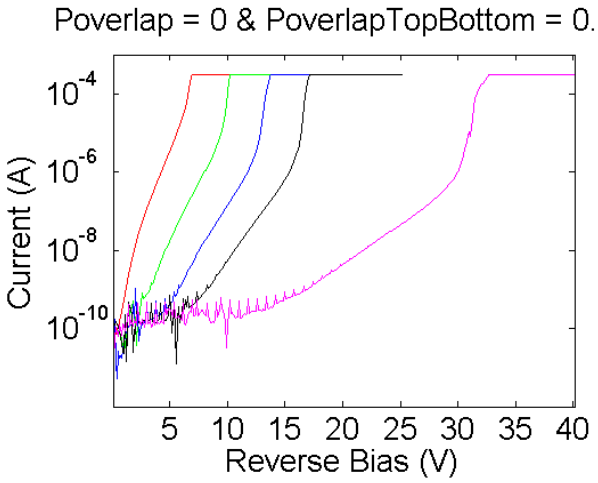

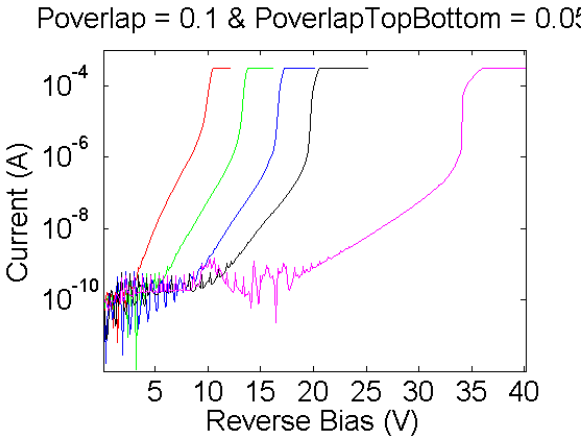

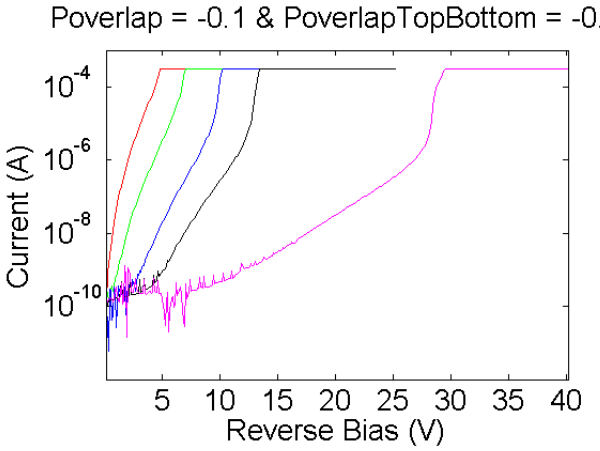

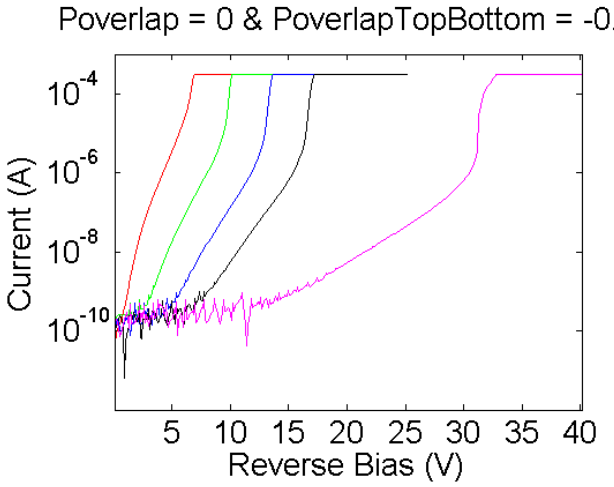

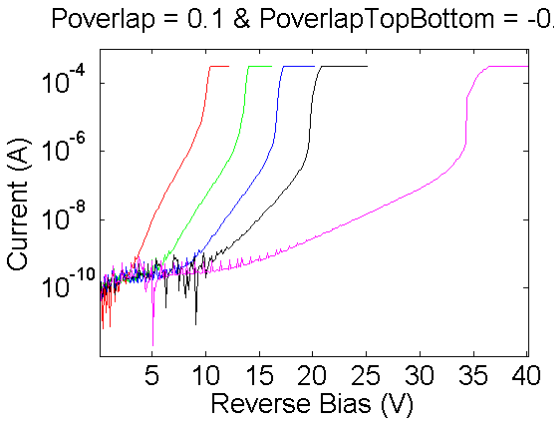

A closer look at the dark current

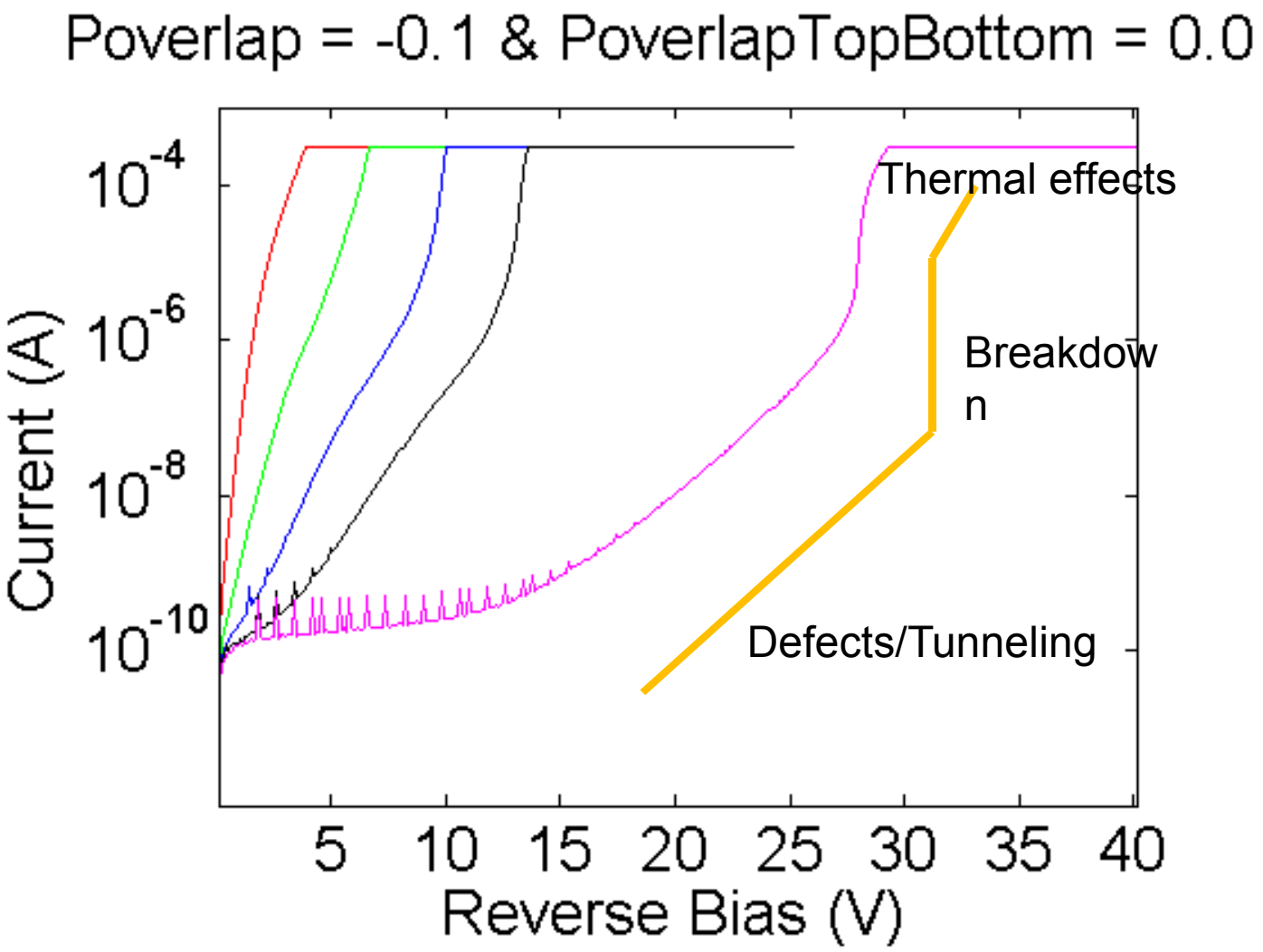

Dark Characteristics L = 8

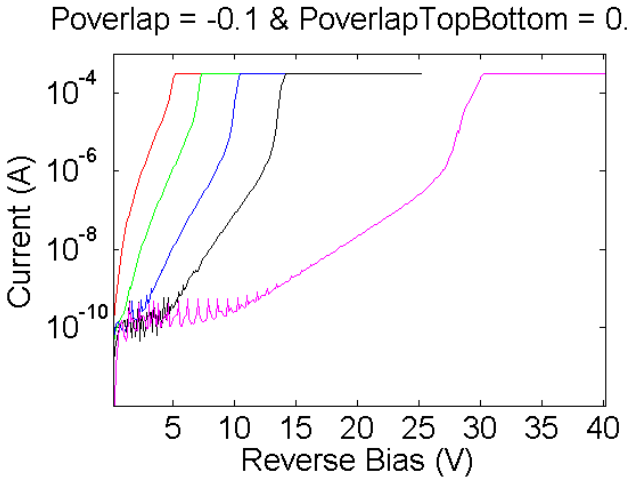

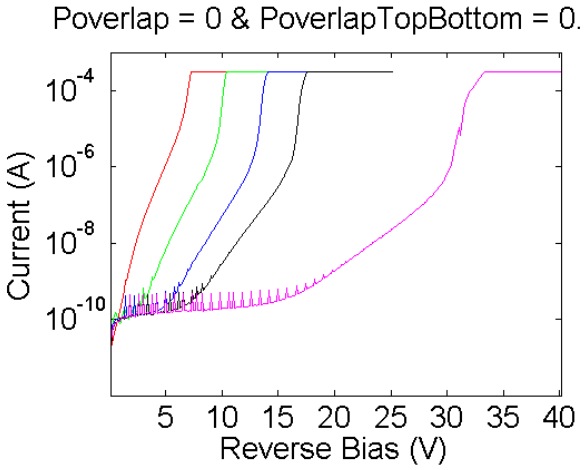

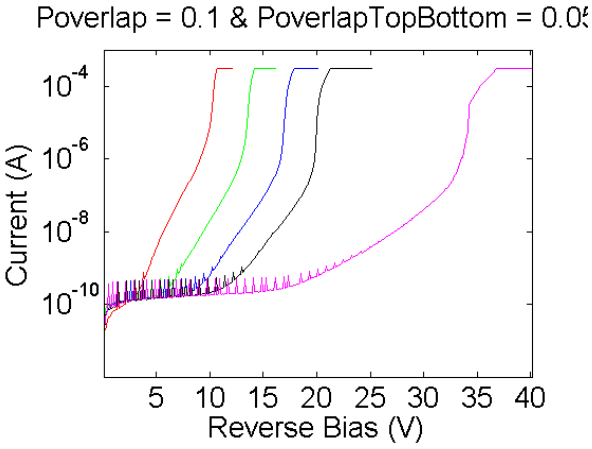

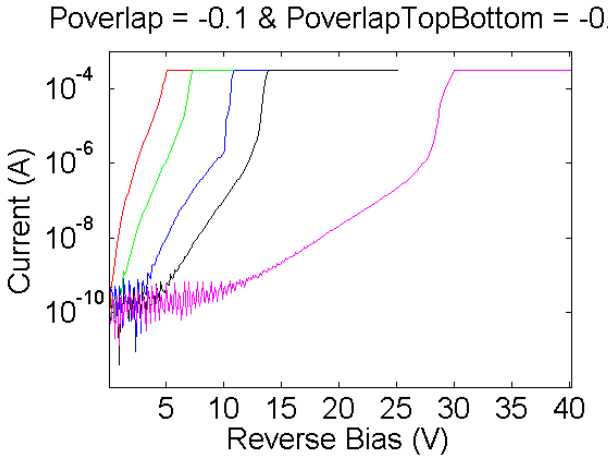

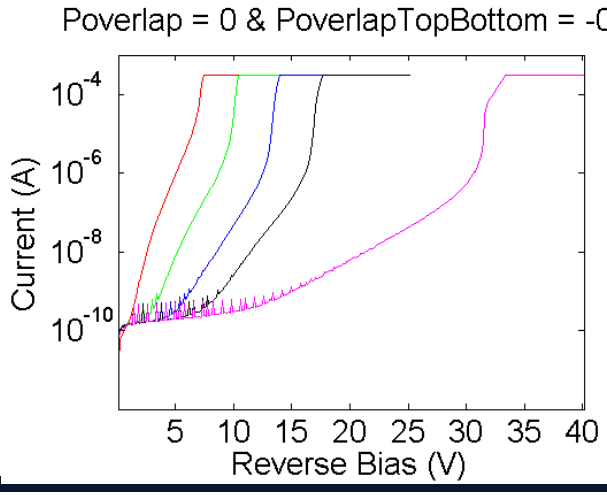

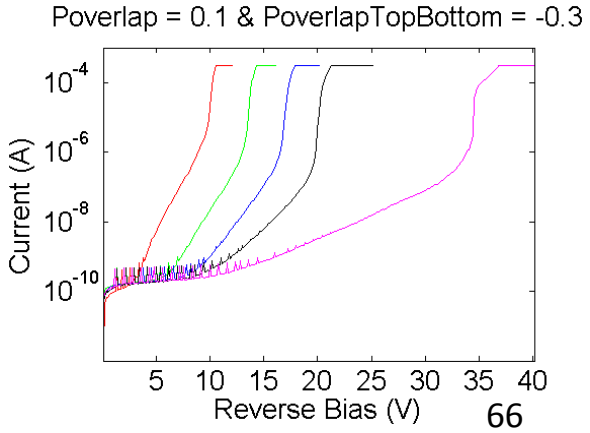

Dark Characteristics L = 4

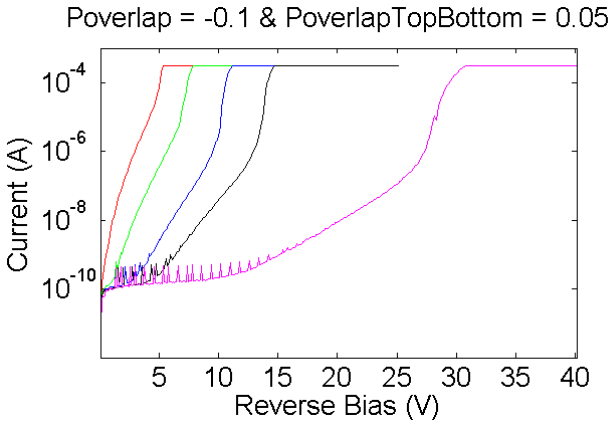

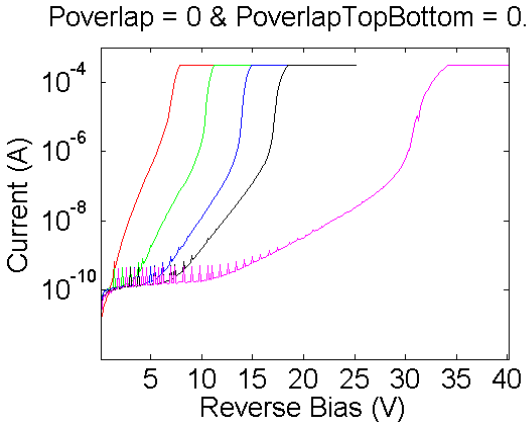

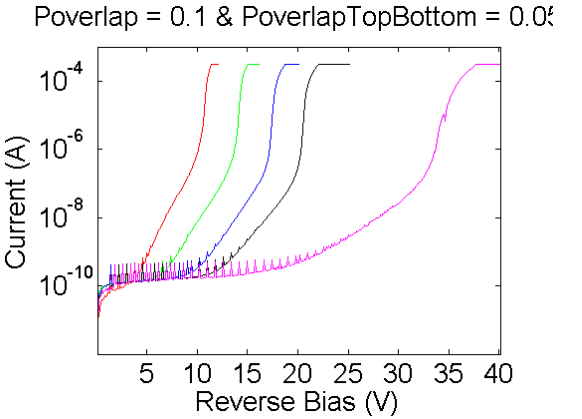

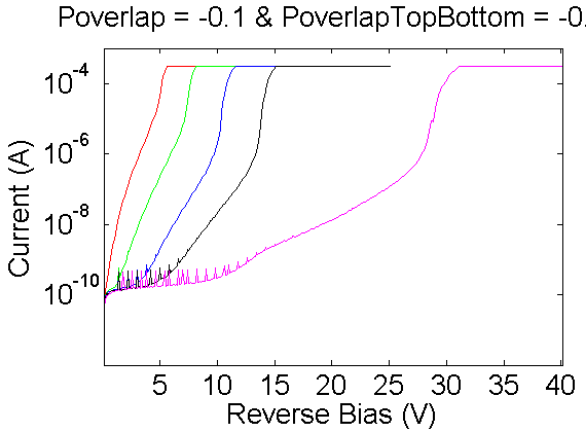

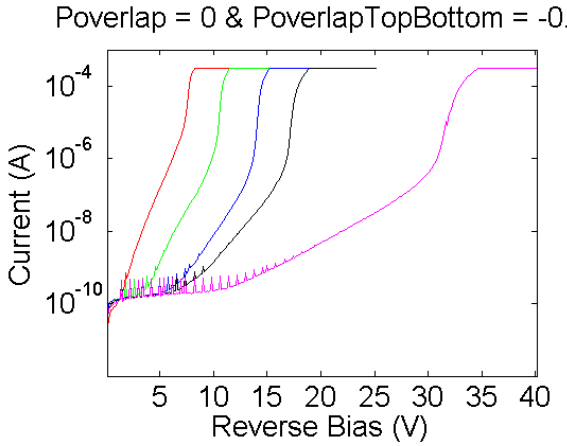

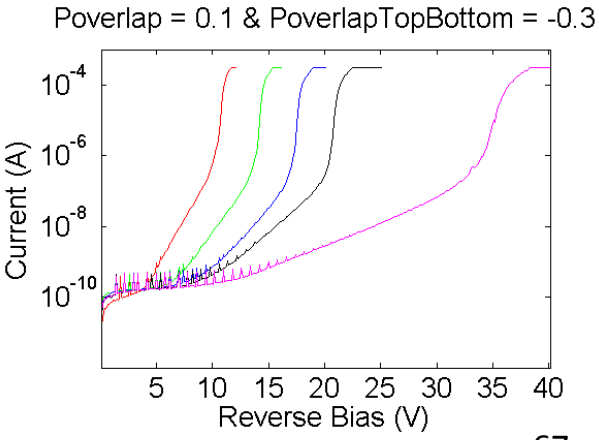

Dark Characteristics L = 2

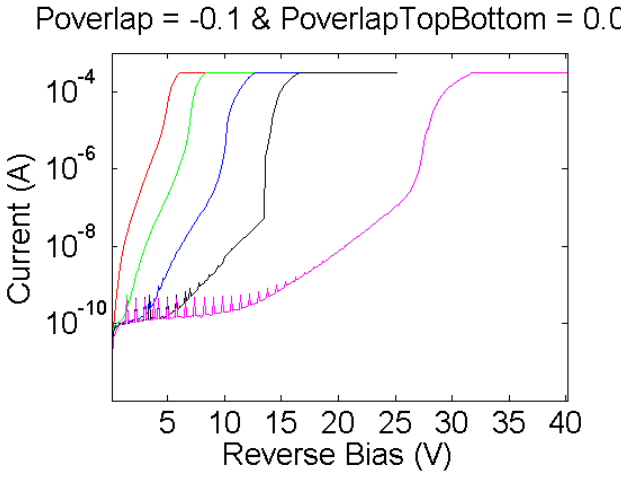

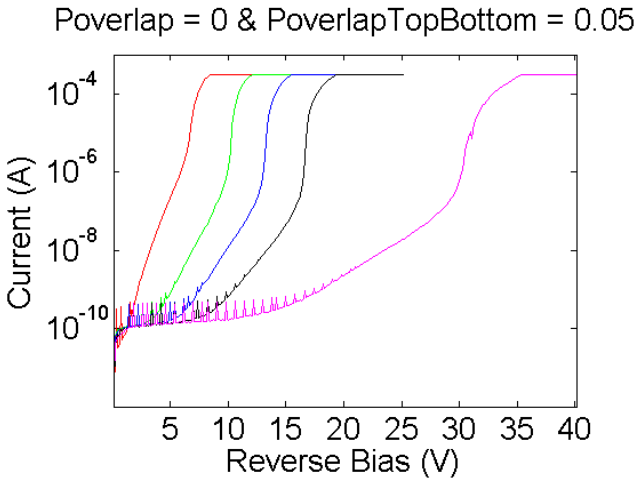

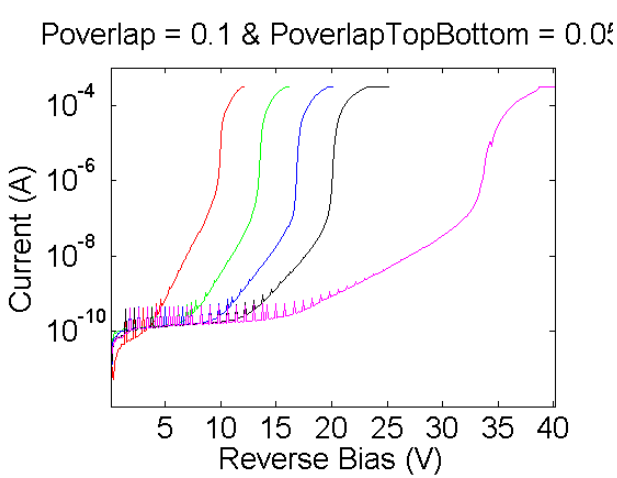

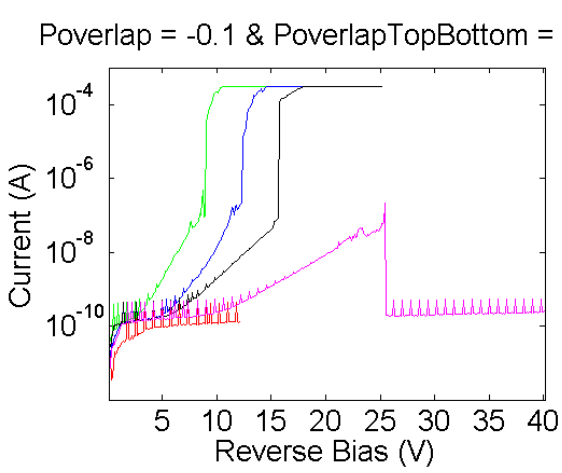

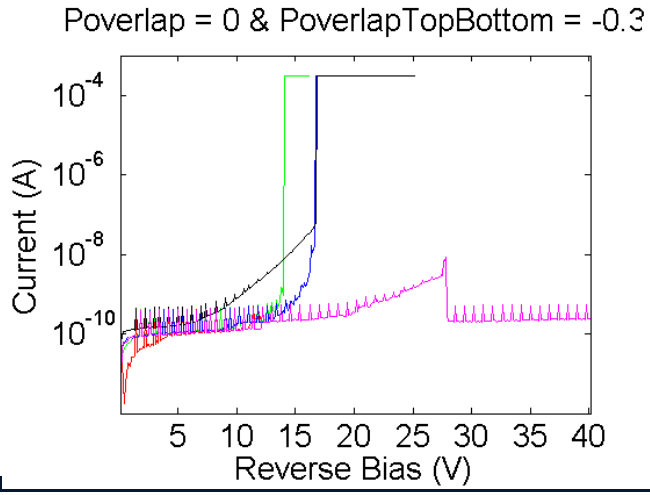

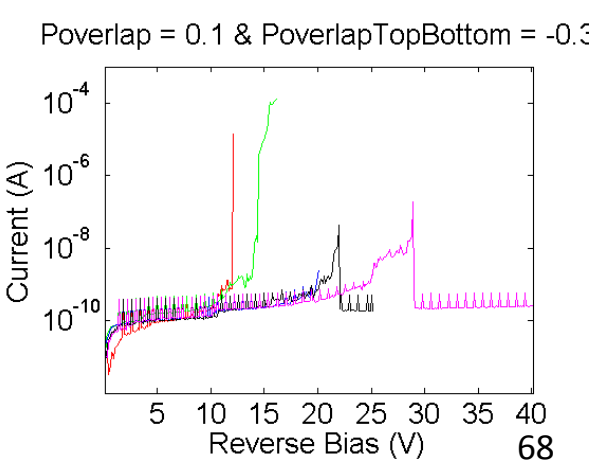

Effect of Poverlap

8um long 0.5 um Wmult

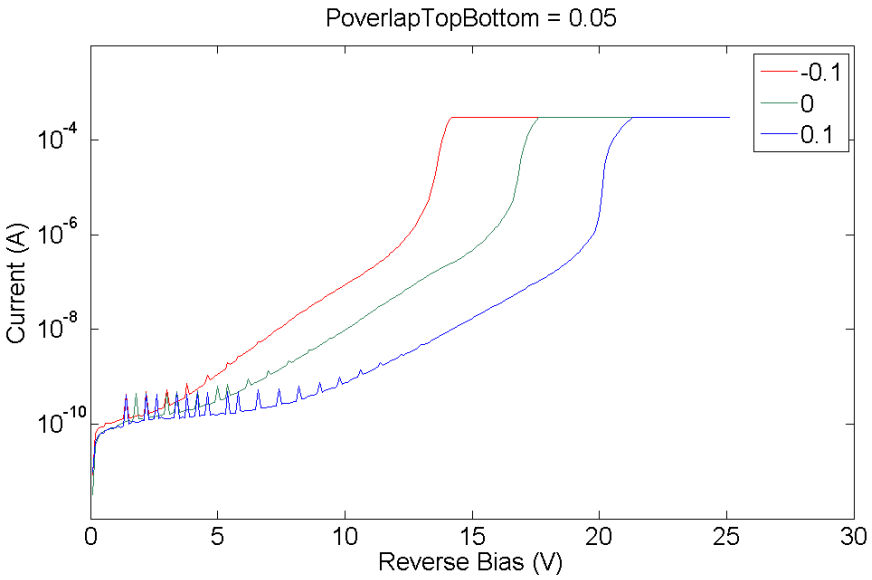

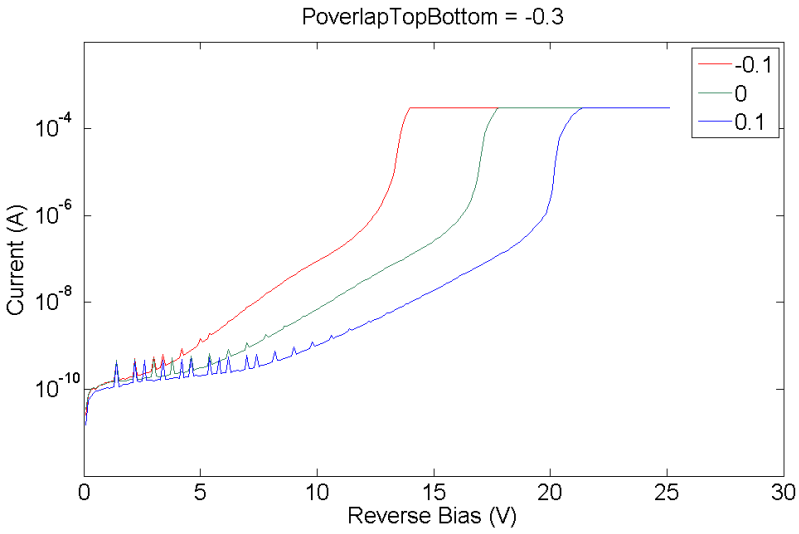

Increasing Poverlap pushes breakdown out due to widening depletion region

Effect of PoverlapTopBottom

8um long 0.5 um Wmult

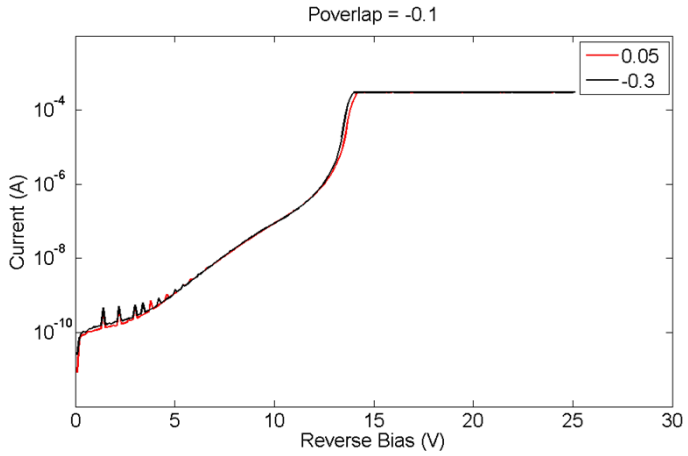

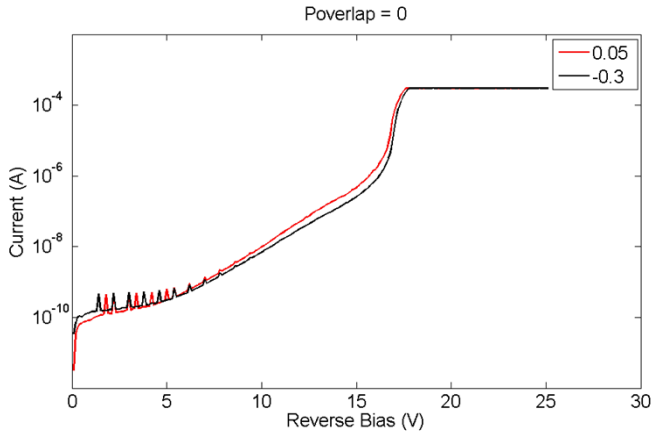

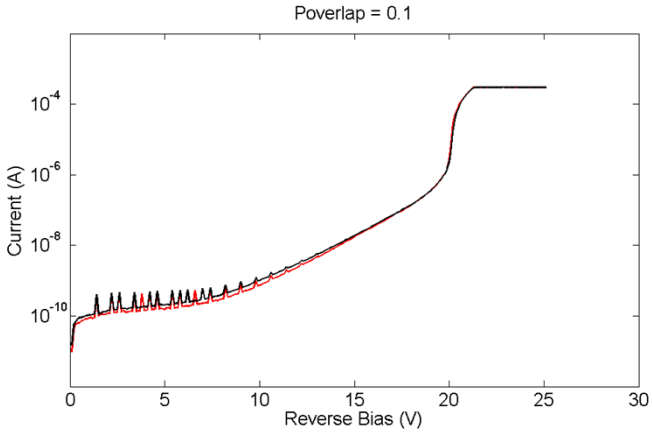

Little effect seen with PoverlapTopBottom in 8um device

Effect of PoverlapTopBottom

2 um long device

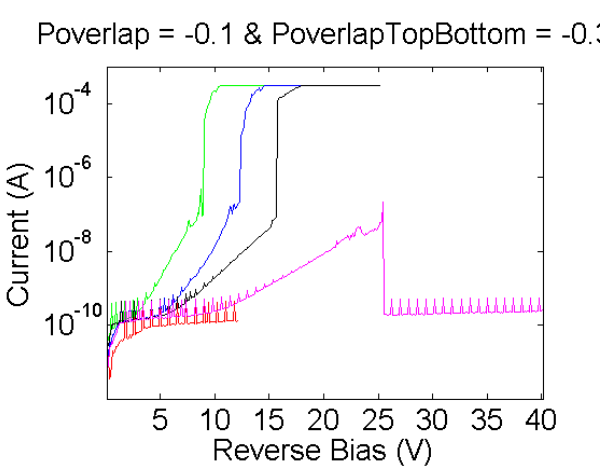

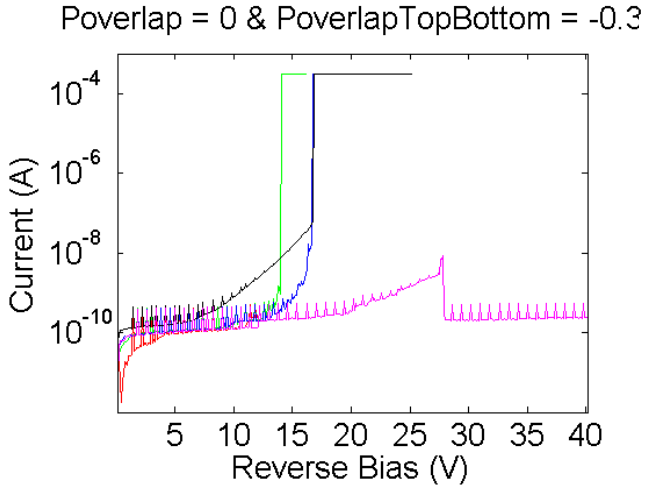

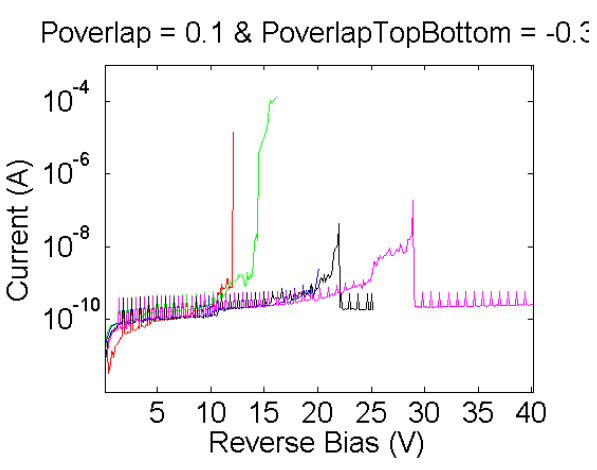

Reverse curves with reduced overlap are poor – now a significant portion of device le

Light On Measurements

- Done with 100 uW incident on grating coupler
- Wavelength set to 1540 nm.
- Estimate ~ 8 uA photocurrent in equivalent PIN structure.
- Fiber array position optimized for each measurement.

Photodiode Measurements

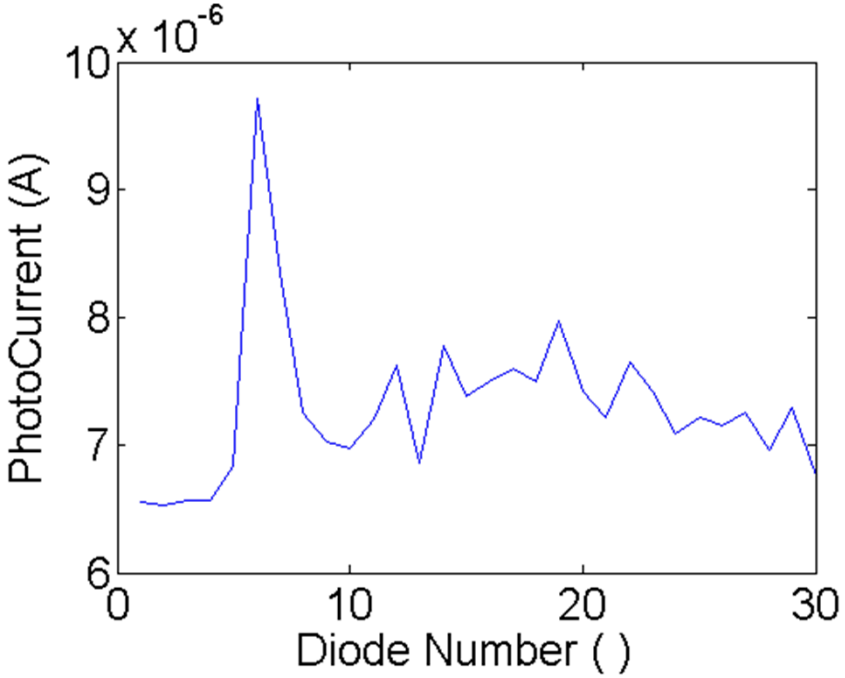

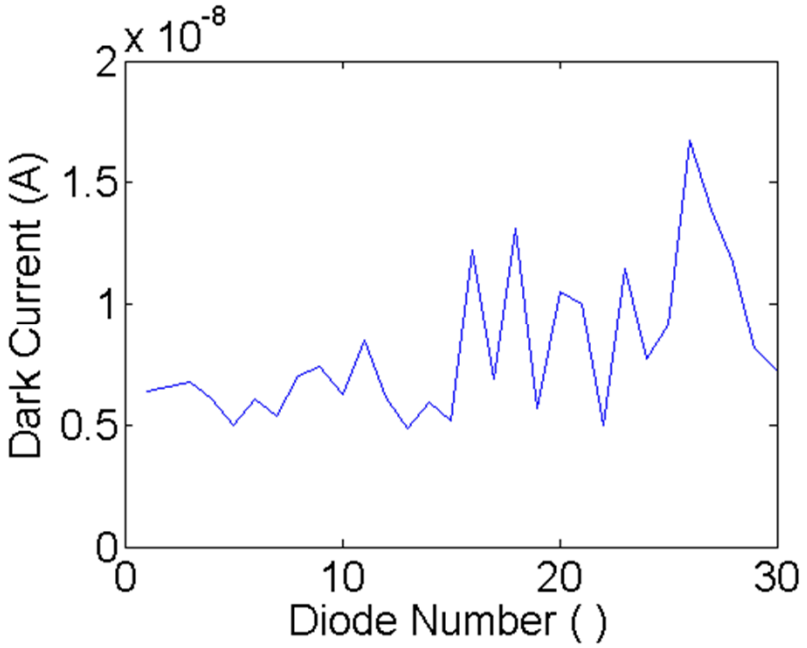

Measured photo and dark currents in 30 1.3x8 um photodiodes in the adjacent die the average photocurrent was 7.3uA and the average dark current was 8.1 nA. I used 8 uA as unit gain in the APD analysis.

Light On (Dashed Curve) L = 16

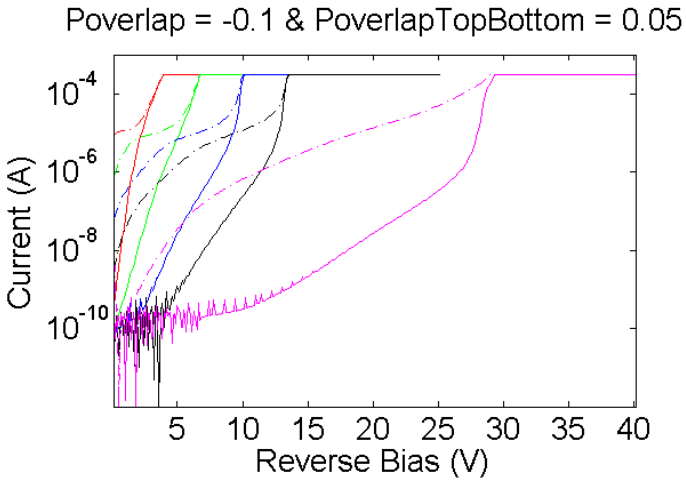

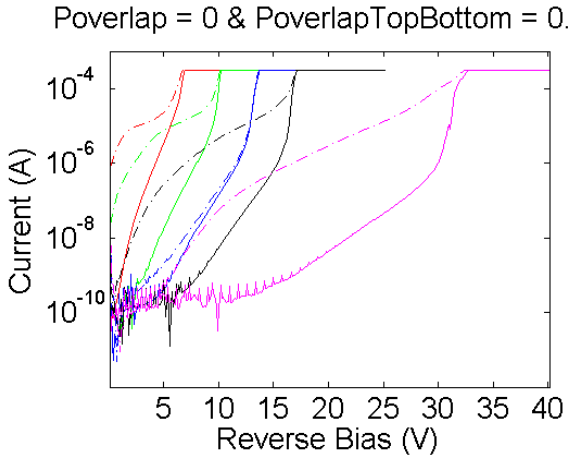

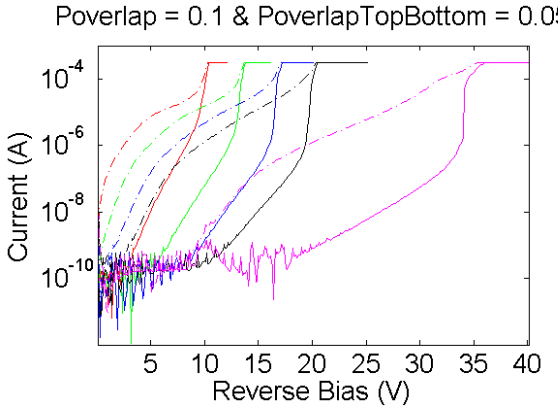

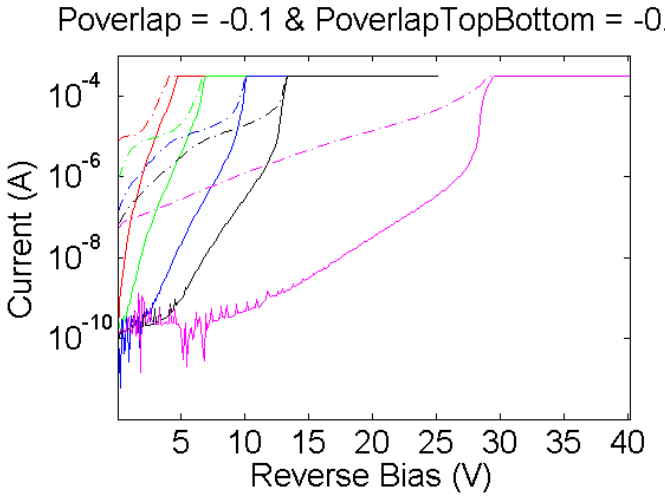

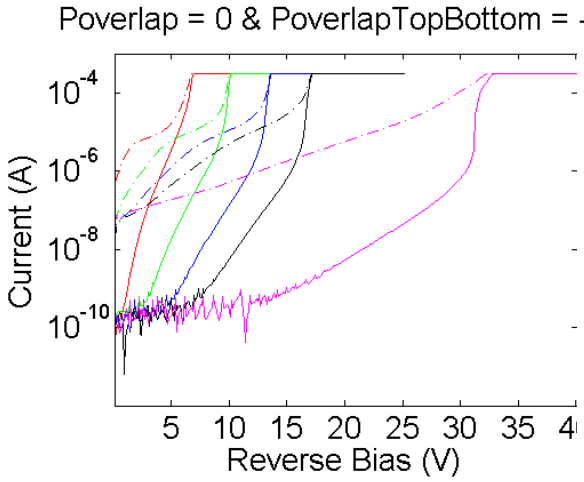

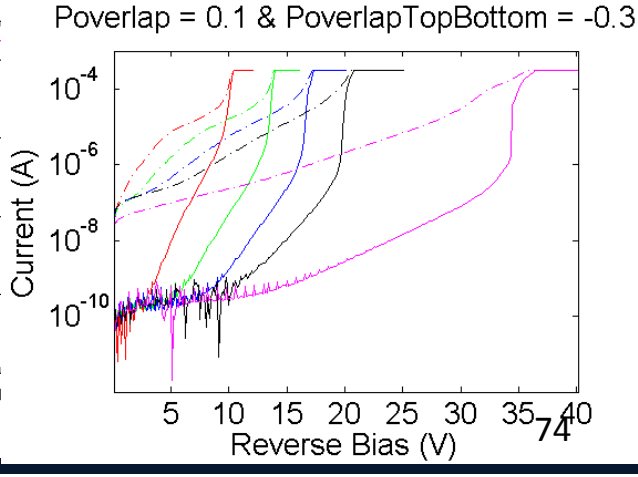

A closer look at photocurrent

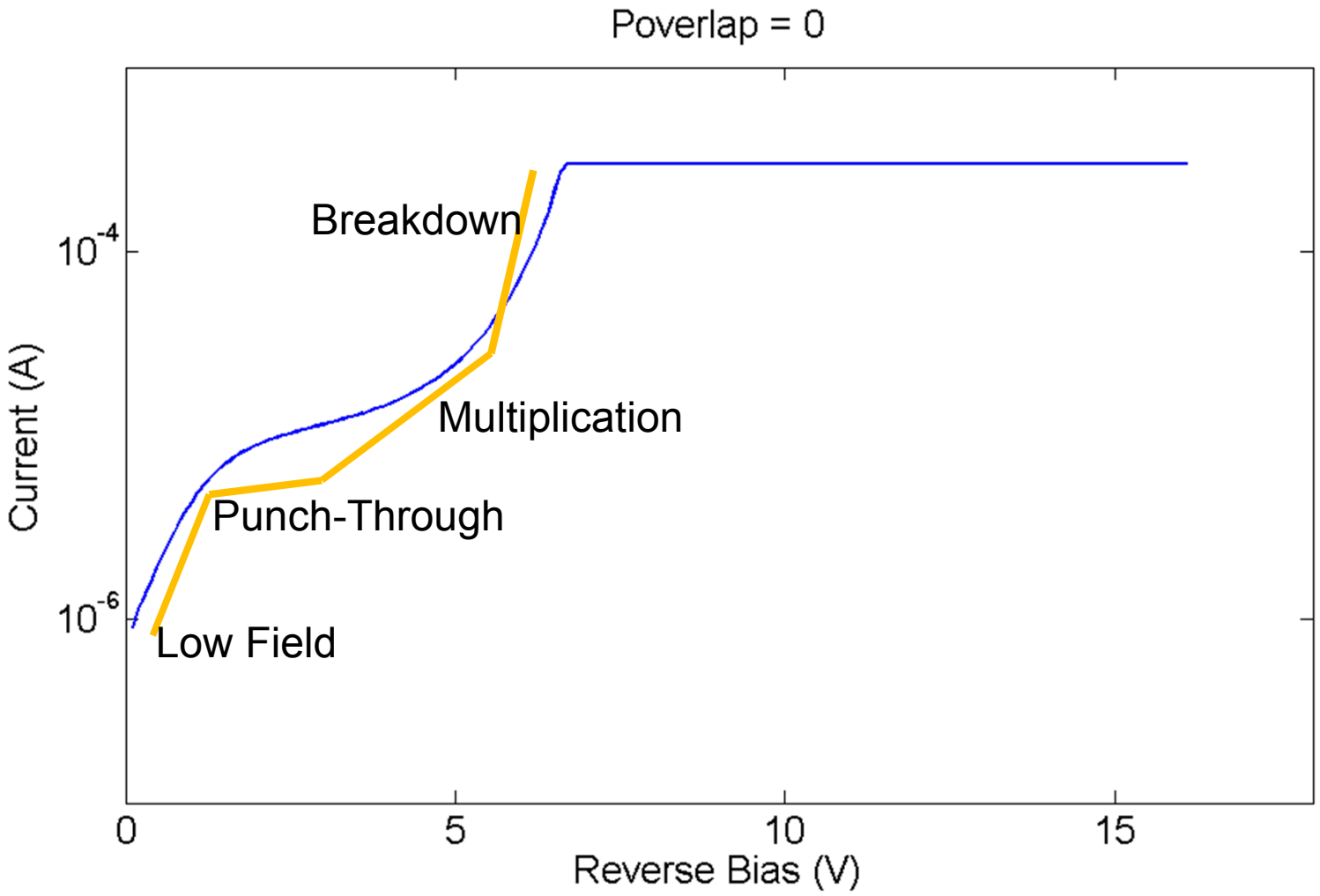

Light On (Dashed Curve) L = 8

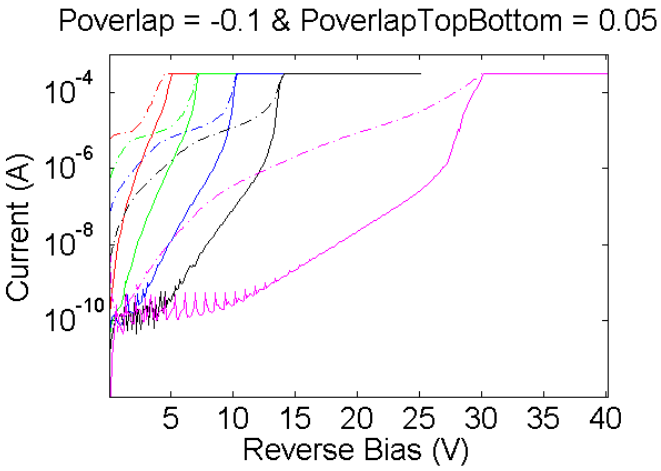

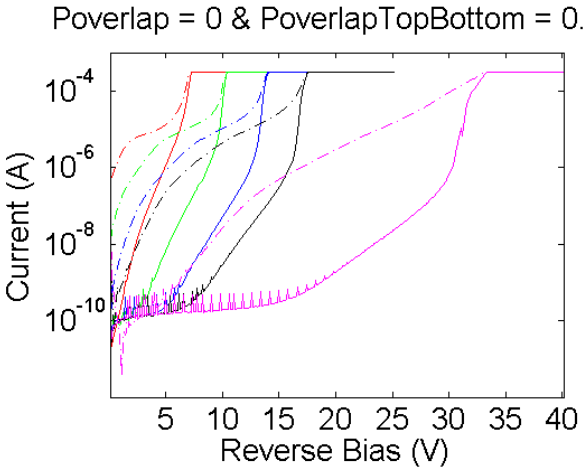

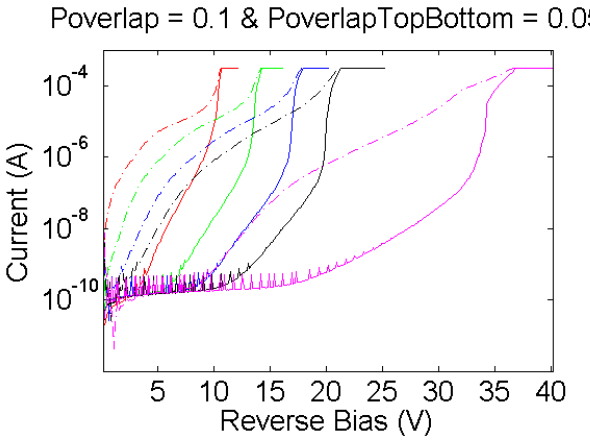

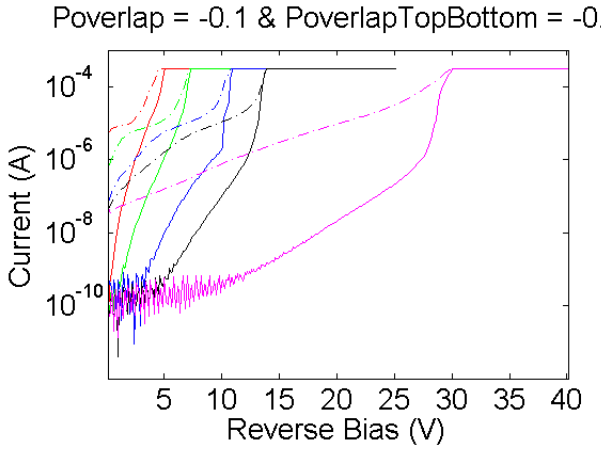

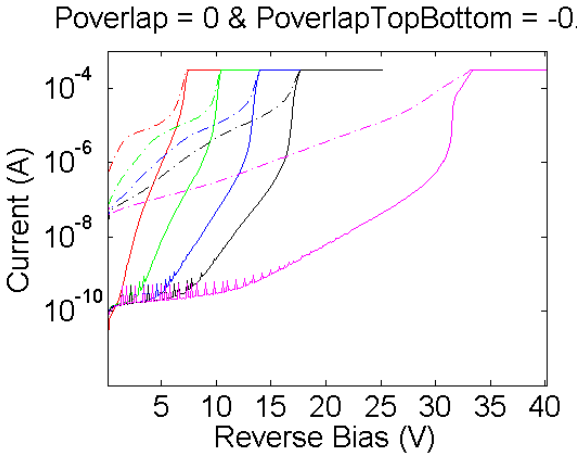

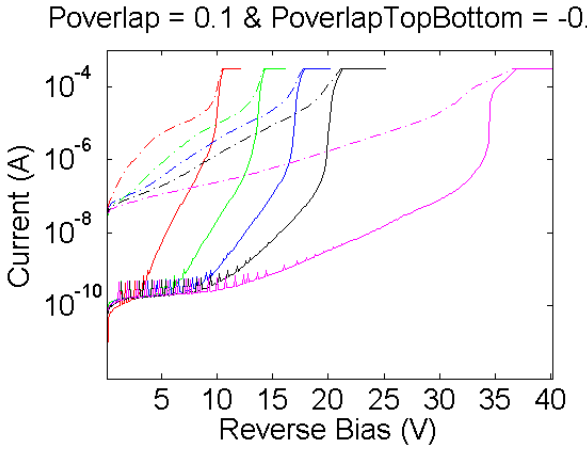

Light On (Dashed Curve) L = 4

Sandia National Laboratories

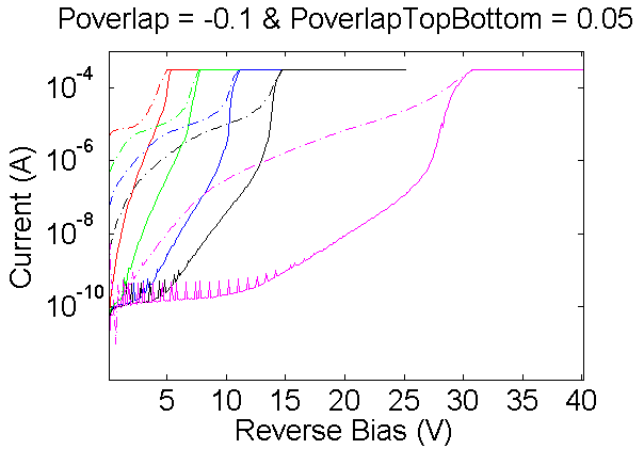

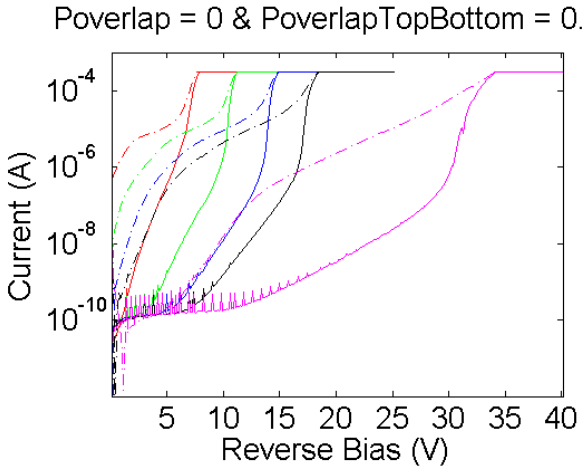

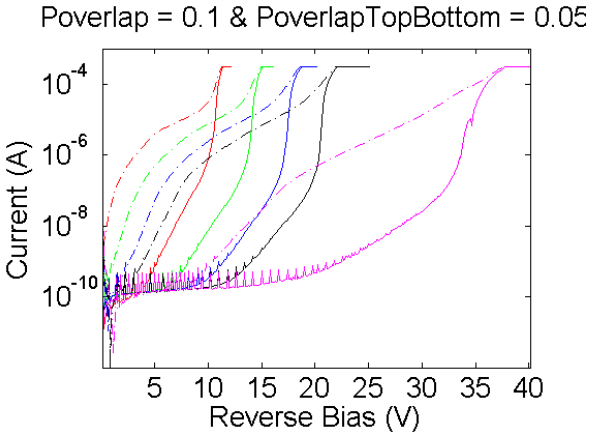

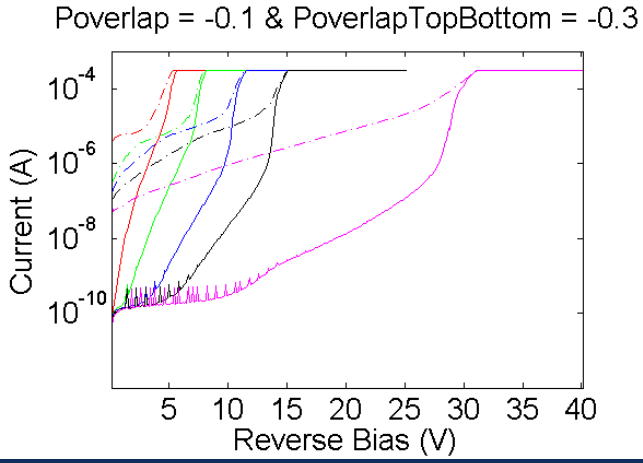

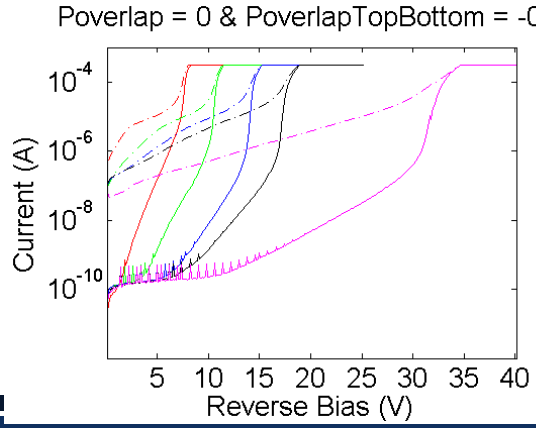

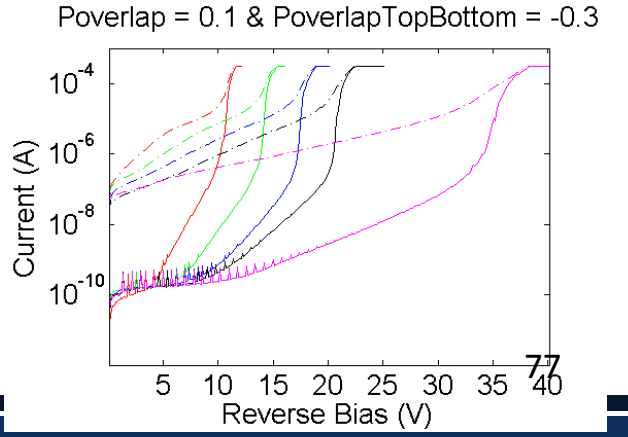

Light On (Dashed Curve) L = 2

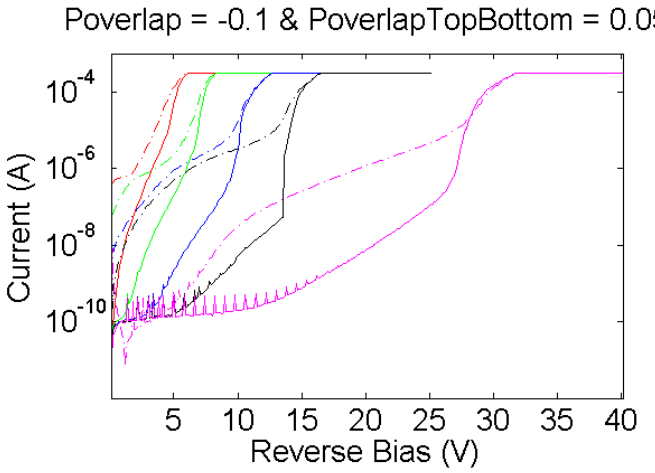

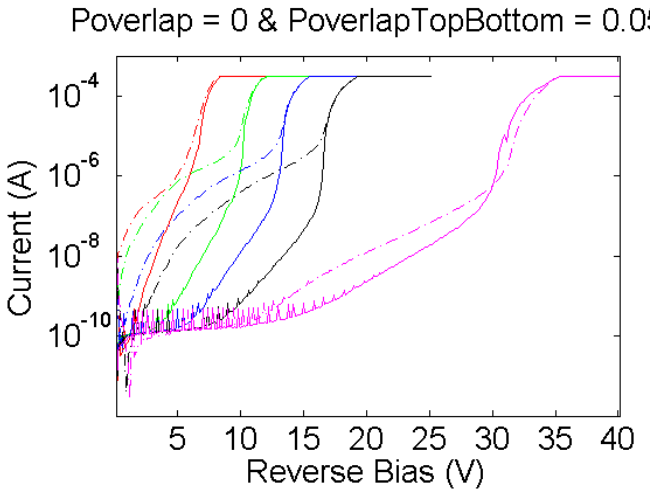

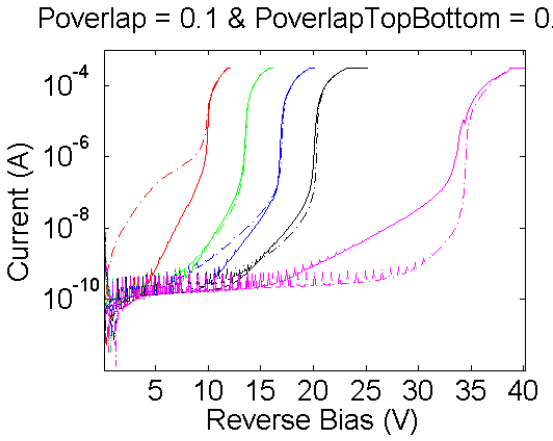

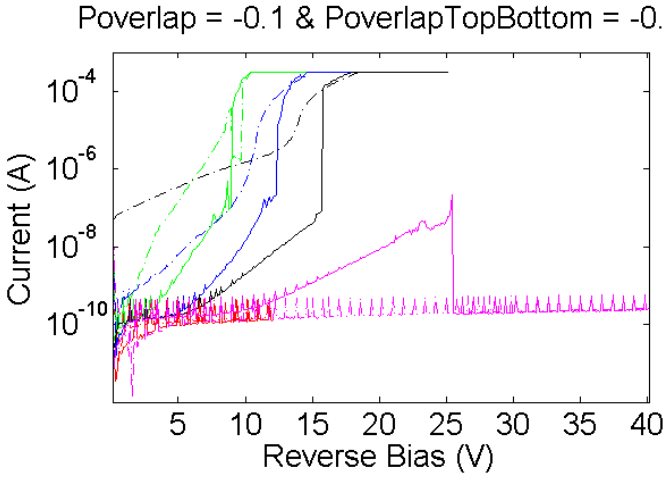

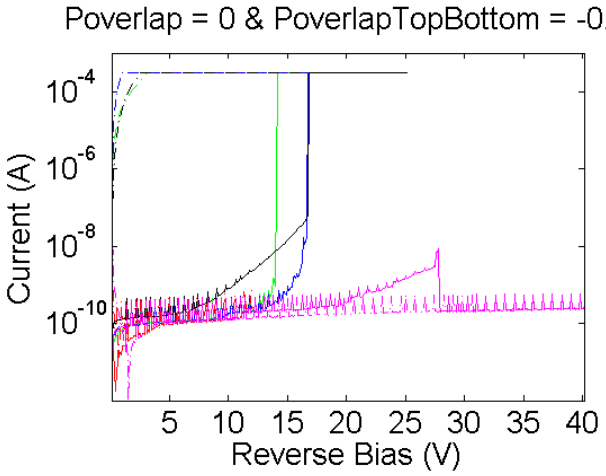

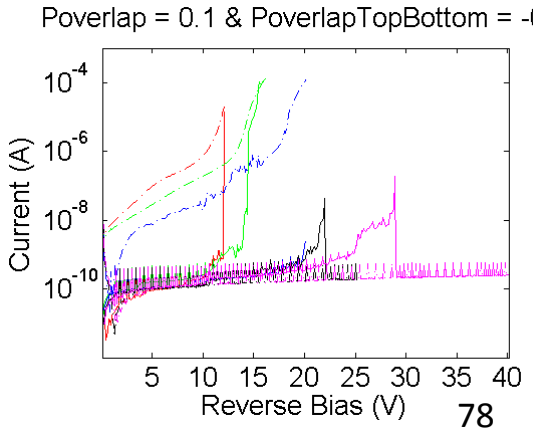

Permanent change in device?

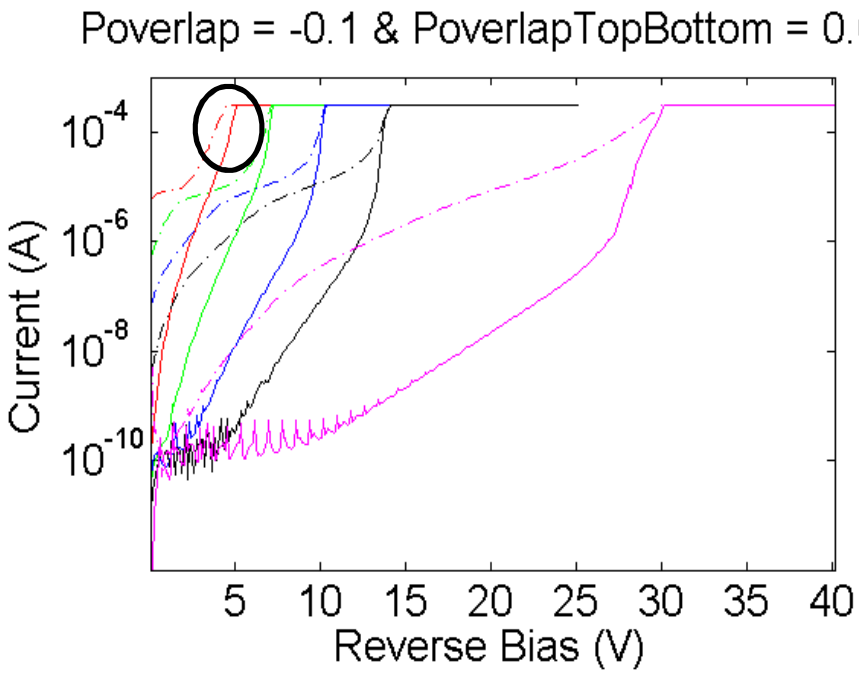

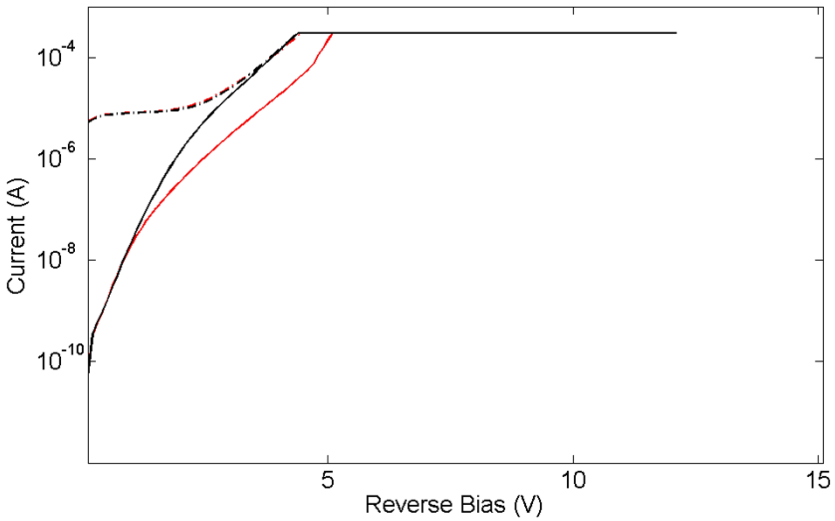

Some devices look particularly good. But… remeasuring the same device we see a hyster
effect on the dark current

A clear gain picture emerges

$M = (i_{light} - i_{dark})/8uA$

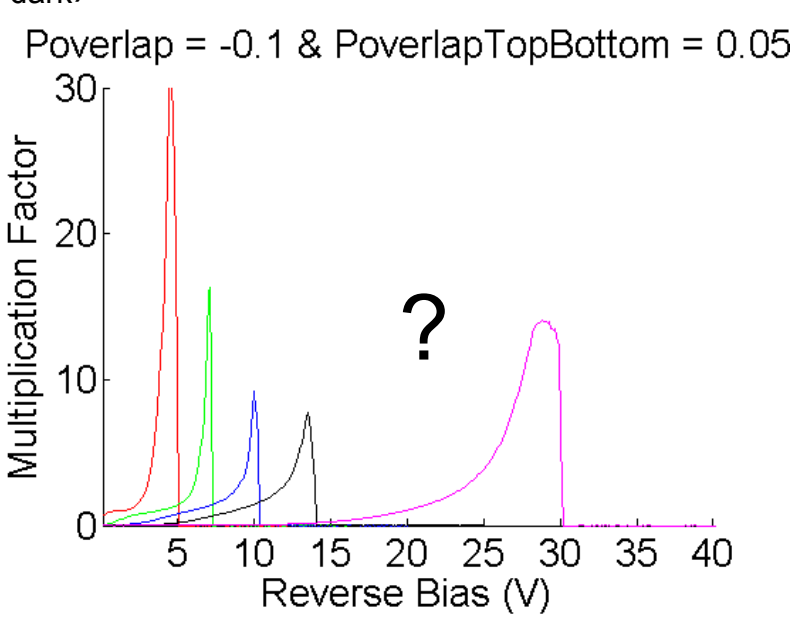

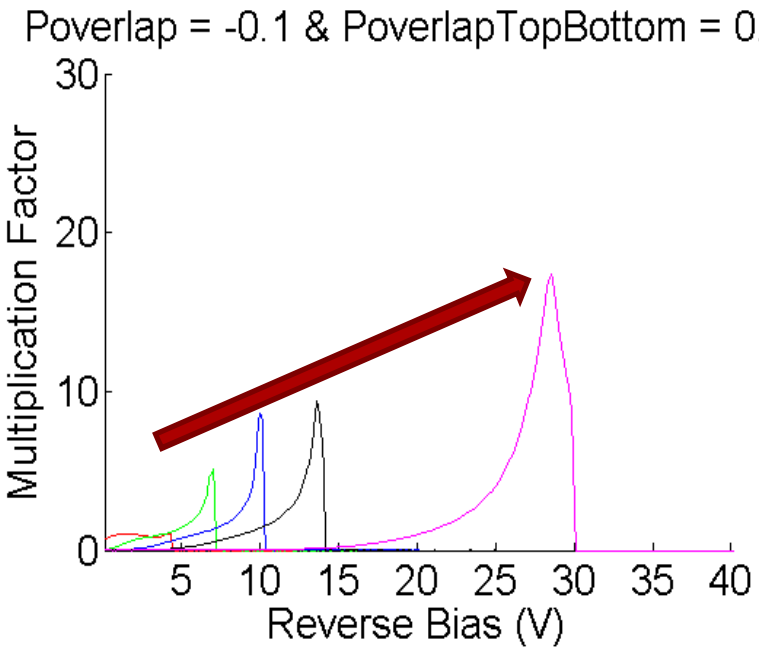

We expect that the avalanche multiplication gain is proportional to the size of the gain region. After hysteresis/burn-in is taken into consideration a very clear gain dependence on width of the avalanche region appears.

Multiplication L = 16

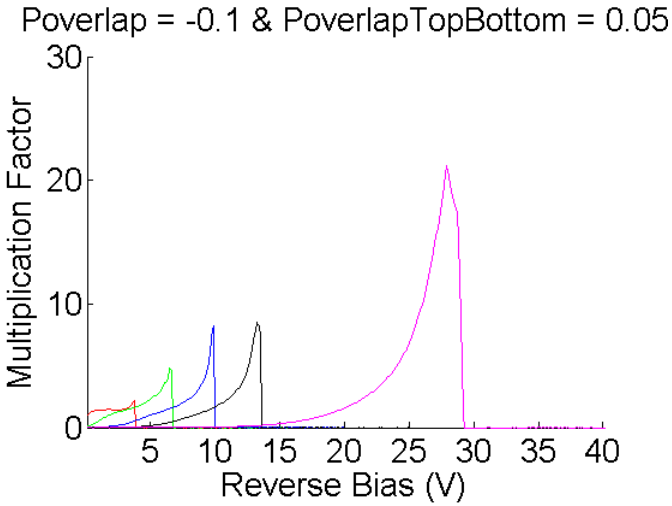

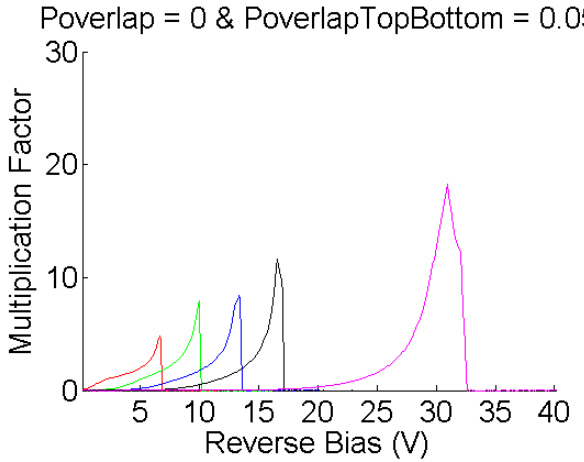

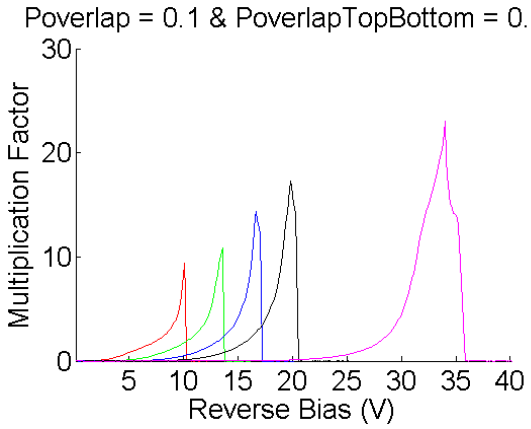

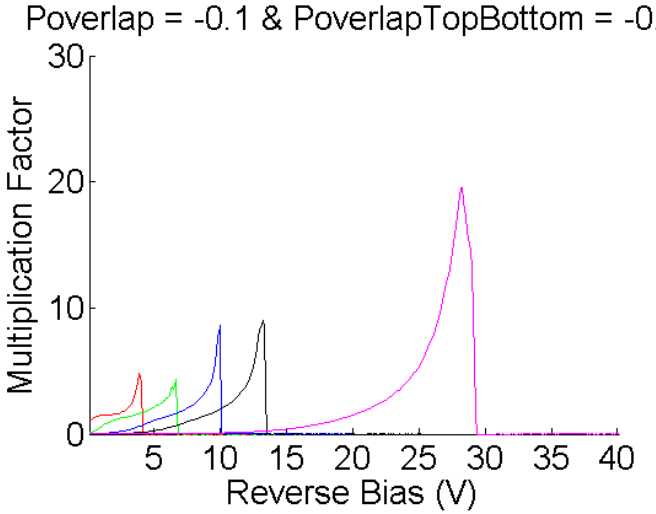

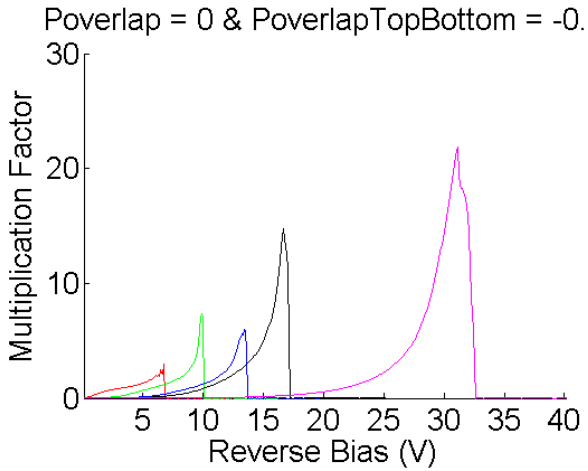

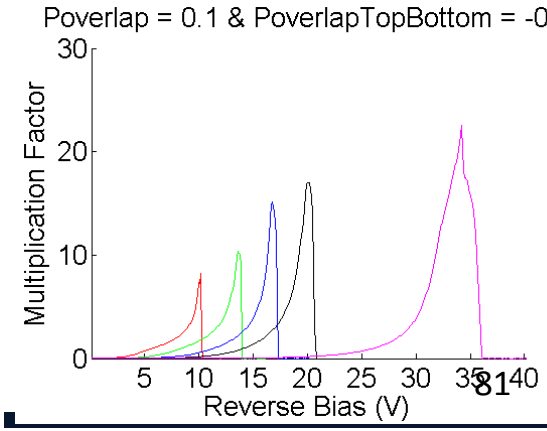

Multiplication L = 8

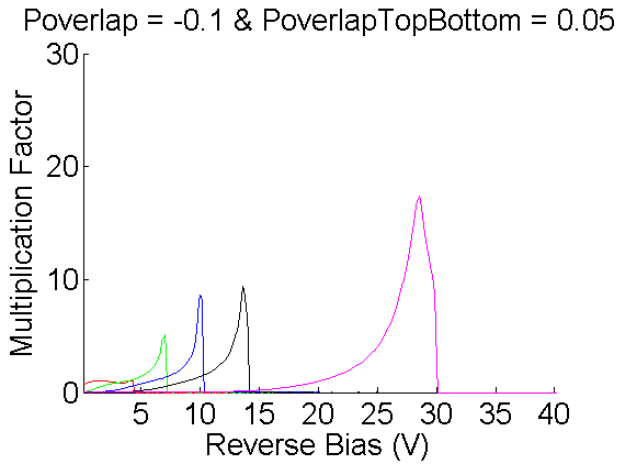

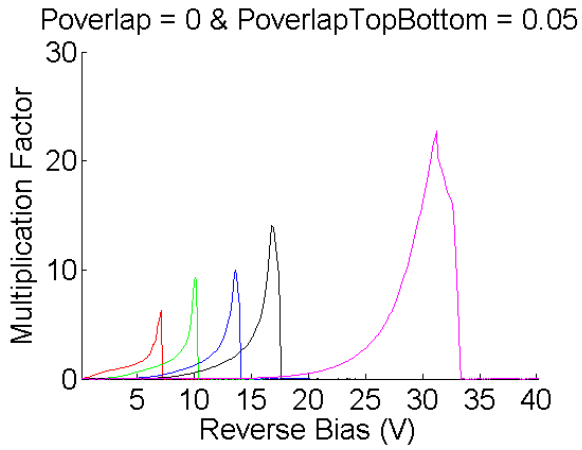

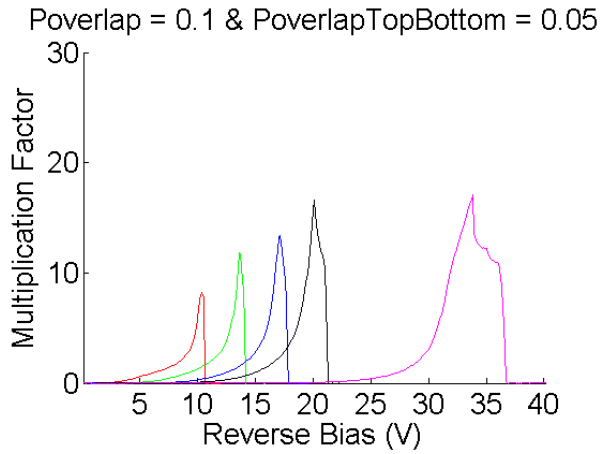

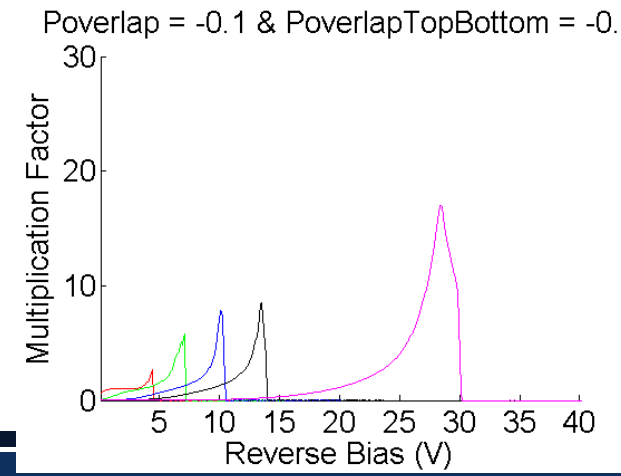

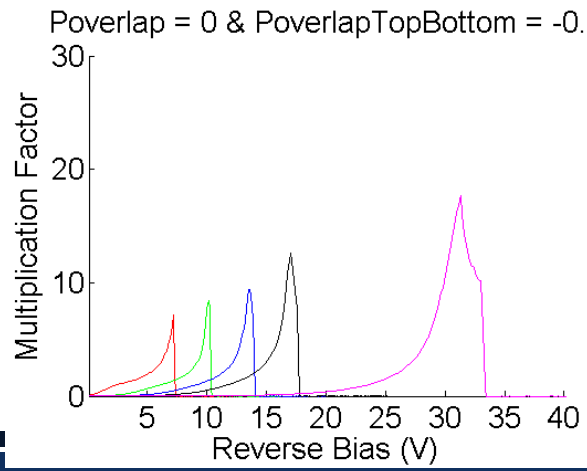

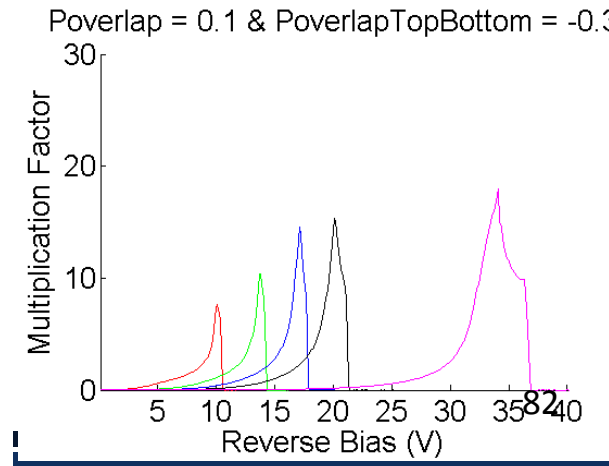

Multiplication L = 4

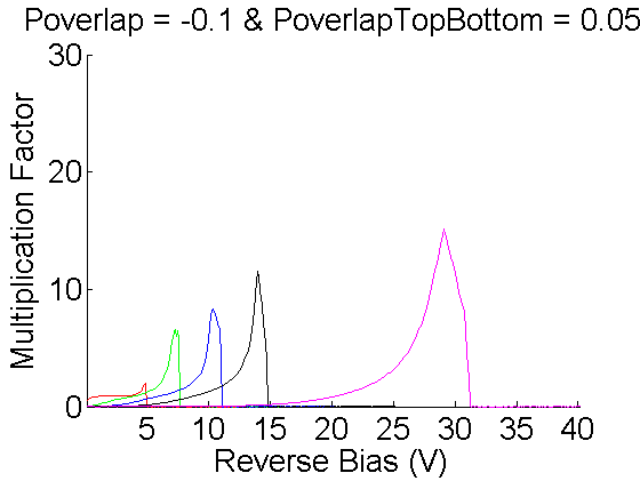

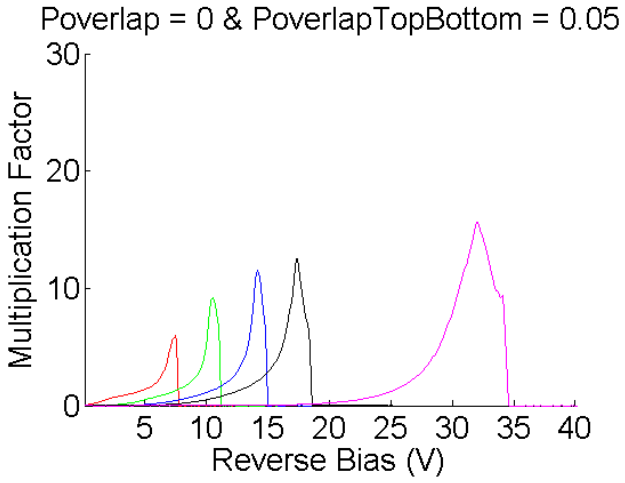

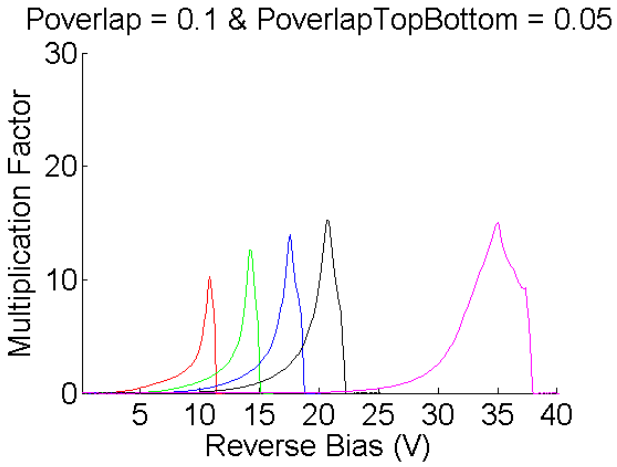

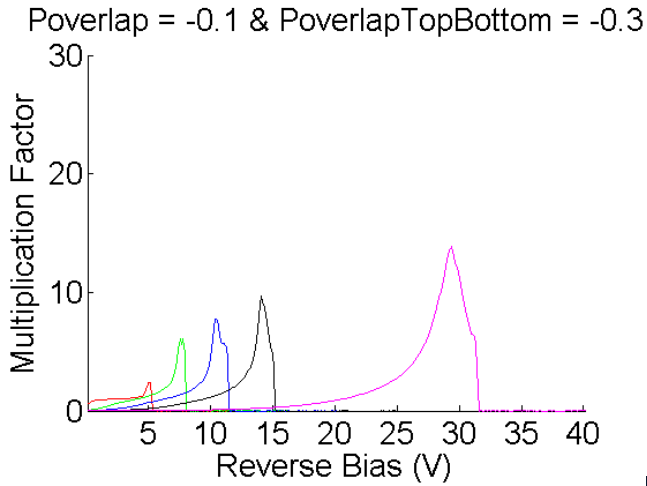

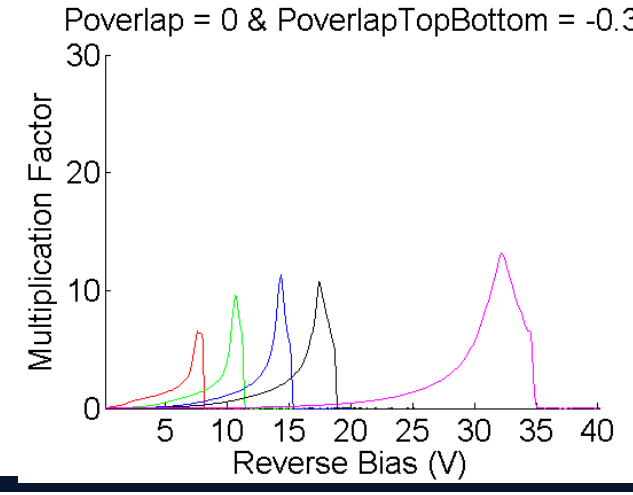

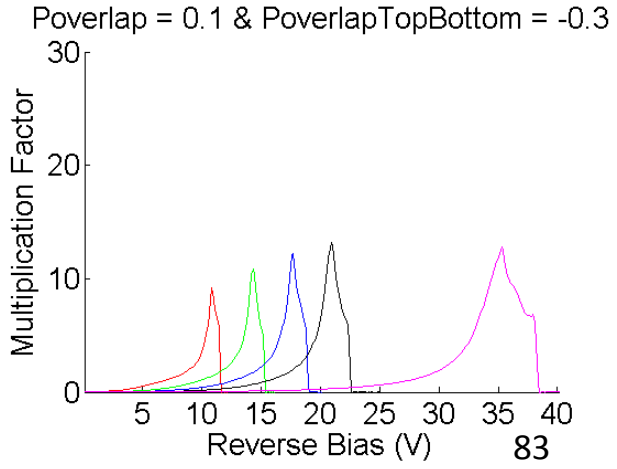

Multiplication L = 2

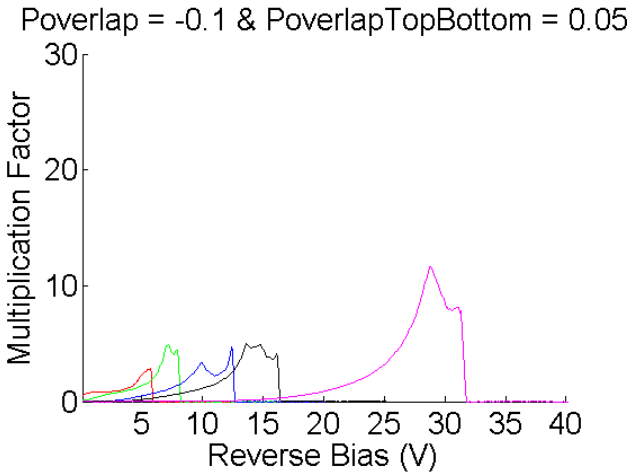

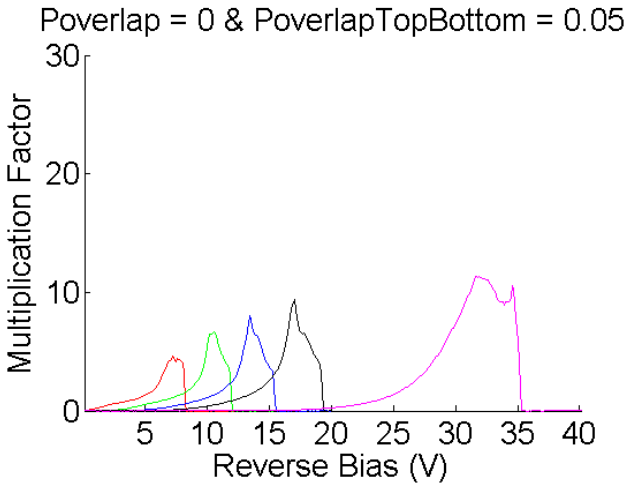

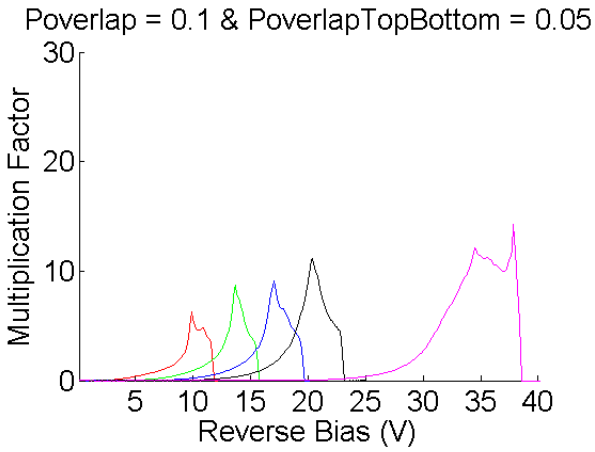

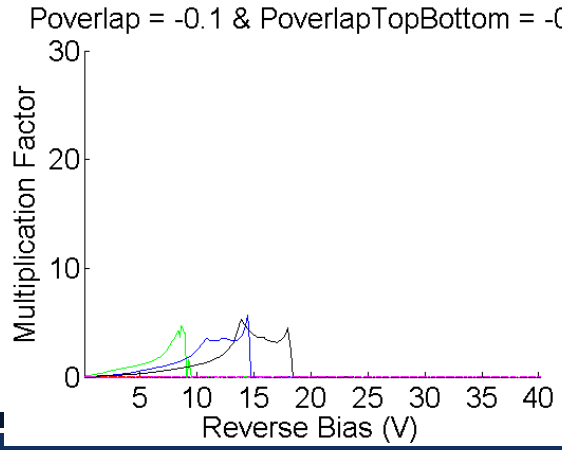

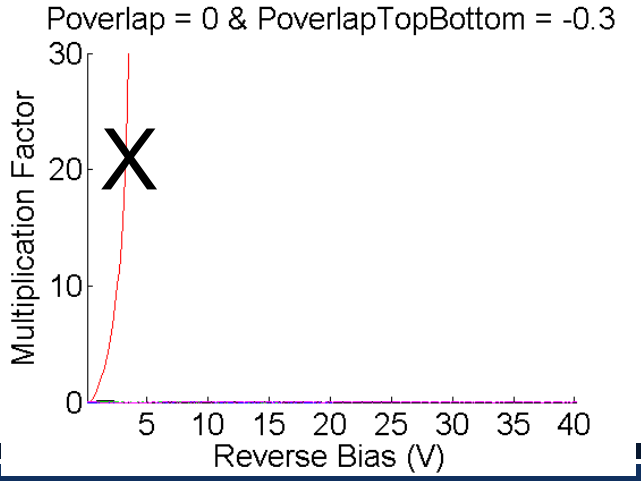

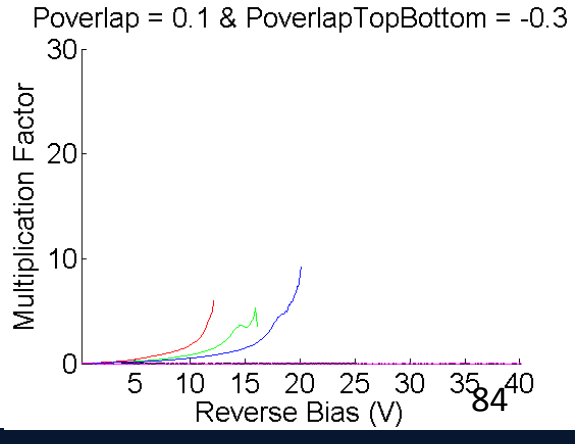

Effect of PoverlapTopBottom

16um long 1.0 um Wmult, Poverlap = -0.1

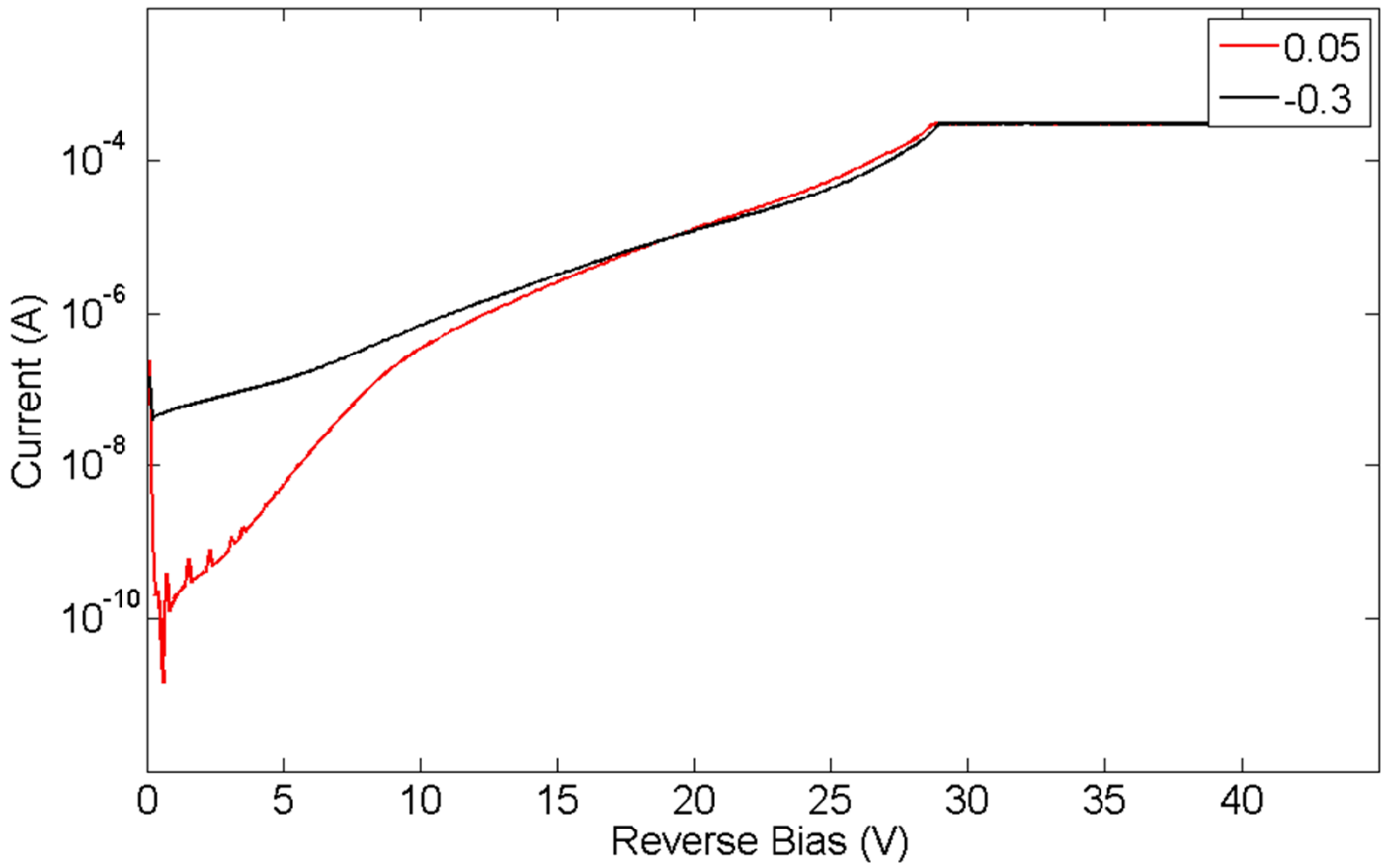

Photovoltaic mode observed at low voltages with reduced PoverlapTopBottom

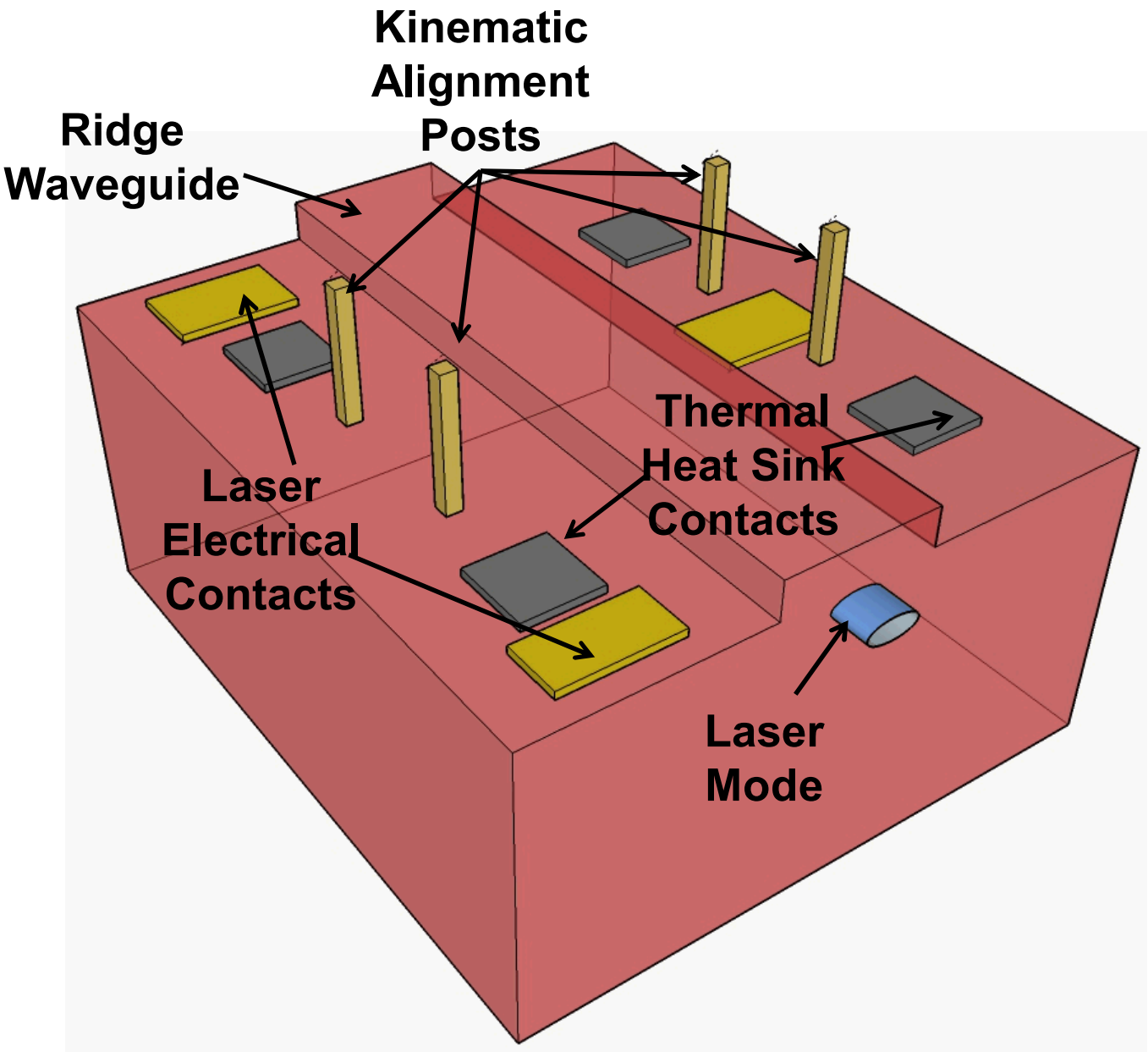
Kinematic
Alignment
Posts
Ridge
Waveguide
Thermal
Heat Sink
Contacts
Laser
Electrical
Contacts
Laser
Mode

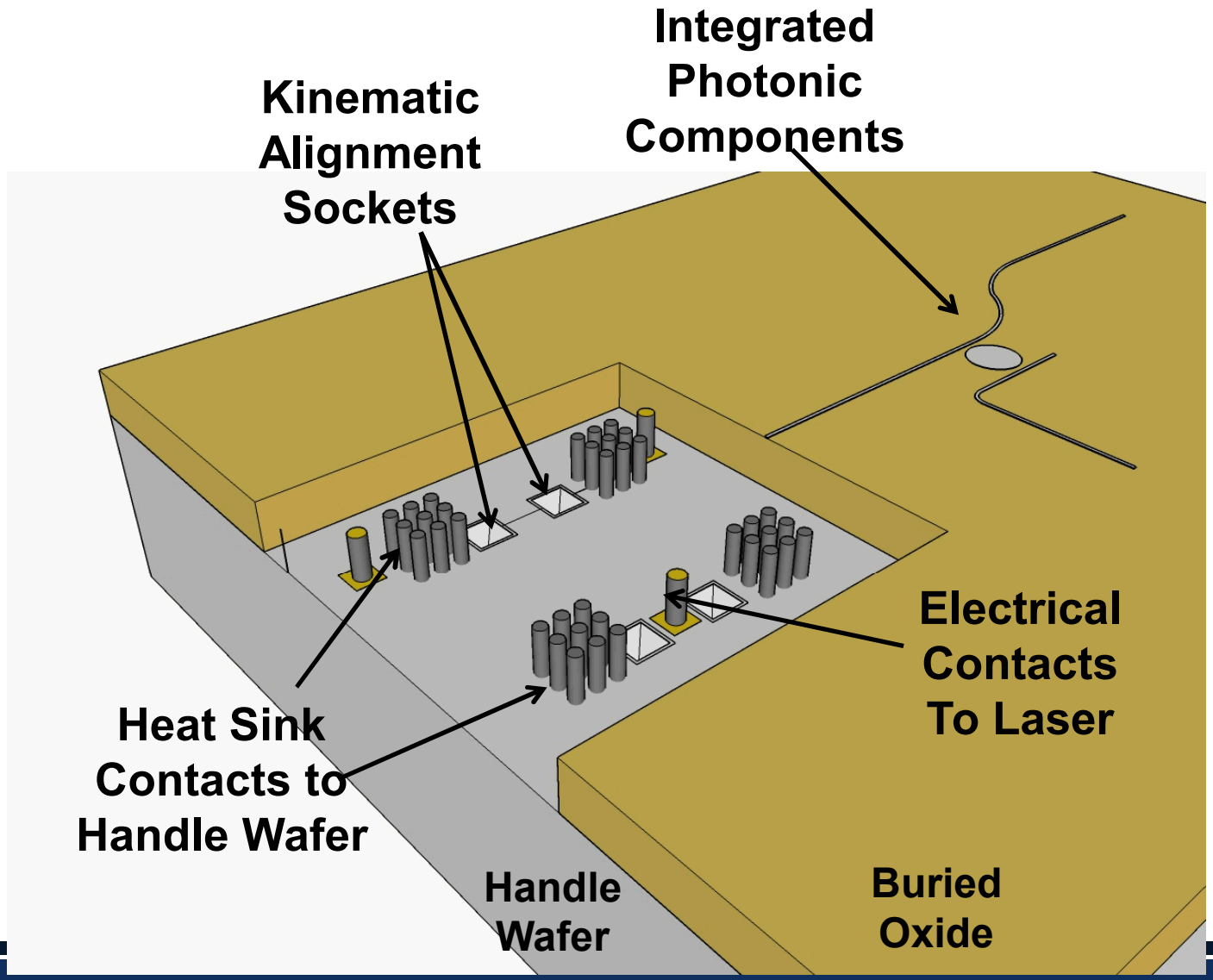
Integrated
Photonic
Components
Kinematic
Alignment
Sockets
Electrical
Contacts
To Laser
Heat Sink
Contacts to
Handle Wafer
Handle
Wafer
Buried
Oxide

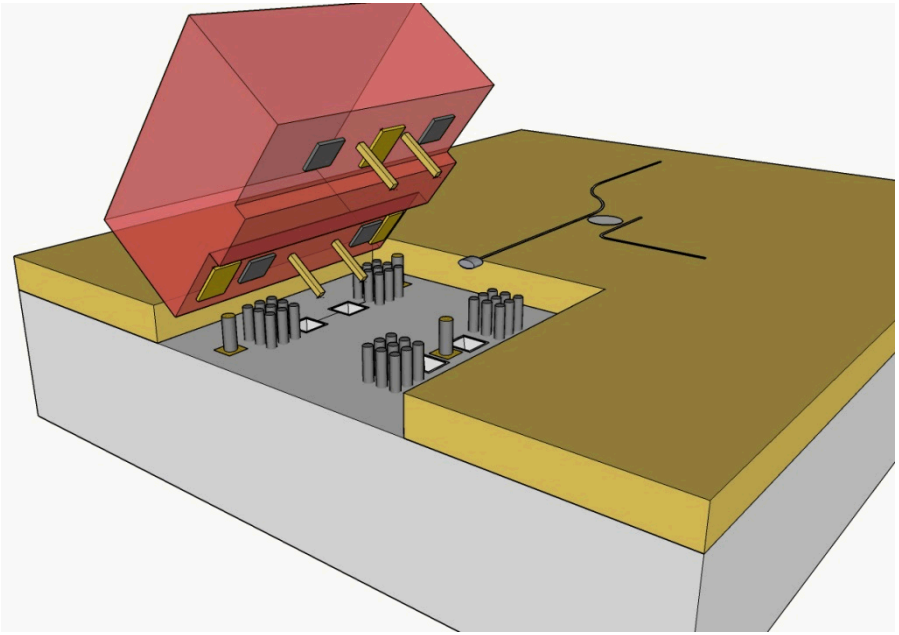

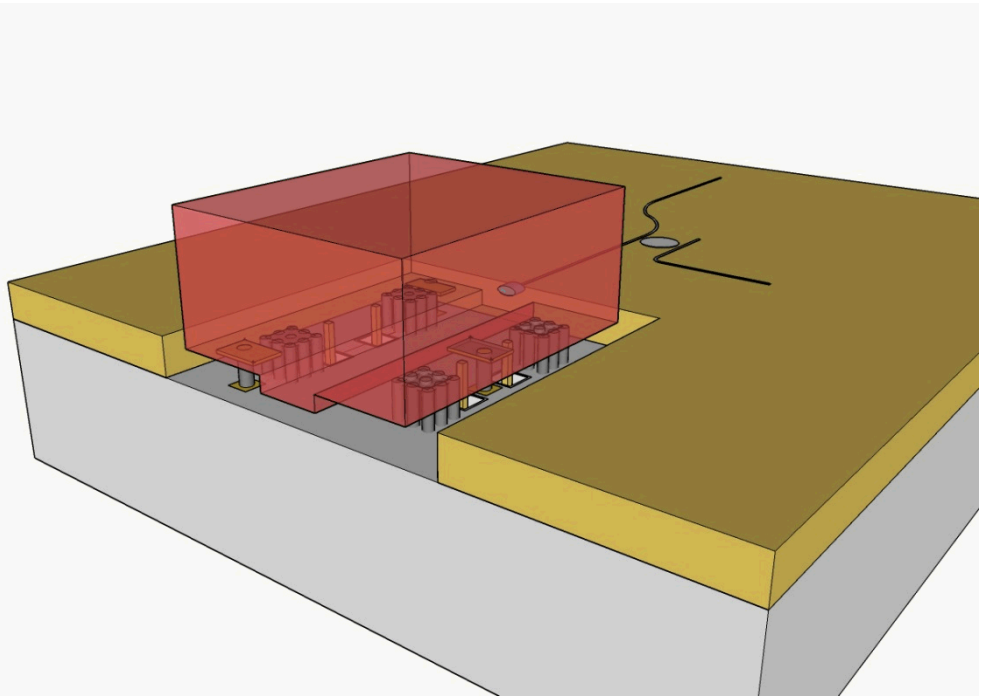

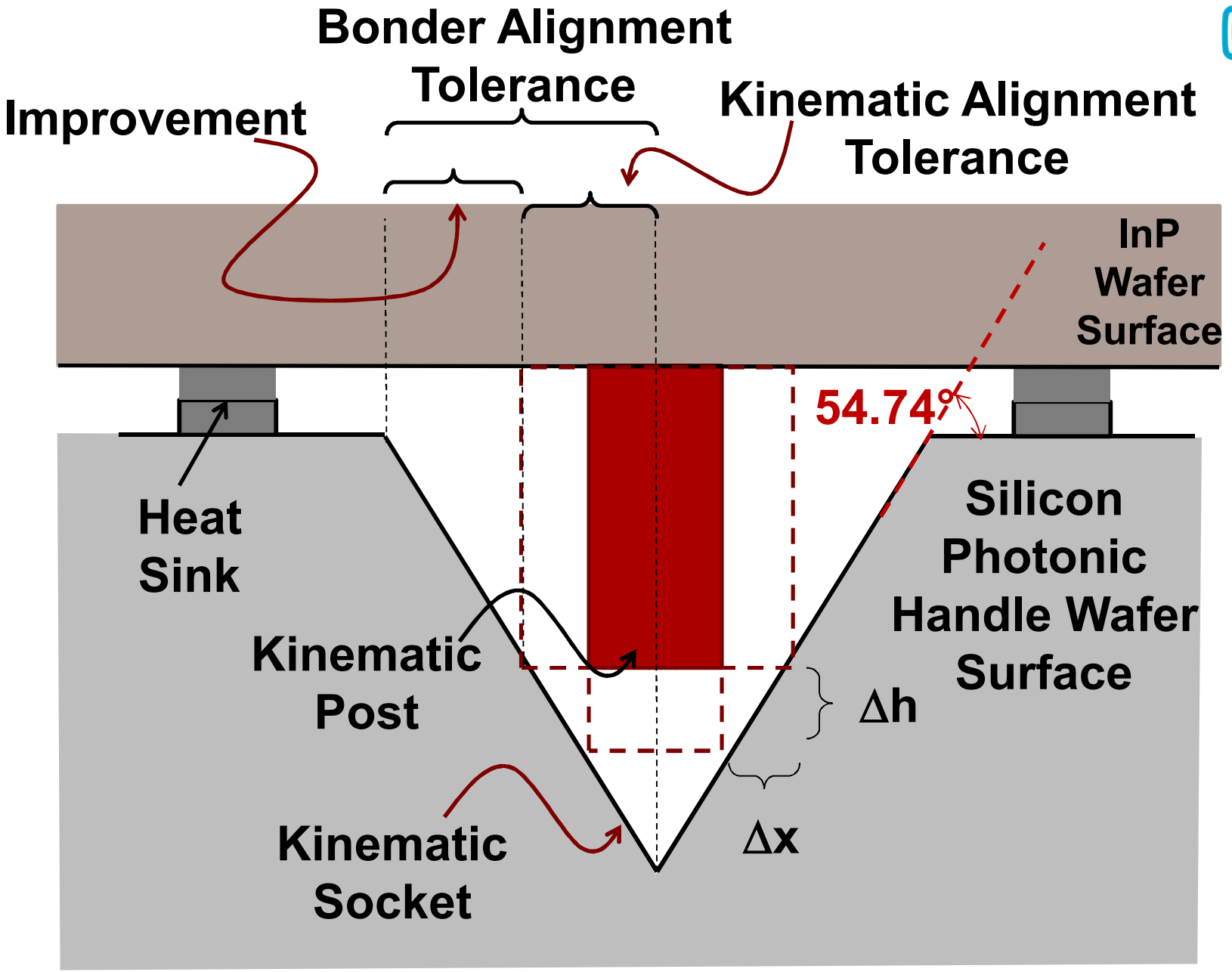
Bonder Alignment Tolerance
Improvement
Kinematic Alignment Tolerance
InP Wafer Surface
54.74°
Heat Sink
Silicon Photonic Handle Wafer Surface
Kinematic Post
Δh
Kinematic Socket
Δx

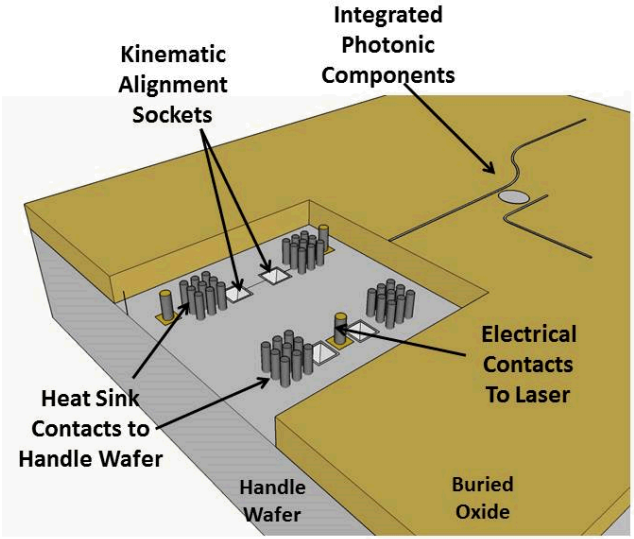
Kinematic
Alignment
Sockets
Integrated
Photonic
Components
Electrical
Contacts
To Laser
Heat Sink
Contacts to
Handle Wafer
Handle
Wafer
Buried
Oxide

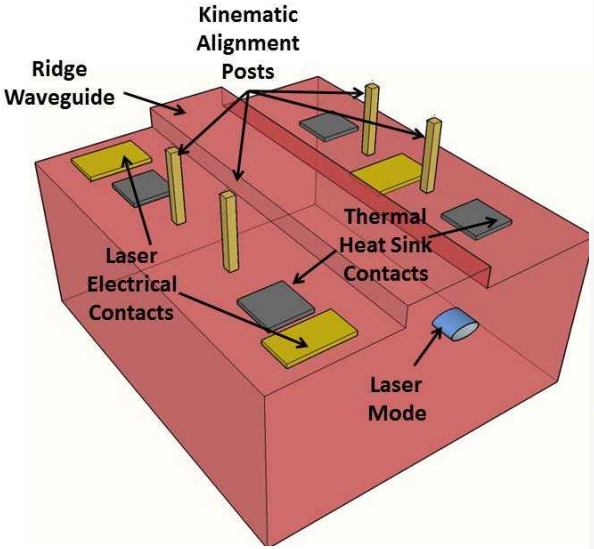
Kinematic
Alignment
Posts
Ridge
Waveguide
Thermal
Heat Sink
Contacts
Laser
Electrical
Contacts
Laser
Mode

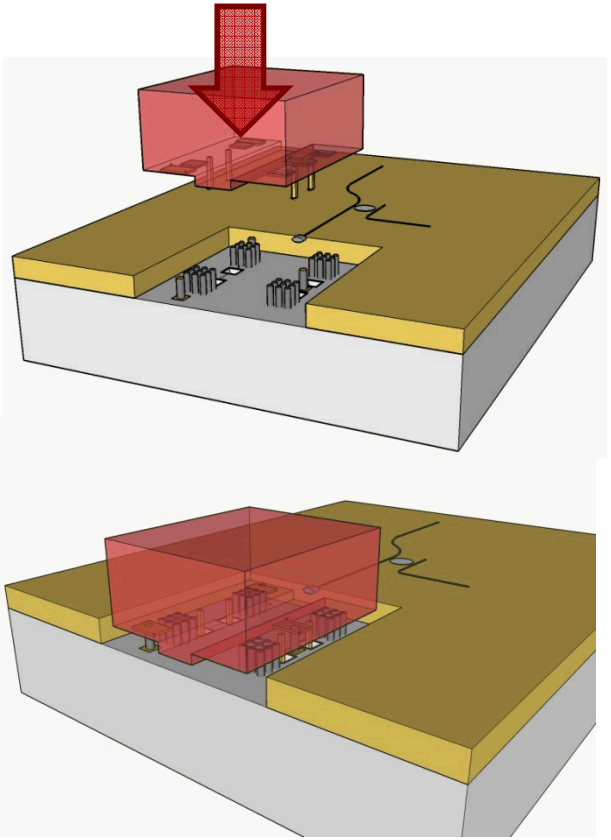

A.

B.

C.

Sandia National Laboratories

Post Reticle Socket Reticle

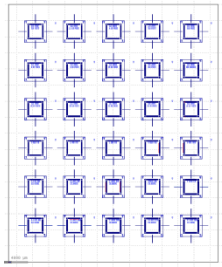

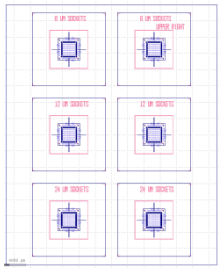

flip over

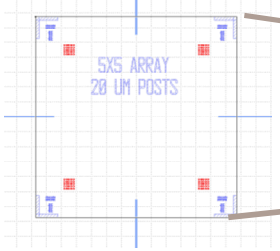

Post Die

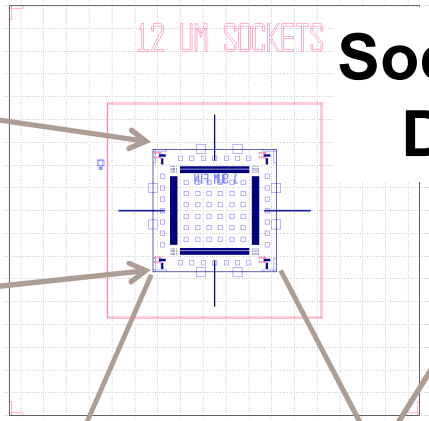

Socket Die

High Mag GDS Kinematic Alignment Features

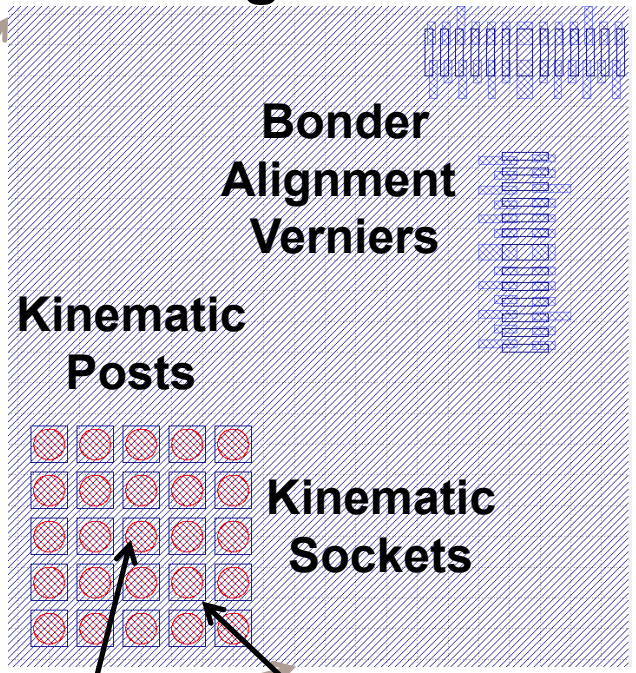

Bonded Socket-Post Die

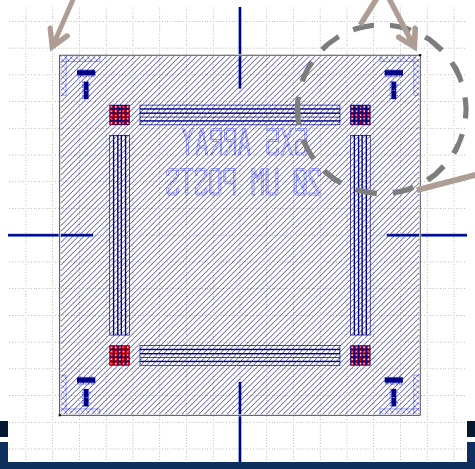

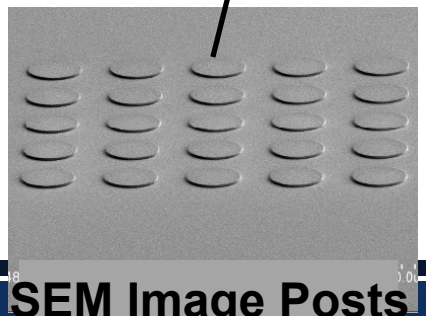

SEM Image Posts

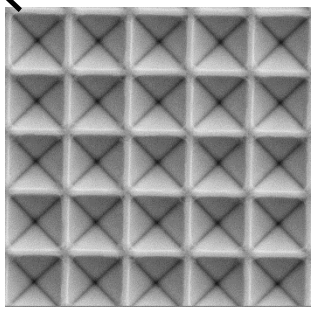

SEM Image Sockets

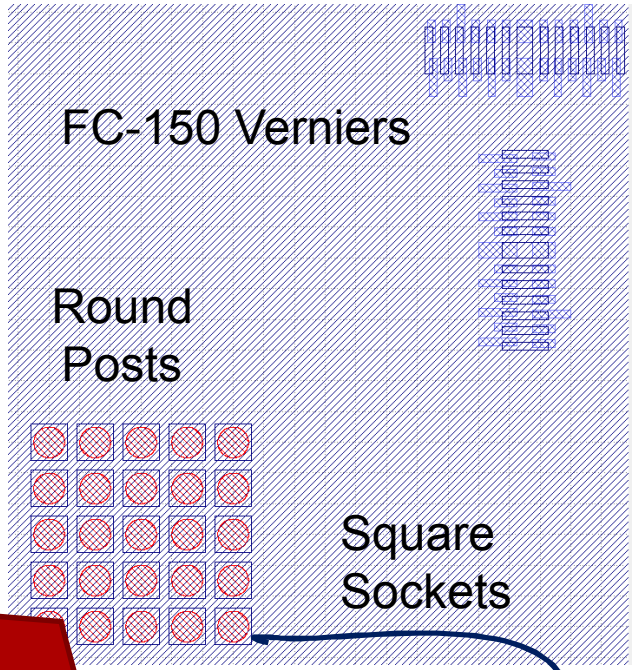

5 x 5 Post Array

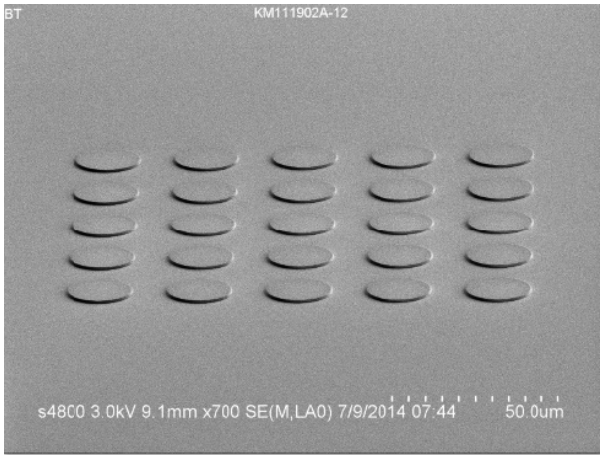

Note low aspect ratio

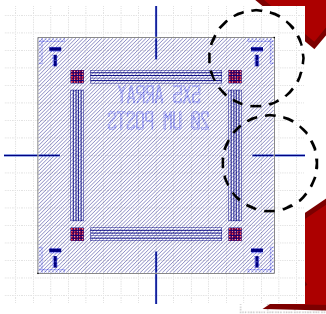

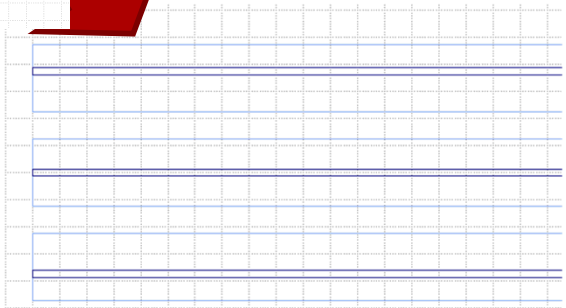

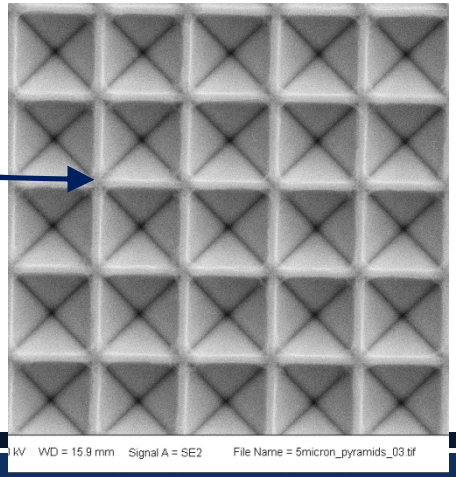

5 x 5 Socket Array

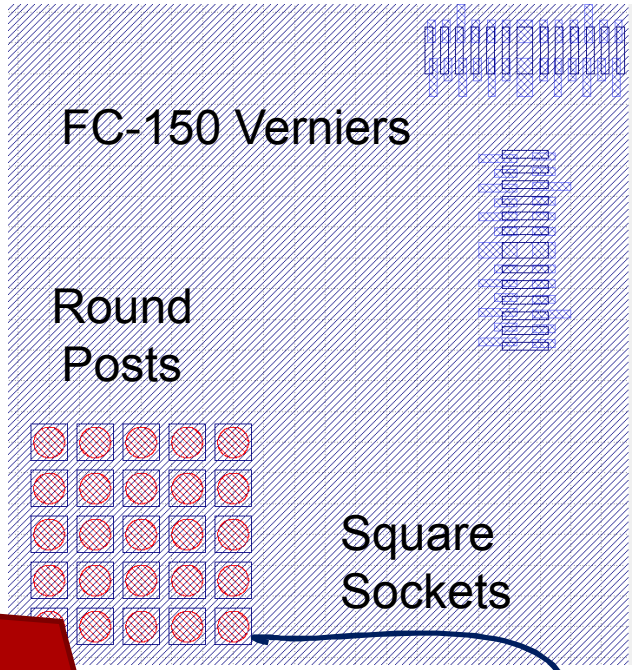

5 x 5 Post Array

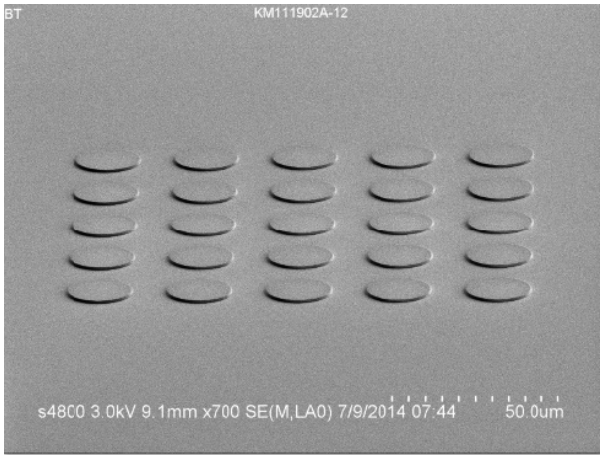

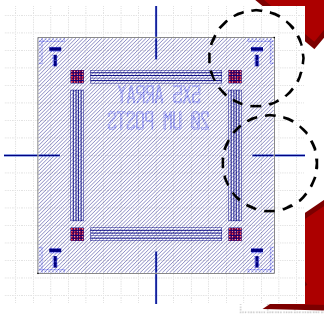

Note low aspect ratio

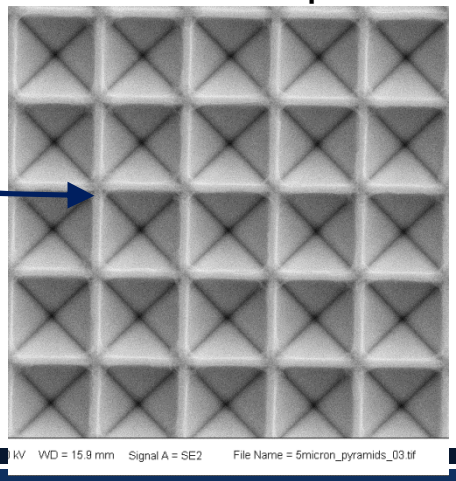

5 x 5 Socket Array

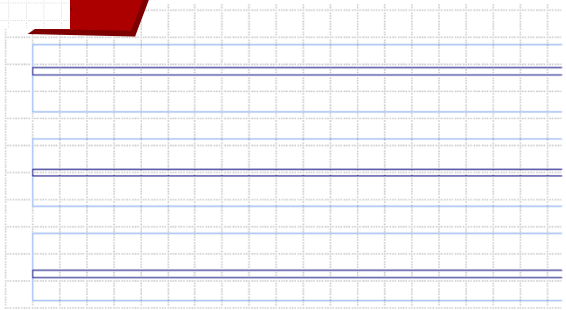

3-Element Vernier (3-Element Tauke-Pedretti)